L

Design of Steel Piles for Integral Abutment Bridges

Hans Pétursson

LULEÅ
UNIVERSITY
OF TECHNOLOGY

Design of Steel Piles for Integral Abutment Bridges

Hans Pétursson

Division of Structural and Construction Engineering
Department of Civil, Mining and Natural Resources Engineering
Luleå University of Technology
SE-971 87 Luleå
www.ltu.se/sbn

"Any fool can know. The point is to understand."
— Albert Einstein

Division of Structural and Construction Engineering/Steel Structures

Department of Civil, Environmental and Natural Resources Engineering

Luleå University of Technology

Academic dissertation

That by due permission of The Technical Faculty Board at Luleå University of Technology will be publicly defended, to be awarded the degree of Doctoral of Engineering, in Hall F1031, Luleå University of Technology, Friday, October 30, 2015, 09:00.

Opponent /Examiner: Professor Ian May, Heriot Watt University, Edinburgh

Examining Committee: Professor Niels Gimsing, Technical University of Denmark, Copenhagen

Associate Professor Mohammad Al-Emrani, Chalmers University of Technology

Adjunct professor Costin Pacoste, Royal Institute of Technology, Stockholm

Chairman: Professor Peter Collin, Luleå University of Technology

Supervisor: Professor Peter Collin, Luleå University of Technology

Assistant supervisor: Professor Bernt Johansson, Luleå University of Technology

Front page: The picture shows piles during construction of the bridge over Leduån.

Preface

The research project presented in this thesis was carried out between 1999 and 2014. The first part of the research, presented in a licentiate thesis written by the author in 2000, addressed bridges with integral abutments with an emphasis on composite bridges and cross shaped steel piles (X-piles). The second part was carried out between 2005 and 2008 to a great part within the RFCS research and development project INTAB (Pak et. al 2008). The project was financed by SBUF, Ramböll Foundation, Ramböll Sweden, FinRoad and Ruukki. Financial and moral support have also been given by Swedish Transport Administration (and its predecessor Swedish Rail Administration and Swedish Road Administration). The third part was carried out between 2008 and 2012 when paper II to V was written and the laboratory tests described in Paper V were performed. This thesis was than written during 2014 and 2015.

I would like to take the opportunity to thank the people and who made this work come true.

First, I would like to thank my supervisor Peter Collin, for giving me the opportunity to perform this research at Luleå University of Technology and Ramböll.

Bernt Johansson who introduced me to the subject in the first place, supervised me when I wrote the licentiate thesis and took the time to read this thesis and to give comments.

People at the laboratory at Luleå University of Technology that with skill performed the monitoring of the bridge over Leduån and the tests that is described in the thesis.

Last but definitely not least, I would like to thank my lovely wife Eva for all the love, patience and support she has given me through the years and my children Axel, Kalle and Moa. You are my everything!

Falun, September 2015

Hans Pétursson

Abstract

This thesis deals with integral abutment bridges, with focus on the design of steel piles carrying such bridges.

As outlined in Chapter 1, integral abutment bridges have large advantages over bridges with expansion joints and bearings. However, there are some questions to be answered and some of these questions are formulated as research questions in this thesis.

Cross shaped steel piles were axially loaded to failure, simulating the effect of the bridge length varying with the annual temperature variations.The tests showed that 25 mm imposed deformations of the pile tops do not significantly influence ultimate capacity of the piles (Chapter 2 and Paper I).

In order to study how steel piles in integral abutments are used in different countries an international workshop was arranged in Stockholm (Collin et. al. 2006 and Paper II) and a literature study was conducted (Chapter 3).

Furthermore the bridge over Leduån was designed, built and monitored. The monitored values with respect to deflections and pile stresses gave a fairly good agreement with FEA carried out with soil parameters from the Swedish Bridge Code Bro 94 (Chapter 4, Paper III and Paper IV).

In order to investigate the behavior of steel piles in fatigue with strains exceeding yield strains, bending tests of piles encased in concrete were carried out (Paper V). The tests demonstrated that a pile can accommodate strains many times the yield strain and still last for hundreds of cycles.

Finally the results above are discussed and a design method is suggested in Chapter 5. In Chapter 6 answers to the research questions from Chapter 1 are formulated and discussed.

Keywords: integral abutment bridges, joint-less bridges, steel piles

Sammanfattning

I denna avhandling studeras broar med integrerade landfästen, med fokus på stålpålar i dessa broar. Som beskrivs i Kapitel 1 har broar med integrerade landfästen stora fördelar jämfört med konventionella broar med lager och övergångsanordningar. Vidare formuleras i Kapitel 1 ett antal forskningsfrågor.

Försök med X-pålar genomfördes år 2000. Försöken visade att 25 mm tvångsförskjutning; tänkt att simulera effekten av att brolängden ändras vid temperaturväxlingar mellan sommar och vinter; inte nämnvärt påverkar pålarnas bärförmåga i tryck (Kapitel 2 och Paper I).

En internationell workshop genomfördes i Stockholm, med deltagare från 9 länder (Collin et. al. 2006 och Paper II) med syfte att se hur länder använder och dimensionerar broar med integrerade landfästen. Det framkom att det råder en stor skillnad mellan olika länders utformning av och dimensioneringsfilosofi rörande broar med integrerade landfästen. Dessutom genomfördes en litteraturstudie med avseende på bland annat dimensioneringsregler samt fullskalemätning (Kapitel 3).

En bro över Leduån dimensionerades, byggdes och försågs med instrumentering för såväl korttidslaster (trafik) som långtidslaster (temperaturvariationer). De uppmätta värdena med avseende på såväl deformationer som pålspänningar visade relativt god överensstämmelse med FE-analys genomförd med jordparametrar beräknade enligt den tidigare svenska bronormen BRO94 (Kapitel 4, Paper III och Paper IV).

För att undersöka hur stålpålar påverkas av töjningsvidder flera gånger större än flyttöjningen, genomfördes deformationsstyrda försök där stålpålar ingjutna i betong böjdes. Försöken visade att en påle kan utsättas för upprepade töjningar många gånger större än flyttöjningen, och ändå klara hundratals cykler innan en utmattningsspricka börjar propagera (Paper V).

I Kapitel 5 föreslås en dimensioneringsmetod för stålpålar i broar med integrerade landfästen och slutligen besvaras och diskuteras i Kapitel 6 de ovan nämnda forskningsfrågorna, och framtida forskningsinsatser föreslås.

Nyckelord: broar, integrerade landfästen, stålpålar

Table of Content

Notations, symbols and abbreviations

Roman upper case letters

A	Cross-sectional area	[m^2]
A	Constant	[-]
B	Width of the abutment backwall	[m]
B	Constant	[-]
C	Detail fatigue category factor	[Pa]
C_1	Dimensionless parameters, used to calculate p_u.	[-]
C_2	Dimensionless parameters, used to calculate p_u	[-]
C_3	Dimensionless parameters, used to calculate p_u	[-]
C_i	Compression flange buckling factor	[-]
D	Diameter of pile	[m]
E	Modulus of elasticity	[Pa]
E_s	Modulus of elasticity of soil	[Pa]
E_p	Modulus of elasticity of pile	[Pa]
H	Distance between the neutral axis of the superstructure and the clamped section of the pile	[m]
I	Area moment of inertia	[m^4]
K	Soil pressure coefficient	[-]
K_a	Active soil pressure coefficient	[-]
K_0	At rest soil pressure coefficient	[-]
K_p	Passive soil pressure coefficient	[-]
L	Length	[m]
L_b	Bridge length	[m]
L_f	Minimum pile length	[m]
L_e	Equivalent cantilever length	[m]

M	Moment	[Nm]
M_p	Plastic moment	[Nm]
M_p'	Plastic moment resistance reduced because of	
	the simultaneous axial force in the pile	[Nm]
N	Axial load	[N]
N_c	Critical axial buckling load	[N]
N_d	Axial design load	[N]
N_f	Number of cycles until failure	[-]
N_u	Maximim axial factored load	[N]
Q_{ik}	Axle load	[N]
T	Temperature	[°C]
$T_{e,max/min}$	Max/min uniform temperature component	[°C]
U'	Non-dimensional buckling coefficient for piles in	
	soils where soil stiffness is constant with depth	[-]
V'	Non-dimensional buckling coefficient for piles in	
	soils where soil stiffness is linearly increasing	
	with depth	[-]
W	Elastic section modulus	[m^3]
Z	Plastic section modulus	[m^3]

Roman lower case letters

b	Width of pile	[m]
b	Fatigue strength exponent	[-]
c	Fatigue ductility exponent	[-]
c	Outstanding flange width or the web depth	[m]
c_u	Undrained shear strength in cohesive soils (cohesion)	[Pa]
e_0	Initial imperfection	[m]
f_y	Yield strength	[Pa]

k_{eh}	Equivalent uniform lateral soil stiffness parameter	[Pa]
k_h	Lateral soil stiffness parameter	[Pa]
l_c	Critical pile length	[m]
l_e	Embedded length of L_{equ}	[m]
l_u	Not embedded pile length	[m]
m	Slope of log-log S-N curve	[-]
n	Number of cycles, number of segments, number of piles	[-]
n_h	Coefficient of subgrade reaction	[N/m^3]
p	Soil pressure	[Pa]
p_a	Active soil pressure	[Pa]
p_p	Passive soil pressure	[Pa]
p_u	Ultimate soil pressure	[Pa]
q_k, q_{ik}	Distributed traffic load	[Pa]
t	Material thickness	[m]
t_d	Time measured in days	[days]
t_o	Constant	[-]
y	Horisontal displacement of pile	[m]
y_u	The ultimate pile displacement, further displacement will not increase the soil pressure against the pile	[m]
z	Soil depth	[m]

Greek letters

α	Constant	[-]
α	Adjustment factor for traffic load.	[-]
α_e	Thermal coefficient of a material	[°C^{-1}]
β	Constant	[-]
β	Adjustment factor for traffic load.	[-]
γ	Constant	[-]

Design of Steel Piles for Integral Abutment Bridges

γ	Unit weight of a material	[N/m³]
δ	Constant	[-]
δ_{px}	Horizontal displacement of the pile head along the x-axis of the pile that is associated with the plastic-moment resistance M_{py}	[m]
ε	Strain	[-]
ε_a	Strain amplitude	[-]
ε_f	Elongation at fracture	[-]
ε'_f	Fatigue ductility coefficient	[-]
ε_y	Yield strain	[-]
ε_{50}	Soil strain at half the ultimate shear stress	[-]
θ	Rotation angle	[-]
θ_i	Coefficient of inelastic rotation capacity	[-]
μ	Mean value	[-]
ρ	density	[kg/m³]
σ	Standard deviation	[-]
σ	Stress	[Pa]
σ_u	Ultimate tensile strength	[Pa]
σ'_f	Fatigue strength coefficient	[Pa]
ϕ	Soil friction angle	[°]
φ	Load factor	[-]
φ_{rc}	Resistance factor for compression	[-]
ψ	Reduction factor	[-]
Γ	Displacement magnification factor	[-]
$\Delta\varepsilon$	Total strain range	[-]

$\Delta\varepsilon_e$	Elastic strain range	[-]
$\Delta\varepsilon_p$	Elastic strain range	[-]
$\Delta\sigma$	Stress range	[Pa]
ΔL_b	Changes in bridge length	[m]
ΔT	Temperature range	[°C]
ΔT_E	Range non-linear temperature distribution	[°C]
ΔT_M	Range of linearly varying temperature component	[°C]
ΔT_N	Range of uniform temperature component	[°C]

Abbreviations

AASHTO	American Association of State Highway and Transportation Officials
AISC	American Institute of Steel Construction
EBT	Effective Bridge Temperature
FE	Finite Element
FEM	Finite Element Method
LRFD	Load and Resistance Factor Design
PC	Pre-cast concrete
RFSC	Research Fund for Coal and Steel
SBUF	Svenska Byggbranchens Utvecklingsfond

1 Introduction

1.1 Background

Figure 1 A leaking joint that has caused severe corrosion on the steel beams and bearings of the bridge in the left picture. Joints that need to be repaired or replaced cause much disturbance for traffic as shown in the right picture.

Infrastructure maintenance costs are constantly increasing, and bridges are no exception to the rule. It is thus interesting to find technical solutions that, in addition to low investment cost, require minimal maintenance. One way is to design bridges so that water is diverted from the bridge and to have as few parts as possible that require maintenance. Joints are generally a weak point of many bridges. When bridge joints start to leak, the water can find its way to the bridge structure. Water contaminated with road salt accelerates the natural decomposition processes such as steel- and rebar-corrosion and degradation of concrete. Bridges without joints are thus preferable. The definition of a bridge with integral abutments is not the same everywhere. In this thesis it means that the superstructure and abutment are built in one integral unit without joints and bearings. When a bridge abutment has a rotational joint (e.g. a bearing) but no transition joint it is called a semi-integral bridge. This thesis focuses mainly on integral abutments with one row of slender steel piles under each abutment, but bridges with integral abutments come in various shapes and configurations and some do not even have piles supporting them.

Integral abutment bridges are becoming more popular around the world, but the traditions differ from country to country, as described in Paper II. This leads to

different technical solutions for the same problem in each country and details even differ in neighbouring states in USA. To behave as desired during use, bridges with integral abutments are dependent on proper detailing and construction. The construction sequence is important (see Figure 2) because undesired stresses can be introduced if an unsuitable sequence is applied. Before the superstructure and the abutment are joined together as a unit it is important to place as much of the weight of the bridge as possible to avoid transferring rotation of the bridge end to the piles. Even after finishing construction of the bridge structure, to avoid unnecessary bending of the piles, it is important not to fill the embankment material against the bridge abutment-walls in an un-symmetrical sequence.
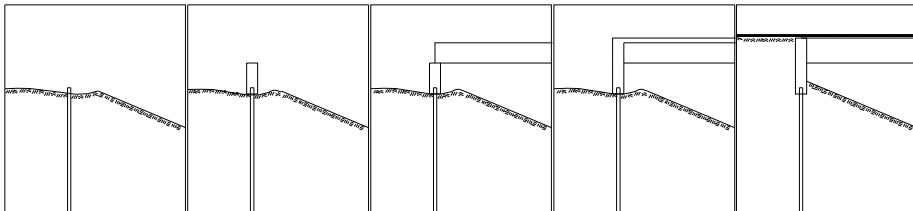

Figure 2 The sketches show the order in which a bridge with integral abutments should be built. First the piles are driven and the lower part of the abutment is cast. Then the beams are placed and the concrete slab is cast, beginning in mid-span. When the formwork is removed, the embankments can be filled and compacted at approximately the same rate at both abutments.

In Sweden, various concepts for building integral abutment bridges have been used. The most common bridge type in Sweden for short spans is a concrete frame bridge with integral abutments. Most of those bridges have short spans, less than 10 m, but some have spans up to 37 m and there are multi-span integral abutments of this type with lengths up to 120 m. For medium length bridges, 20 m-70 m, the most common bridge in Sweden is the semi-integral bridge. The research that has led to this thesis is however aimed at integral bridges with one row of slender steel piles under each abutment. In Paper IV the construction sequence for the bridge over Leduån is described. The sequence included the filling of a softer material around the pile tops in order to minimize the bending stresses in the piles due to thermal movements.

In 1999, research was started at Luleå University of Technology with the purpose of collecting experiences from the U.S. and the UK and transferring them to Swedish conditions. Since then at least 20 integral bridges with one row of piles under each abutment have been built in Sweden and a European research project INTAB (Feldman et. al. 2010) has been completed. Most of the bridges are short and it is the personal experience of the author that it is difficult to design integral abutment bridges that are longer than 40 m and at the same time avoid yielding in the piles at the serviceability limit state. The reason for this is that piles in integral abutment bridges can experience severe strains during service due to soil restraint and annual fluctuations in bridge temperature, which displace and rotate the ends of the piles that are clamped to the superstructure. These bending strains in the piles are not a consequence of load transfer from bridge to soil and could be eliminated by using a

hinged pile design. However, hinged piles are more expensive and might require frequent maintenance, making clamped pile joints preferable in practice. Most design codes do not allow strains exceeding the yield point at the serviceability limit state such as EN 1993-2 (CEN 2009b). This will limit the possibility to build longer integral abutment bridges founded on steel piles. EN 1990 3.4 (CEN 2010) states that "The limit states that concern: – the functioning of the structure or structural members under normal use; – the comfort of people; – the appearance of the construction works, shall be classified as serviceability limit states". None of these criteria are violated if the pile top experiences some inelastic strain. Some might consider the wording about appearance of construction work to be violated. One thing that could endanger a structure's functionality during normal use of piles is if there were to form fatigue cracks in the steel piles enhanced by accumulation of plastic strains. However most current codes do not prohibit plasticization of the pile cross section at the ultimate limit state, if the cross-section have enough rotation capacity. Since bridges are designed to be used 100 years or more (120 years is the normal design life for bridges in Sweden), the strains caused by the annual temperature variations should be considered as a low cycle fatigue problem. Low-cycle fatigue is not covered in the Eurocodes but in this thesis an attempt is made to give guidance how to handle the problem.

1.2 Purpose of the thesis

The aim of this thesis is to improve the design method for steel piles in integral abutment bridges. The intent is to enable the designer, with less effort, to make a safer or equally safe design as before, by using the methods described in this thesis. The thesis will therefore describe how the analysis and design of piles of an integral abutment bridge can be achieved.

To fully analyse the piles in a bridge with integral abutments, many load cases have to be considered and models with different parameters must be used. The modulus of subgrade reaction is an uncertain parameter and both high and low values should be considered. The steel pile will corrode with time and the effective cross section will be reduced. The soil behind the abutment will counteract the movement of the abutment when the abutment moves towards the soil, the stiffness of the soil can be different on each side of the bridge and thus different soil stiffnesses behind each abutment should be considered if relevant. To design the piles, at least two design situations must be studied; one causing the largest rotation (largest strains) and one causing the largest axial force (buckling and second order effects). The piles are analysed at the serviceability limit state and the ultimate limit state. At the ultimate limit state both static and fatigue load cases have to be considered as the traffic will cause stress variations in the piles. All of this gives a large number of load cases for different models and a time consuming job to analyse all design situations.

Bridges with integral abutments have a length limit that cannot be exceeded without causing problems of some sort. This length depends on a lot of parameters and a length limit cannot be generally set. One limiting factor that is stated in some bridge codes (e.g. EN 1993-2, CEN) is that the steel must not have strains exceeding the yield limit at the serviceability limit state. If this limit is applied to steel piles in integral abutment bridges it will limit the concept very much.

To be able to present a suggested design method for piles in bridges with integral abutments some questions need to be answered.

Research question 1: *Do integral bridges perform as expected under load and will the stresses/strains in the piles be as large in reality as expected according to the design codes?*

Research question 2: *How do the yearly temperature variations influence the static load-carrying resistance of the piles?*

Research question 3: *Is it possible to allow strains exceeding the yield point in steel piles and still have a safe design for 120 years?*

Research question 4: *What fatigue spectra can steel piles in integral abutment bridges be expected to experience, during their lifetime? What design criteria should be used for the piles?*

Research question 5: : *If yielding is allowed, what model should be used to analyse strains in piles, to verify the adequacy against low cycle fatigue?*

1.3 Limitations

Firstly, this thesis is limited to integral abutments with a single row of slender steel piles under each abutment. Other types, such as frame bridges, abutments on spread footings, abutments with piles that resist abutment rotation etc. are not discussed in depth.

Secondly, the focus of this thesis is on the design of the piles of integral abutment bridges and no other parts.

Thirdly, the focus of this thesis is on structural design and not geotechnical design, although the interaction with the soil is considered.

Fourthly, the top of the piles are assumed to be encased in an abutment of concrete.

1.4 Scientific approach

To achieve the objectives and answer the research questions of this thesis,

the following scientific approach has been used.

Step 1: Information about the status of the research and practice concerning bridges with integral abutments has been gathered. This has been done generally by performing the literature survey that is described in Chapter 2. The author has also been involved in the design work on three bridges with integral abutments as well as the planning, arrangement and reporting of an international workshop with participants from eight countries.

Step 2: The critical detail, i.e. the pile top, have been identified and the focus has been set on this detail.

Step 3: Experimental methods have been used to study the identified detail. The behaviour of the critical parts of the bridge has been tested in the laboratory and observed by field measurements.

Step 4: The experimental results have been evaluated and compared to FE-analyses and analytical models.

Step 5: The results from steps 1 to 4 are summarised by this thesis and areas for further research are pointed out and design criteria are suggested.

Step 6: An example design method has been presented.

1.5 Outline of the thesis

This thesis consists of six chapters, four appended papers published in peer-reviewed international journals (Papers II-V) and two appended conference papers (Papers I and VI).

In Chapter 2, a summary of the author's licentiate thesis is presented. The thesis was written in Swedish and there is no English summary in it and thus the English summary is included here.

In Chapter 3, the results from a literature survey are presented. International research around the world dealing with integral abutment bridges is discussed.

In Chapter 4, the design, construction and monitoring of the bridge over Leduån is described and discussed. The bridge was a part of the research project INTAB and the piles were designed by the author. Some results from the long-term monitoring are presented and discussed.

In Chapter 5, the design method suggested by the author is described and discussed.

In Chapter 6, general conclusions are drawn and topics for future research are suggested.

The first part of the thesis is ended with a reference list.

Furthermore six papers are appended..

1.6 Summary of appended papers

Paper I Pétursson H. and Collin P., Innovative solutions for integral abutments, 10th Nordic Steel Construction Conference 2004, Copenhagen (2004) pp. 349-359.

In paper I it is investigated whether cross shaped steel piles (X-piles) are suitable for use in integral abutment bridges and the conclusion was that the decrease in load bearing resistance due to rotations and translations of the pile top should not limit the use of these piles in integral abutments. The paper includes laboratory tests of X-piles on elastic foundation with transversal end deformation, simulating effect elongation/shortening of a bridge due to temperature variations. The piles were loaded axially to failure.

Paper II White H. 2nd, Pétursson H. and Collin P., Integral Abutment Bridges: The European Way, Practice Periodical on Structural Design and Construction, Vol. 15, No. 3, August 2010, pp. 201-208.

Paper II presents results from a European survey that was conducted in early 2007 to illustrate the design criteria used by each different country for Integral Abutment Bridges. The survey requested information useful to a designer comparing the design requirements and restrictions of various European countries. As an added measure of comparison, these results were compared to some recently conducted surveys of design practices in state agencies in the USA.

Paper III Pétursson H. and Kerokoski O., Monitoring and Analysis of Abutment-Soil Interaction of Two Integral Bridges, Journal of Bridge Engineering, Vol. 18, No. 1, January 2013, pp. 54-64

Paper III is divided in two parts. The first part is about field tests of two joint-less bridges, focusing on the magnitude and significance of earth pressure behind the abutments. This part is written by Olli Kerokoski. The second part is written by the author and describes some of the measurements done on the bridge over the Leduån. The bridge was fitted with strain and displacement gauges and short-term measurements were made using a loaded lorry. The field test results for this bridge were verified with calculations based on an abutment rotation stiffness calculation model developed during the research presented in this paper.

Paper IV Pétursson H., Collin P., Veljkovic M. and Andersson J., Monitoring of a Swedish Integral Bridge, Structural Engineering International, Volume 21, Number 2, May 2011, pp. 175-180(6)

In paper IV, results obtained while monitoring the Swedish bridge over Leduån are presented. The responses of the piles and the superstructure were measured for both

thermal and traffic loading. The results agreed well with calculations but the connection between the pile and the abutment did not seem be rigid.

Paper V Pétursson H., Möller M. and Collin P., Low-cycle Fatigue Strength of Steel Piles Under Bending, Structural Engineering International, Volume 23, Number 3, August 2013, pp. 278-284(7). This paper describes bending tests of clamped piles demonstrating that a steel pipe pile can accommodate large inelastic deformations under strains six times greater than the yield strain for several hundred load cycles.

Paper VI Hällmark R., Collin P., Pétursson H. and Johansson B. (2007) Simulation of Low-Cycle Fatigue in Integral Abutment Piles. IABSE Symposium – Improving Infrastructure Worldwide, September 19-21, 2007, Weimar, Germany

In Paper VI a model to simulate strain variations caused by temperature variations and traffic loads was created from real temperature data and traffic loads measured by Bridge-Weigh-In-Motion technology. Daily and annual temperature changes as well as the varying traffic loads were simulated by using the Monte Carlo method. Pile strains were calculated, and their fatigue effect were evaluated. The work was carried out as a M.Sc. project by Robert Hällmark supervised by the author and Prof. Peter Collin.

2 Summary of licentiate thesis

The authors licentiate thesis was written in Swedish. A summary of that thesis is presented in this chapter.

In the first chapter a short introduction to the concept of bridges with integral abutments is given and the purpose of the thesis is described. The purpose of the research project was to obtain knowledge of experiences that had been made in USA and UK and transfer them to Swedish conditions. The research questions that the thesis tries to answer are:

- How large are the costs for maintenance and replacement of joints and bearings?

- Is a bridge with integral abutments more economical than a conventional bridge in the long run?

- Can the steel piles withstand the strains that are imposed on them due to the rotation and displacement of the abutment?

The second chapter describes what the author learned from literature studies and from a study trip to USA.

The third chapter describes the laboratory tests that were conducted, in which two X-piles were tested for maximal axial load while displaced 25 mm transversely at the pile top (see Figure 3). The tests showed that the piles could reach the same load as was expected without the top displacement, for the given conditions.

Figure 3 Laboratory tests on specimen made of X-piles.

The fourth chapter describes different analysis methods for piles in bridges with integral abutments. Different soil models for soil-pile interaction analysis are presented.

The fifth chapter presents a parametric study conducted with FE-analysis. The parameters studied were initial geometric imperfection of the X-pile, soil stiffness and displacement. The FE-model was first calibrated to the tests (see Figure 4).The ultimate loads for 75 cases were determined with non-linear FE-calculations for the range of parameters.
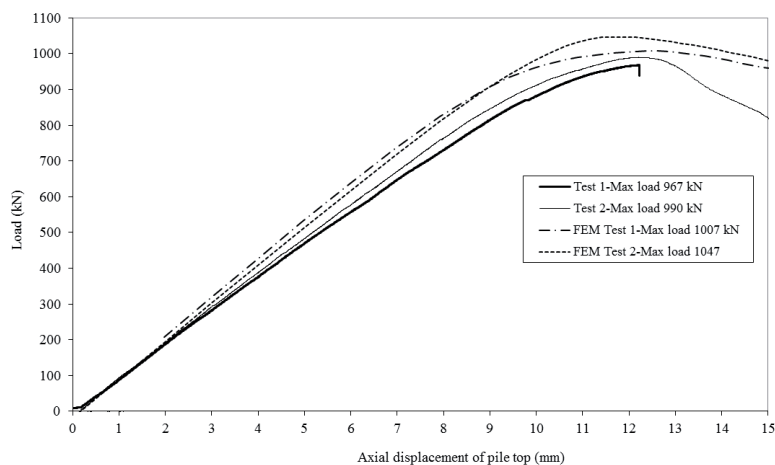

Figure 4 Results from FE-analysis compared to test results.

In the sixth chapter, the building of a Swedish bridge with integral abutments is presented. The bridge was the first of its kind in Sweden and parts of it, as the abutment piles, were designed by the author.

In the seventh chapter, a suggestion is given of how bridges with integral abutment could be designed and analysed.

In the eighth chapter, a comparison of costs for three similar bridges with different abutment designs is presented. The costs are for building and maintaining the bridges for 120 years. The bridges studied are 120 m long three-span composite bridges. One has integral abutments, one semi-integral abutments and the third is equipped with bearings and transitions joints at the end. It was concluded that about 13 % of the cost could be saved using the integral design compared to a bridge with transition joints and bearings.

3 Literature review

3.1 General

European experience with integral abutment bridges is significantly less than in USA, but the experience gained has been positive. As a result, the trend is that a larger percentage of newly constructed bridges across Europe has integral abutments. In Switzerland, many integral bridges were built during the period 1960-1985, which was the construction period of the national motorway network (Kaufmann et. al 2012). The majority of these bridges were concrete frames or strut frame bridges. In China not many bridges with integral abutments have been built to date but the concept is being introduce and in the years to come. There are projects being built and during 2014 Fozhou University arranged a workshop with international experts on the subject (Zhuang et. al. 2014).

Although integral abutment bridges have been built for more than 50 years, the design is usually not conducted according to precise theories. Experimentation, intuition and field observations have driven the development forward. Inspections of many bridges with damaged joints have shown that direct damage has not always had disastrous effect. The ability of piles and abutments to absorb thermal expansion has often been underestimated. This has meant that engineers have dared to build increasingly longer bridges without joints, despite analytical tools being absent or prohibitively time consuming. This is not the case everywhere. Some authorities demands accurate calculations to prove structural safety before a bridge is built. This is however a complicated task for piles under integral abutments as the interaction of elastic structural elements and the surrounding soil causes a number of uncertainties.

In the following chapter, a literature review on the subject of integral abutment bridges, especially those with steel piles supporting the integral abutments is presented and discussed.

3.2 Loading

Loads are the same for integral abutment bridges as other bridges and are in Europe specified by the Eurocodes and the relevant National Annexes. The Eurocodes that are applicable are EN 1991-1-1, EN 1991-1-4, EN 1991-1-5 and EN 1991-2 (CEN2009c, CEN2003a, CEN2003b and CEN2005b). Some actions cause displacement and rotations at the top of the piles and this gives unwanted strains in the piles that supports an integral abutment.

The stiffness behind the abutment relieves these effects to some extent, depending on material, confinement, water content and friction. It is therefore a rational approach to consider the earth pressure as a load with a permanent part, the at-rest earth pressure, and a variable part, the active and passive earth pressure. The difference between the active and the at-rest earth pressures is small and can usually be ignored. The difference between the passive and at-rest earth pressures are included in load cases that causes the abutment to displace and rotate into the embankment (when the bridge expands due to temperature rise, coupled with traffic loading).

3.2.1 Thermal actions

Two types of thermal actions need to be considered. First, a uniform temperature change, which means that the abutment is displaced horizontally. The magnitude of the bridge movement depends on the difference between the mean temperature of the structure at the time that the superstructure is locked to the abutments and in the design situation. Also, an uneven temperature distribution across the depth of the superstructure causes movements of the piles as the end of the superstructure rotates and cause a horizontal displacement of the pile top. The mean bridge temperature is dependent mainly on the ambient air temperature but also on wind and rain effects and solar radiation. Temperature gradients through the depth of the bridge beams generate bending of the superstructure and rotation of the end. The maximum temperature differentials (with positive gradient) occurs when the concrete deck slab is exposed to sun radiation during the summer and winter, resulting in a concrete deck slab that is warmer than the steel beams and thus the rotation of the end of the superstructure will occur in the opposite direction to that due to the traffic load. The minimum temperature differential (with negative gradient) occurs when the concrete deck slab is suddenly drenched with cold rain or snow, thus cooling the concrete deck slab at a faster rate than the steel beams. This will give rotation of the superstructure end in the same direction as the traffic load in the framed arrangement of an integral bridge. Sudden temperature changes will also affect the temperature in lower flange faster than the concrete slab thus creating a temperature gradient trough the superstructure.

The temperature of the bridge varies continuously (see Figure 5). The seasonal variations have the largest amplitude, but a small number of cycles. The design life

of a bridge in Sweden is set to be 120 years, which gives 120 stress cycles of annual temperature variations. The daily variations are more frequent and will induce $365 \times 120 = 43\ 800$ stress cycles. The ranges of these temperature cycles is not constant (see Figure 6).
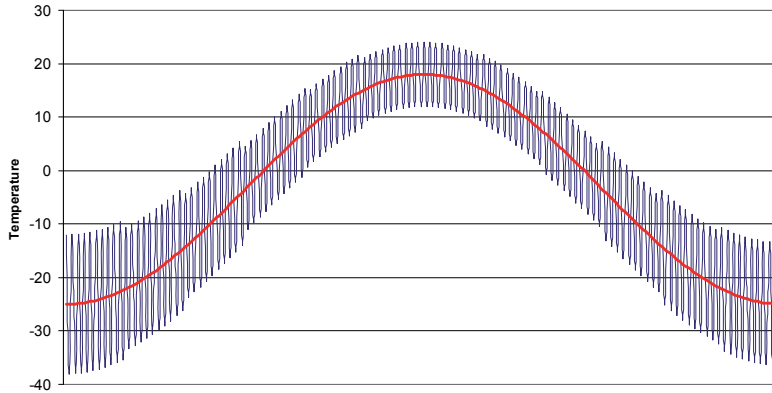

Figure 5Theoretical ambient temperature variation over one year. The black line represents daily changes and the red line the annual change (Hällmark 2006).
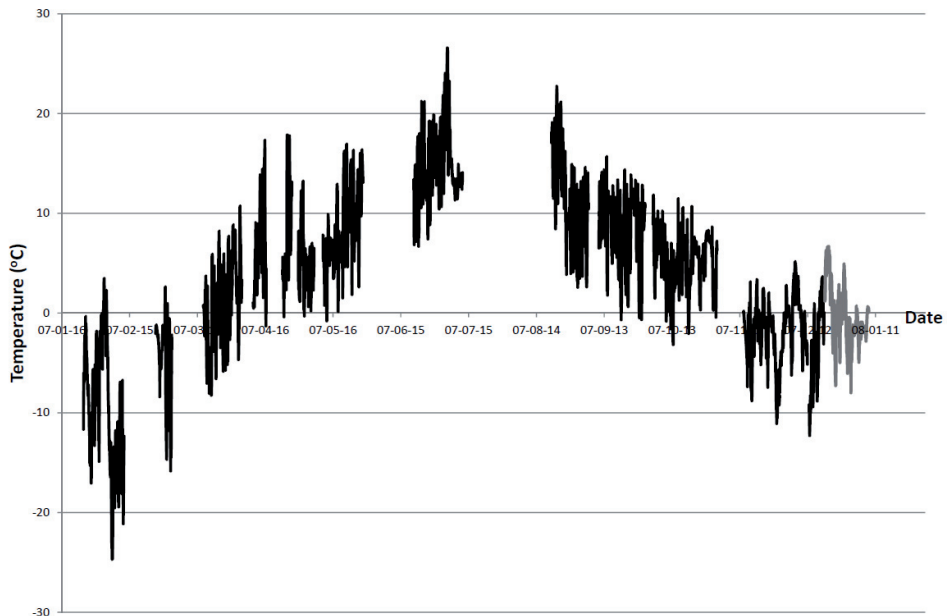

Figure 6 Air temperature variation during one year of monitoring the bridge over Leduån. Not all days are recorded, due to problems with the equipment.

It is not common to measure the bridge temperature and it is thus valuable to have models to estimate the bridge temperature from ambient temperature. The estimation

is mostly based on the shade air temperature but there are more sophisticated models (Fu et. al. 1990, Moorty et al. 1992 and De Jong et. al 2004). In Eurocode EN 1991-1-5 (CEN 2003) a diagram is presented to estimate the maximum and minimum uniform bridge temperature components $T_{e,min}$ and $T_{e,max}$ from the minimum and maximum shade air temperatures and this is reproduced in Figure 7.
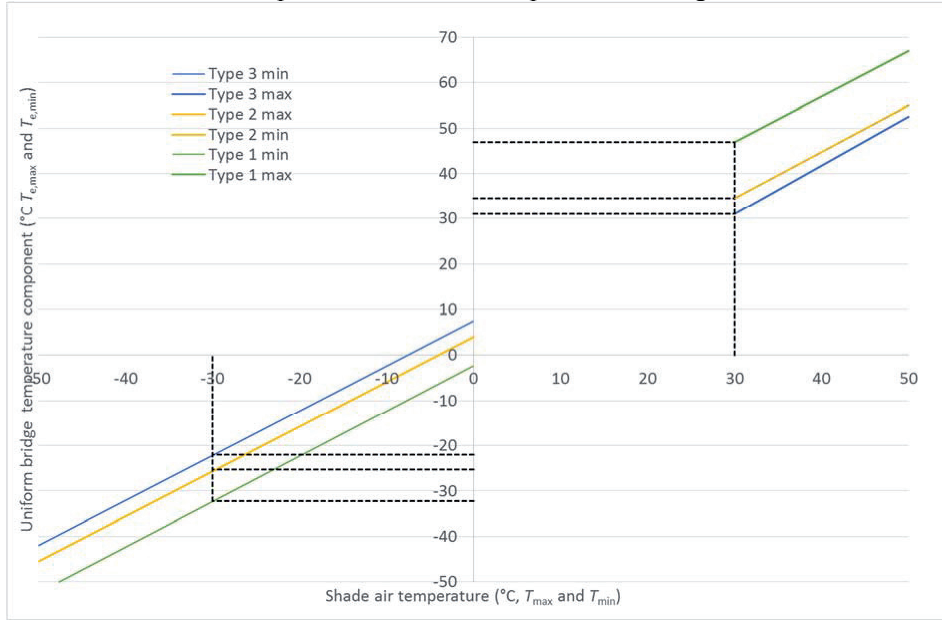

Figure 7 Correlation between minimum/maximum minimum/maximum uniform bridge temperature component(taken from EN 1991-1-5 (CEN) Figure 6.1).

Bridge decks are grouped in three different groups in Eurocode EN 1991-1-5 (CEN 2003b) for the purpose of differentiating between massive bridge deck that take longer time to heat and cool from lighter bridge decks that are more rapidly heated and cooled. The three groups are Type 1: Steel deck, Type 2: Composite deck and type 3: Concrete deck. As seen in Figure 7 the maximum/and minimum bridge temperatures are 5° C above the corresponding shade air temperatures for type 2 while the range is larger for Type 1 and smaller for Type 3. The overall range of the uniform bridge temperature is:

$$\Delta T_N = T_{e,max} - T_{e,min} \tag{1}$$

The shade air temperature used for design is a temperature with the annual probability of being exceeded of 0,02 or once in 50 years. As an example value for Stockholm, Sweden is T_{max}=36 ° C (TRVFS) and T_{min} =-29 ° C and the range of the bridge temperature thus becomes 65° C for a type 2 deck. As can be seen in Table 1 the maximum range of temperature within any one yearfor the past 52 years is 56.6° C (Moberg et. al. 2002) if instant values are used. If the daily mean temperature is used to calculate the annual temperature range, which is closer to the mean bridge

temperature, the maximal air shade temperature range is 46.6 ° C The design values can thus be regarded as conservative.

Table 1 Temperature measurements in Stockholm 1961-01-01 to 2011-12-31 (Moberg et. al. 2002). The measurements are updated continously.

| | Daily temperatures | | | | | Annual temperature ranges. | |
	T_{max}	T_{min}	T_{mean}	ΔT_{daily}	ΔT_{mean}	ΔT^{1}	ΔT^{2}
Max.	35.4	22.4	28.3	20.4	14	56.6	46.6
Min.	-22.1	-25.5	-23.9	0.3	0	32	23.5
Mean	10.5	4.1	7.1	6.3	1.7	45.8	36.1
Median	10.0	4.0	6.9	5.9	1.3	46.2	36.1

In Eurocode EN 1991-1-5 (CEN 2003b) the maximum and minimum temperatures are in Figure 7 based on daily temperature ranges of 10° C which is 13% of the maximal annual temperature range. Measurements in the UK (Emerson 1977) showed that the daily temperature range in a composite bridge were at most about 25% of the annual.

For integral abutment bridges the bridge temperature variations will cause strain variation in the piles that are substantial. An estimate for fatigue calculations should aim to give a constant value for the amplitudes that gives the same fatigue damage as the real case.

The author's estimate, which most likely is an overestimate, is that the daily variations give the same fatigue effect of the material as if the daily variations were of constant amplitude and 10% of the annual ones. It is estimated that 80% of the values given in Eurocode EN 1991-1-5 (CEN 2003b) is sufficient to use to calculate annual temperature ranges for fatigue calculation.

3.2.2 Traffic loading

Most of the published research/studies about integral bridge design that can be found in the literature are concerned with thermal effects and soil pressure behind the abutments. Not many studies have been made on the effect that the traffic load has on piles in integral abutment bridges.

---

[1] Calculated from maximum and minimum readings during one year.

[2] Calculated from maximum and minimum daily mean estimations during year.

Mourad et. al. (1998 and 1999) conducted a study by using a 3D FE-model to calculate the pile forces from gravity loads produced by two side-by-side HS20-44 lorries. Two bridges with different slab thickness and beam cross section were analysed. The bridges had 11 and 12 steel HP300×79 piles under each abutment. Two of those were under the free end of each wing-wall and the rest placed in one row under the abutment. The conclusion of the study was that the abutment wing-wall system did not act like a rigid block under truck load and the corner piles are not always the most heavily loaded piles. The bending moments in the piles are significant from truck load and cannot be neglected in design. It is the author's experience that the bending stresses from the traffic can be substantial. How large these bending stresses will become depends on the bridge geometry and detailing. The configuration of piles in the study, with a pile under the free end of the wing wall, is not usual in Europe. The wing wall pile could carry some of the load from the corner pile and that might be the reason that the corner pile was not the most loaded pile. With transversal loads added, due to wind and transverse breaking force, and truck load placed as far sideway as possible, the corner pile would always be the most loaded pile.

In the Eurocodes there are two load models for road bridges, representing the most severe traffic expected in practice on the main routes of European countries. There are two adjustment factors α and β to adjust the loads to differences between countries and different roads. Only one load model is described here as it is the only one that is used for pile design.

Load model 1 consist of two axle loads, Q_{ik}, and a distributed load q_{ik} with values in each lane according to Table 2. Each lane is 3 m wide and the distance between the axle loads is 1.20 m.
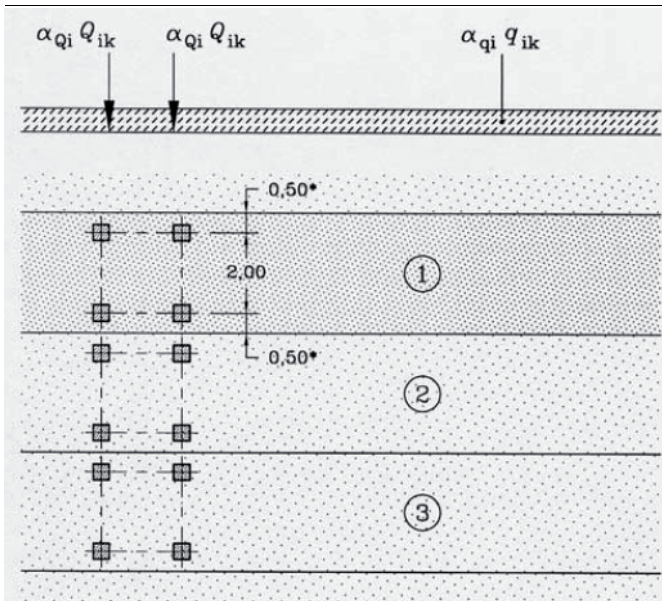
Figure 8 Traffic load model 1(EN 1991-2)

Table 2 Load values for traffic load model 1 (EN 1991-2).

Location	Tandem system TS Axle loads Q_{ik} (kN)	UDL system q_k(or q_{ik}) (kN/m²)
Lane Number 1	300	9
Lane Number 2	200	2.5
Lane Number 3	100	2.5
Other Lanes	0	2.5
Remaining area (q_0)		2.5

3.3 Structural details

Integral abutment bridge solutions are chosen to get rid of poor and maintenance-expensive details such as joints and bearings. But rain and snow will still fall on the bridge and details must be designed so that the water will find its way from the bridge with the least damage possible to the structure. The embankment behind the bridge will be pushed away from the bridge by the abutment in the summer when the bridge length expands and the soil pressure will increase. When the bridge length decreases in the winter, the soil pressure will decrease again. This will repeat every year and it is likely that a bump will form in the embankment adjacent to the bridge.

The piles of an integral abutment are attached to the abutment and the abutment is attached to the superstructure, so all displacements and rotations that occur at the end of the superstructure will transfer to the pile and cause bending moments and shear forces in the piles. Appropriate design of the details in an integral abutment bridge is vital to avoid problems. In the following chapter some of the details that are used in integral abutment bridges are reviewed and discussed.

3.3.1 Connection between superstructure and abutment

It is not only temperature that causes horizontal displacement of the pile top. All loads that cause beam end rotation will result in the pile top displacing horizontally.

In composite bridges, if the concrete deck is placed on the steel beams on site, the self-weight of the concrete is a significant load and will cause a relatively large rotation at the superstructure end. If the superstructure is locked to the piles before the concrete slab is cast, the strain in the piles will be unnecessarily large. To avoid rotations from the self-weight an integral abutment bridge should be built according to a scheme similar to Figure 2. The construction scheme affects how the dead loads are introduced into the piles and it is therefore important to plan the concrete casting for composite superstructures. Following the sequence in Figure 2, first concrete is cast around the piles. The beams can then be placed on the concrete block on top of the piles without introducing any rotation to the piles. To fix the bridge beams to the concrete block horizontally and vertically without restricting the rotation of the beam ends, different techniques are used. One is to place threaded rods in the concrete block to fix the beams. The beams are either placed on rubber cushions through which the threaded rod passes or onto a nut which is threaded on the rod and with a lock nut above the bottom flange (see Figure 9). The second option offers better adjustability in height and does not require the same precision of the cast surface. An alternative way to support the beams is to construct simple bearings between the steel beams and the concrete.
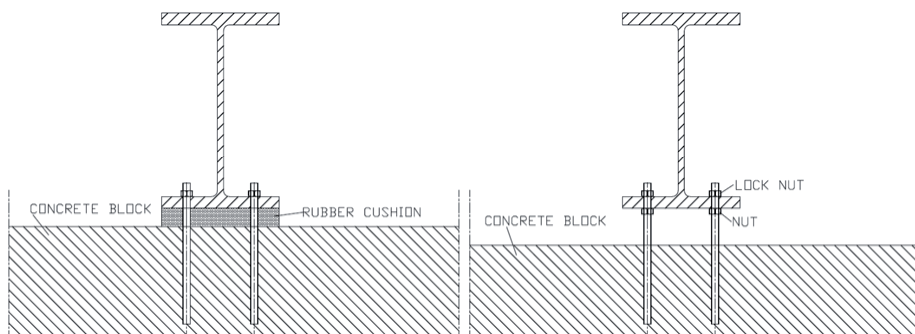

Figure 9 Support of bridge beam at an abutment during construction.. Threaded rods are used to fix the beam to the abutment. In the left figure the bridge beam sits on a rubber cushion and on the right beam sits on nuts threaded onto the rod.

The concrete slab is then cast allowing the bridge beams to rotate freely as the major part of the dead load is placed. The temporary supports of the steel beams are left in the concrete, without any further function.

3.3.2 Connection between abutment and pile

The connection between the abutment and the piles is often considered to be stiff, transferring all of the rotation from the superstructure to the piles. If the piles are stiff, the moment can be substantial and the connections have to be designed accordingly. This is the reason why many designers use slender piles in their design.

In many states in USA, integral abutments are constructed with H-shaped steel piles placed in a row and oriented to be bent around the strong axis when the abutment is subjected to thermal displacement. The reason for this orientation is that the piles ability to absorb thermal expansion is limited when bending in the weak direction, due local flange buckling (Abendroth et. al. 2005). Other states orient the piles to be bent around the weak axis on the basis that the thermal expansion will create lower internal forces from a pile that offers a smaller resistance. This has no relevance in the author´s opinion as the forces can be handled by appropriate design of the abutment.
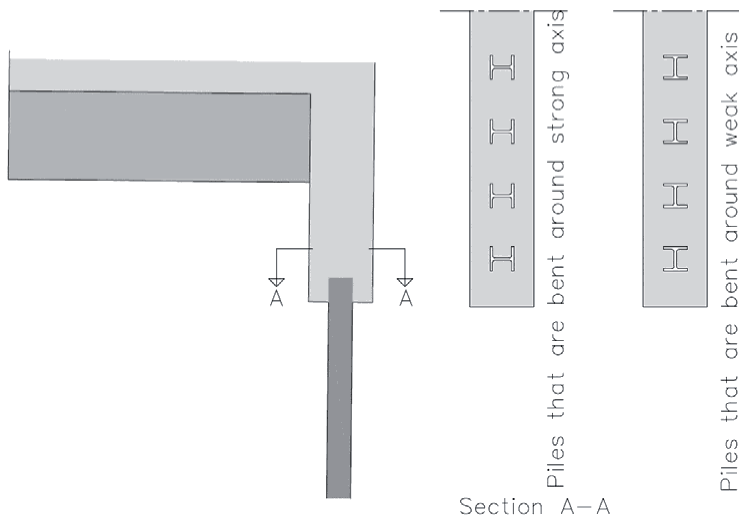

Figure 10 Piles oriented to be bent around the strong axis (to the left) and weak axis (to the right).

Ahn et. al. (2011) studied the connection between piles and abutment in bridges with integral abutments. Three types of new abutment pile connections were developed and analysed. The intention was to increase the stiffness of the connection. FE-analysis and half-scale loading tests were conducted. Only ultimate loads were

investigated and no conclusion regarding the fatigue resistance of the details in integral abutment bridges were drawn.

Some researchers have pointed out that the connection does not behave rigidly in all cases (Khodair 2004) and this can be beneficial as it lowers the bending strains in the piles.

3.3.3 Approach slabs

Since it may be difficult to achieve adequate level of compaction of material in the backfill, approach slabs are often used. Approach slabs have the benefits that they act as a bridge between the abutment and firmer compacted material behind the bridge. If there are differential settlements between backfilling and abutment the approach slab evens the difference over a greater distance. This makes the transition between the bridge and the embankment smother and the dynamic influence from the traffic load smaller. Carefully designed approach slabs help to dissipate water from the bridge preventing the water from pouring down to the filling just behind the bridge and thus preventing erosion of backfill material as well as freeze damage. Approach slabs are anchored to the abutment to prevent the approach slab separating from the bridge when it contracts and then falling off its support on the abutment. The approach slab is designed to rotate independently of the bridge.
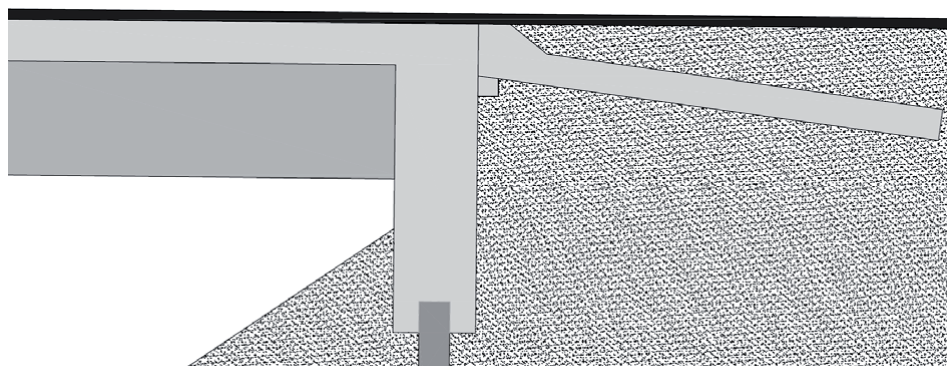

Figure 11 Inclined approach slabs that are buried in the embankment are commonin Europe.

In Europe, the most common design is to have an inclined approach slab that is buried in the embankment, see Figure 11. In the USA it is more common to have the approach slab above ground, as a bridge span between the bridge and a sleeper pad at some distance (the distance can be between 2 and 6 m) that is founded on densely compacted embankment. In Finland, Kerokoski (2006) monitored the earth pressure against the abutment on a bridge with buried approach slabs.

3.3.4 Replacing soil around pile top

One way to limit the stresses in piles in integral abutments, that seems to be used by many designers, is to replace the soil around the upper part of the pile with some

other softer material. Holes are prepared where the piles are driven, usually around 2 m deep, and the void around the pile head is filled with sand or some other soft material that is kept loose to limit the lateral support of the pile. There are not any studies available on how loose the material is in the end of a period of 120 years. One idea is to use a compressible material that will not be compacted as shown in Figure 12.

Arockiasamy et. al. (2004) reviewed the construction and design practise for integral abutment bridges. In the review a parametric study was conducted to investigate the effects of placing piles in holes where sand could be placed around the upper part of the pile. The parameters studied were different degree of compaction of the sand in the holes, elevation of water table, soil type and pile orientation. It was observed that only marginal increase in pile stress was obtained with dense sand in the hole and it was concluded that pre-drilled holes do not contribute significantly to stresses in the pile. Though the stresses in a pile in a pre-drilled hole are lower the pile length required will be greater. The water table elevation was shown to have very little significance on the response of piles in an integral abutment. Moment was, as expected, shown to be higher in piles in stiffer soils.
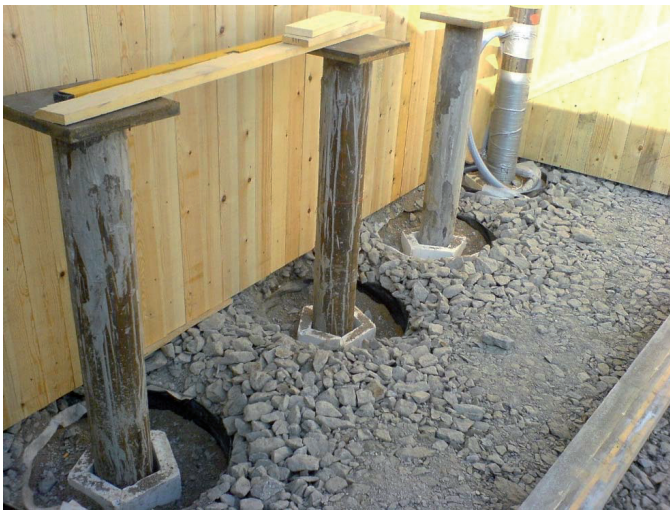

Figure 12 Piles placed inside metal sleeves of diameter 600 mm and depth 2 m. Styrofoam sheets are placed round the piles and the void is filled with sand.

Khodair (2004) studied the pile-soil interaction and the effectiveness of sand filled pre-drilled holes to limit the stresses in piles in integral abutments, the lateral earth pressure in the retained soil behind integral abutments and the buckling resistance of single piles in integral abutments. To do this, a bridge was instrumented and monitored and non-linear FE-models were developed. The monitored bridge was a 45.5 m long continuous bridge in two spans supported on 19 HP 360×152 steel piles under each abutment. The width was 33 m and the skew 15 °. The deck was a composite deck with ten steel girders and a reinforced concrete deck on top of them.

The piles were installed in 0.76 m diameter holes and concrete was poured in the holes around the piles over 60 % of the pile length or 7.62 m. Then a corrugated steel sleeve was placed on top of and supported by the concrete. The sleeves, which ended at the top of the piles, were filled with sand. Conclusions from the research were the following:

- A realistic soil model should be used when designing integral abutment bridges. The model should be based on experimental measurements.

- When designing piles in integral abutment bridges as beam columns one should divide the pile in two separate portions, divided at inflection points, and both should be designed as beam columns.

- It is very conservative to overlook the lateral support surrounding the piles when they are checked according to beam columns rules/equations. It is therefore recommended that FEM is used.

- The designer should avoid plastic strains in the piles by limiting the span of the bridge in which the detail is used, by increasing the number of supporting piles or by increasing the yield strength of the steel material used in the piles.

- It is desirable to reduce or to eliminate the skew of a bridge in order to reduce the non-uniformity of the pressure distribution behind the abutment.

The two last conclusion are not very realistic or economical. Some degree of skew and plastic strain must be handled to build economical bridges with integral abutments.

3.3.5 Embankment

Backfilling materials for integral abutment bridges are usually friction materials with good drainage capabilities. The material has to be well graded to facilitate compaction in confined areas. To prevent excessive settlements of the bank behind the abutment the material should be well compacted.

The soil behind the abutment resists longitudinal displacement from the temperature expansion in the bridge. It causes the bridge end to rotate and counteracts the displacement at bottom of the abutment. In the winter the abutment moves away from the embankment. But it has been shown that the bridge has a stiffer behaviour in the winter and the pile bending due to traffic load can be expected to be restrained by the frozen soil in the embankment to a larger extent than in summer. Research has also shown that the pressure over time will increase and it will become passive eventually after repeated cyclic movement of the abutment into and away from the embankment behind the abutment (Kerikoski 2006).

Diclei et. al. (2010) investigated what influence the backfill had on the internal forces due to traffic load. A structural FE 2-D frame model was used and the effect of

different parameters as bridge size, abutment height and thickness, pile size and orientation, number of spans and foundation soil stiffness was studied. It was found that it had a big influence on the results if the stiffness of the backfill was included in the structural analysis when analysing a bridge with integral abutments. This was not true for shear forces in the superstructure from traffic load, where the backfill stiffness had a negligible influence. The stiffness of the soil around the piles had no effect on the shape of the influence lines for traffic loads. For multiple span bridges the influence of the backfill stiffness on the internal forces are less significant. It was also found that the equivalent cantilever method does not yield reliable estimates except for shear forces in the superstructure when traffic loads are analysed. The soil stiffness was assumed to be linear in the analysis. The backfill was modelled with linear spring element in the analysis.

The effect of the embankment material is often taken into account in the analysis of the bridge by applying one permanent load representing the at-rest earth pressure and one variable load representing the passive earth pressure that develops at bridge elongation.

The earth pressure against the abutment from the embankment is usually calculated using theories developed by Coulomb (1796) or by Rankine (1857). The theories were developed for retaining rigid walls and are built around a coefficient of lateral earth pressure that is the ratio between horizontal and vertical earth pressure. The largest earth pressure will arise when the abutment moves towards the embankment and passive earth pressure forms. The passive earth pressure will grow as the abutment is moved back and forth and will eventually become higher than is anticipated by Rankine theory (Kerikoski 2006). But high passive earth pressure will decrease the bending in the piles. According to recommendations of Kerikoski (2006) one third of fully passive earth pressure could be expected at zero movement of the abutment.
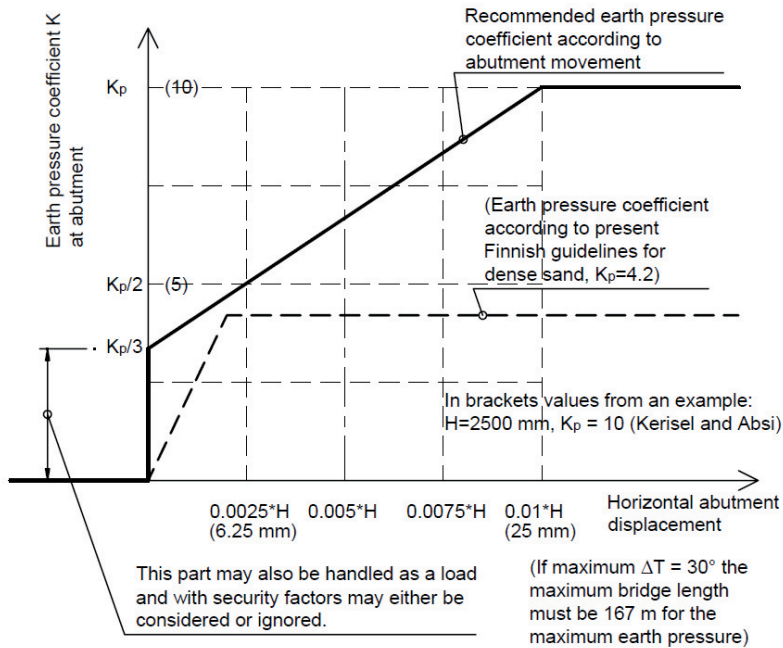
Figure 13 Recommended earth pressure coefficient based on abutment displacement.

3.4 Curved integral abutment bridges

Curved bridge beams can be beneficial for integral abutment bridges as the temperature expansion of the bridge can be radial to some extent and decrease the longitudinal displacement at abutments. Some of the longest integral abutment bridges are curved bridges e.g. Bridge over Happy Hollow Creek on State Route 50 in Tennessee and Sunniberg Bridge in Switzerland.

Curved integral abutment bridges were studied by Kalayci et. al. (2012). The investigation used a detailed 3D FE-model and a parametric study was conducted. A bridge in Vermont, USA, was used as study object, it is a bridge with two spans of 33.8 m and it has an 11.25° curve. Under each abutment, five steel HP 360×174 piles were placed in one row, oriented to be bent around the weak axis. Four different curvatures and loose and dense sands behind the abutment were studied by calculation with FEM. The investigation concluded that as the curvature was increased, in the FE-model, the weak axis bending of the piles decreased. Though the resultant stresses due to strong axis bending was low, interaction between strong and weak axis bending is recommended to be considered by the authors. A further conclusion was that U-shaped wing-walls can partially decrease the strong axis bending moments of the piles.

Figure 14 Sunniberg-Bridge in Switzerland (Picture by Dr. Ana M. Ruiz-Teran).

3.5 Length limits

The ductility, fatigue resistance or the effect of lateral displacement on axial resistance of the piles may limit the length of an bridge with integral abutments. It is not possible to have length limits that are valid for all cases. There are so many parameters that come into play; curvature, soil condition, skew, pile type, slenderness of superstructure, climate and material properties just to mention few. But some researchers have presented studies to decide length limits for integral abutment bridges. One is Diclei et. al. (2003 to 2005), who presented an analytical approach to determine length limits. The governing parameters were flexural strength and low cycle fatigue. The expression used for the low cycle fatigue was the same as was used by Razmi et. al. (2012). In the study, it was assumed that there were 52 small amplitudes for each annual temperature amplitude and that the small amplitudes were 30 % of the large ones. According to the model used by Diclei et. al (2003) the maximal strain amplitude that a pile can sustain is 0.004277 if the service life is 75 years. This corresponds to a strain amplitude 2.5 times larger the yield limit for

a pile in S355 steel (or a strain range of 5 times the yield limit). The conclusions from the studies were estimations of maximum lengths for integral abutment bridges, as shown in Table 3.

Table 3 Different length limits from different papers of Diclei. The piles that was studied were HP (from HP 200* 63 to HP 360*174) section in ASTM A36 steel.

	Steel	**Concrete**	
	(m)	**(m)**	
Diclei (2003)	100-160	190-240	Piles in sand
Diclei (2004a)	120-180	210-260	Piles in clay

Abendroth et. al (2005) presented an expression to calculate the length limit for integral abutment bridges with steel H-shaped piles. The expression is based on only the ductility requirements for the steel piles supporting the abutment. The bridge length is limited by the expression:

$$L \leq \frac{\varphi_{rc} 9 C_i \delta_{px}}{\Gamma \alpha_e \Delta T} \qquad (2)$$

φ_{rc} is a resistance factor for compression that is applied to the inelastic rotation capacity for the pile ($\varphi_{rc} = 0.85$),

C_i is a compression flange local buckling factor calculated with the following expression:

$$C_i = \frac{0.56 \sqrt{\frac{E}{f_y}} - \frac{b_f}{2t_f}}{0.25 \sqrt{\frac{E}{f_y}}} \qquad (3)$$

δ_{px} is horizontal displacement of the pile head along the x-axis of the pile that is associated with the plastic-moment resistance M_{py},

Γ is the displacement magnification factor that is based on a 98% statistical-confidence level to account for uncertainties in the expansion and contraction of a PC-girder bridge

α_e is the coefficient of thermal expansion and contraction

ΔT is the change in the average bridge temperature.

The limiting length will be the shortest length that is calculated for three cases; 1-maximum expansion, 2-maximum contraction and 3-maximum re-expansion.

3. Literature review

Abendroth et. al. (2005) calculated the length limits to be 245 m for a bridge with parameters according to Table 4. In Abendroth's approach, it is assumed that the bending stresses in the pile that the longitudinal displacement produce have no significant effect on pile load bearing resistance but the secondary $P\delta$ effects are accounted for.

Table 4 Parameters for bridge length limit calculation (Abendroth et. al. 2005)

Parameter	Value
Modulus of elasticity for pile material, E	200 GPa
Pile yield stress, f_y	248 MPa
Pile shape	HP 250×63
Pile effective length, shear	3581 mm
Pile effective length, moment	3658 mm
Soil unit weight	2225 kg/m^3
Friction angle	37°
Temperature variation Case 1, Γ=1.60	43.3° C
Temperature variation Case 2, Γ=1.35	49.4° C
Temperature variation Case 3, Γ=1.25	40.0° C
α_e	1.1*10^{-5}

A length limit based on just reaching yield at the serviceability limit state would give the following limiting displacement of the pile:

$$\delta = \frac{f_y W L_e^2}{6EI} = \frac{f_y b L_e^2}{6E2} = \frac{f_y}{E}\frac{L_e^2}{12h} \tag{4}$$

where b is the width of the pile, W is the section modulus and I is the area moment of inertia, all in the direction of the displacement.

But this is for a displacement that generates yield stress in the pile top. The pile will also be subjected to other stresses. Assuming that 50% of the stresses comes from other loads than temperature and that both abutments move the same distance for a given temperature change, the length limit can be derived from the following relationship:

$$\frac{L\Gamma\alpha_e\Delta T}{4} \leq \frac{f_y}{2E}\frac{L_e^2}{12h} \tag{5}$$

The figure four (4) in the dominator above allows for the displacement being equal at both ends and that the displacement from negative and positive temperature changes are equal. Using Abendroth´s parameter, the limit would be:

$$L \leq \frac{f_y}{E} \frac{L_e}{6\Gamma\alpha_e\Delta Th} = \frac{248}{200000} \frac{3658^2}{6 \cdot 1.35 \cdot 1.1 \cdot 10^{-5} \cdot 49.4 \cdot 256} = 20m \qquad (6)$$

Compared to Abendroths 245 m.

This example only is valid for the case with the exact parameters assumed for the example bridge but it shows how limiting the serviceability limit rules would be to integral abutment bridges, if applied. In other words, the limitation of not allowing strains exceeding the yield limit seems to be unnecessarily conservative.

3.6 Monitoring integral abutment bridges

Many bridges with integral abutments have been monitored during the last decades. Some of the findings from monitoring are described below.

In Finland a research project concerning integral abutment bridges was started in the 2003 and it has resulted in two Ph.D. theses (Laksonen (2011) and Kerikoski (2006)). In the project, three bridges were monitored and focus was on earth pressure from the embankments behind abutments. It was concluded that, though it is possible to build long integral abutment bridges, regular pavement maintenance cannot be avoided for bridges with more than about 40 m bridge length and 2.5 m high abutment wall. This might be acceptable for road bridges but is a problem for railway bridges where the tolerances are smaller regarding the vertical positionof the rail. Some of the work is described in Paper III.

In Rochester Minnesota, a concrete bridge with integral abutments was monitored for a little more than seven years (Huang et. al. 2004). More than 150 gauges were placed on the bridge during construction. The bridge was a pre-stressed concrete bridge with three spans of 21.5 m length. Six HP 310×79 piles were driven under each abutment, oriented to be bent around the weak axis as the bridge lengthened or shortened due to temperature variations. Huang et. al. (2008) also conducted a parametric study to extend the results that were obtained during the monitoring. The parameters that were investigated were, among others, pile type, size, orientation and depth of fixity. The investigation concluded that cast in-place concrete piles were not recommended because of the large concrete stresses they cause in the superstructure. H-piles oriented for strong axis bending (from thermal loading) improved the behaviour of the piles but increased the concrete stresses in the superstructure, compared to piles oriented for weak axis bending. It was also concluded that stiffer soils surrounding the piles resulted in larger pile stresses.

Kim et. al. (2012) summarises the monitoring of four integral bridges over periods between 2.5 years and 7 years, starting in 2002. The bridges were between 62 and

420 m long, with span lengths between 18.9 m and 122 m. All abutments were supported by HP310×110 steel piles. The study concluded that the abutments moved significantly over time. Abutments in all four bridges showed highly non-linear and irreversible displacements. The backfill pressure for all bridges reached their passive earth pressure.

Pugasap et. al. (2009) presented an analytical, long term, response prediction methodology and compared results to the measured response. The measurements included abutment displacement, strains in girders, soil pressure against the abutment and ambient temperature. It was concluded that 2D modelling was sufficient in predicting the long-time behaviour of an integral abutment bridge. Displacement comparisons with a more complex 3D model differed by less than 6 % on average. It was also shown that the accumulation of abutment displacement was significant the first three years and continued for approximately 30 years, after which the accumulating effect dissipates. The long term displacement were 1.5 to 2.3 times the calculated short time displacements. It was also concluded that an increase in girder age (concrete) will significantly lessen the abutment displacement, especially at the top of the abutment.

Fennema et. al. (2005) investigated uncertainties of integral abutment bridge design and analysis through monitoring of a bridge and parametric studies with FEM. The monitored bridge was a 52.4 m long concrete bridge with four pre-stressed concrete I-beams. The bridge had three spans of 14.3m, 26.8 m and 10.7 m length (total length 51.8 m) and was supported by 8 HP 310×10 steel piles at each abutment. Both 2D and 3D models of the bridge was built and results from analysis with the two models were compared. A comparison was also made for three different lateral loaded pile models one with a commercial FE-program with pile model as a beam element and soil as multi-linear springs, and one with the pile analysis software COM624P and one with the same software as the first but with linear springs. It was concluded that use of a FE-model with soil modelled as multi-linear springs is a valid approach that eliminates many assumptions and numerous iterations. Pile responses using 2D and 3D numerical models is similar and the extra effort of performing 3D analysis is not needed. It was also concluded, both from monitoring and FE-analysis,that the primary movement was not horizontal displacement but rotation about the base of the abutment.

In Massachusetts, USA, a three span 82 m long bridge with integral abutments was monitored during three years (Breña et. al. 2007). The bridge was also modelled in 2D and 3D and non-linear FE-analysis was performed to make a parametric study (Bonczar et. al 2005). The parameters that were studied were, among others, the effects of pile yielding and pile design assumptions. It was concluded that there was no yielding in the piles and that the equivalent cantilever method provided a reasonable approximation of the moment in the bridge that was studied. It was also concluded that the abutments move rigidly and the displacement can defined by a translation component and a rotation around a point near the base of the abutment. The rotations and translations of the abutment were different every year. The

moments in the piles were lower than the ones corresponding only to translation because the moments from the rotations had opposite sign.

In Oklahoma, a 63.8 m three-span integral abutment bridge with 10° skew was monitored for a year (Kirupakaran et. al. 2012). The bridge has two lanes and seven HP 250×63 steel piles support each abutment. The superstructure consists of four steel girders supporting a concrete slab. The temperatures during the year varied between -10.5° C and 41.4° C (ΔT=51.9 ° C).

On Hawaii, steel H-piles are not used and therefore integral abutments are preferred supported on concrete piles cast in situ in drilled shafts (Phillip et. al. 2010). In the northern part of the island of Oahu, a 24.4 m long and 17 m wide concrete bridge was built and monitored for 45 months. The single-span bridge was supported on five piles in one row under each abutment. The piles were step-wise tapered and the dimensions were 0. 9 m at the pile tip and 1.22 m at the pile top and a distance of 4.4 m down the pile. Among the results from the study that is of interest here is that the pile head did not behave as fully fixed even though the drilled shaft reinforcement extends all the way up the abutment wall.

In Germany, (Pak 2012), a composite integral abutment bridge with two spans (32 m + 26 m) and two main girders was monitored as a part of the INTAB project (Feldman et. al. 2010). The displacements and rotations of the abutments and the bridge temperatures were measured. From the monitoring, results the conclusion was that the earth pressure from the embankment did not influence the displacement of the abutment to any larger extent.

3.7 Laterally loaded piles

3.7.1 Introduction

To analyse piles load bearing resistance with simultaneous lateral displacement, is complicated because it deals with interaction between elastic structural elements and the surrounding soil. The problem is further complicated by the fact that most naturally occurring soils are inhomogeneous and that a disturbance in the soil continuum is created when a pile is installed. Traditionally, analyses are based on empirical methods derived from results of full-scale tests of horizontally loaded piles.

A lot of research has been performed to develop models that can predict the behaviour of a pile subjected to transverse loads (e.g. Broms 1964, Burdette 2004, Reese 1974 and Meyer et. al. 1979). Two main approaches have emerged: one is to regard the pile in an elastic continuum and one where the pile is regarded as a beam on discrete springs.

The soil modelled with discrete springs originates from the work on beams on elastic foundation by Winkler, 1867. In Winkler´s model the pressure, *p*, in a point along a

beam is only dependent of the deflection, *y*, in that point and modulus of subgrade reaction, k_h (force/length³).

$$p = -k_h y \tag{7}$$

The model ignores that the soil is a continuum; it is assumed that soil pressure in one point does not affect the soil at other points along the pile. Piles are considered as beams and to calculate deflections, moment and shear forces an element of the pile is studied as shown in Figure 15. The equilibrium of moments of a pile element leads to the equation (Euler-Bernoulli):

$$(M + dM) - M + Ndy - Vdz = 0 \rightarrow \frac{dM}{dz} + N\frac{dy}{dz} - V = 0 \tag{8}$$

By differentiating with respect to *z* the following equation is obtained:

$$\frac{d^2M}{dz^2} + N\frac{d^2y}{dz^2} - \frac{dV}{dz} = 0 \tag{9}$$

Recognising that $\frac{d^2M}{dx^2} = EI\frac{d^4y}{dx^4}$, $\frac{dV}{dx} = p$ and $p = -k_h y$ he following differential equation has to be solved:

$$EI\frac{d^4y}{dz^4} + N\frac{d^2y}{dz^2} + p = EI\frac{d^4y}{dz^4} + N\frac{d^2y}{dz^2} + k_h y = 0 \tag{10}$$

where y is the lateral displacement of the pile at the depth *z* below the surface of the soil. *EI* is the flexural stiffness of the pile, *p* is the soil pressure against the pile, k_h is the modulus of subgrade reaction, a measure of the stiffness of the soil and *N* is the axial load in the pile.
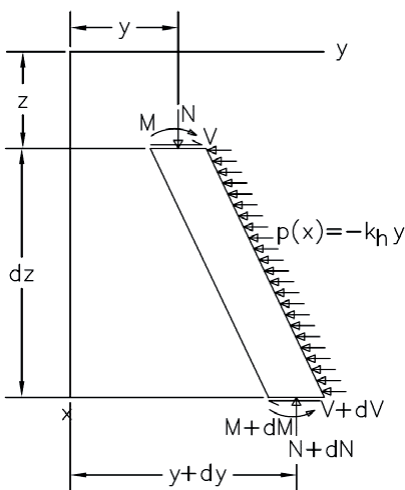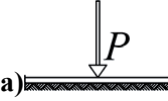

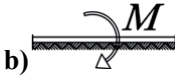*Figure 15 An element of a pile.*

The solution to the above equation is dependent on the assumption that is made regarding the variation of the modulus of subgrade reaction, k_h, with depth. The solution can be found either analytically or numerically. Analytical solutions are only possible in a handy form if k_h is a constant that does not vary along the pile. But most soils behave nonlinearly with respect to lateral displacement and also vary with depth. Iterative numerical solutions must thus be used.

For the most elementary case where soil and pile material can be regarded elastic, the formulas for springs on elastic foundations can be used to calculate displacements, rotations, moments and shear forces. The analytical solutions for infinite beams are used for cases where the pile top is restricted from rotation or displacement and semi-infinite beams are used for cases with pinned pile top with a point load or point moment applied at the pile top shown in Table 5.
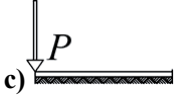
Table 5 Solutions of the differential equation for beams on elastic foundation for the cases a) point load on infinite beam, b) moment on infinite beam, c) point load on semi-infinite beam and d) moment on semi-infinite beam.

	a)	b)	c)	d)
y	$y_0 \alpha$	$-\theta_\theta L \beta$	$\dfrac{2P}{k_h L} \delta$	$-\dfrac{2M}{k_h L^2} \gamma$
$\acute{y}$	$\dfrac{-y_0}{L} \beta$	$-\theta_\theta \gamma$	$-\dfrac{2P}{k_h L^2} \alpha$	$\dfrac{4M}{k_h L^3} \delta$
M	$\dfrac{-L^2 k_h}{2} \gamma$	$\dfrac{-L^3 k_h}{2} \delta$	$-PL\beta$	$M\alpha$
V	$-k_h L \delta$	$\dfrac{-k_h L^2}{2} \alpha$	$P\gamma$	$-\dfrac{2M}{L} \beta$

The following functions are used in cases where the axial force is neglected:

$$L = \sqrt[4]{\frac{4EI}{k_h}} \tag{11}$$

$$\alpha = e^{-\frac{z}{L}}\left(cos\left(\frac{z}{L}\right) + sin(\frac{z}{L})\right) \tag{12}$$

$$\beta = e^{-\frac{z}{L}}sin(\frac{z}{L}) \tag{13}$$

$$\gamma = e^{-\frac{z}{L}}\left(cos\left(\frac{z}{L}\right) - sin(\frac{z}{L})\right) \tag{14}$$

$$\delta = e^{-\frac{z}{L}} \cos\left(\frac{z}{L}\right) \tag{15}$$

and z is the depth under the soil surface.

For piles where there is an axial force present the solution can be written in the same way as in Table 5 but with the length L and α, β, γ and δ are changed and expression for this can be found in Svahn et. al. 2006.

The cases above are only valid for cases where the modulus of subgrade reaction is constant with depth and linearly dependent on the lateral displacement of the pile.

For cases where the soil stiffness reaction increases linearly with depth it is convenient to define the coefficient of subgrade reaction as:

$$k_h = n_h z \tag{16}$$

where n_h is the constant of horizontal subgrade reaction (force/length^3). Factors, such as soil stiffness varying with depth and soil layers with different properties, may be considered using numerical methods such as finite difference method or the finite element method or special computer programs developed for pile design. It is also possible to calculate an equivalent constant soil stiffness along the pile and use with analytical solutions (Greiman et. al. 1987). All the above mentioned methods are still treating the soil as elastic springs. In reality the soil behaves highly nonlinearly in most practical applications and the practising engineer needs to apply nonlinear analyses or make conservative approximations. For the nonlinear analysis load-displacement curves for nonlinear springs must be decided as is described in section 3.7.2.

3.7.2 Parameters of soil surrounding the piles

The properties of the soil surrounding the piles are of great importance when the actions on the piles are to be calculated. Places where piling for bridges is considered often consist of soft soils. Because the properties of natural soils are uncertain and have a large variation it may be adviseable to make safe assumptions and make analyses for several cases.

In order to be able to predict how a pile will behave in an integral abutment, a material model for the soil around the pile is needed. A number of soil models have been suggested in order to be able to calculate the bending moment and deflection, as a function of depth, of piles subjected to lateral loads. Linear elastic methods are not generally applicable because the nonlinear behaviour of soil parameters. Soil reaction can be described by three types of dependencies: force-displacement relation in the horizontal direction along the pile, the force-displacement in the vertical direction along the pile (friction and cohesion) and the load-displacement relation for the pile tip in the vertical direction. A number of researchers have attempted to correlate the theoretical lateral load-displacement expressions with the results from

soil samples subjected to laboratory tests (Meyer and Reese 1979). Poulus (1971) developed methods where the soil was modelled as a continuum with linear elastic properties. In other models the soil is represented by discrete springs that have properties that correspond to the properties of the soil (Broms 1964, Meyer and Reese 1979). The springs can have an infinitesimal small distance between them but are uncoupled. The correlations that are produced often have the form:

$$p = \frac{k_h y}{1 + \left(\frac{y}{y_u}\right)^{\frac{1}{n}}} \tag{17}$$

The relationship between the pressure, p, and the pile displacement, y, is not linear when the pressure is approaching the maximum pressure that can be mobilised against the pile. It is not unusual for the displacement to be so large that the soil response is clearly nonlinear. It can therefore be important to take into account the nonlinear behaviour of the soil when analysing piles in integral abutment bridges. This can be done in different ways. One way is to regard the soil as a perfect elastic-plastic material. The soil will then theoretically behave perfectly elastically, which is represented by the modulus of subgrade reaction, k_h, until the ultimate soil pressure, p_u, is reached where after the pressure is constant regardless of how large the horizontal displacement of the pile, y, is.

The operating line is regarded to behave in the same manner in both direction. This does not mean that there can be tension stresses in the soil but that the other side of the pile is pressured when the pressure becomes negative. If the pile is surrounded with clay it is possible that a void is created behind the pile as it is displaced and when elastic de-loading occurs the void will not be completely closed when the pressure drops to zero again. The pressure will then be zero until the pile reaches is original position before the pressure on the back side of the pile begins to rise. An operation line as described is of course a rough estimate and modulus of subgrade reaction and limiting pressure for design must be chosen carefully to be safe.

According to the Eurucodes (7.7.3 in CEN 2009d) "The calculation of the transverse resistance of a long slender pile may be carried out using the theory of a beam loaded at the top and supported by a deformable medium characterised by a horizontal modulus of subgrade reaction." There is no guidance how to obtain the modulus of subgrade reaction and it is up to the designer to decide a suitable model from experience and literature. Some models from the literature are descired in sections 3.7.2 and 3.7.4

3.7.3 Soil with cohesion (clay)

If the soil surrounding the piles is considered to be an elastic continuum with Young's modulus E and Poisson's ratio of 0.5 the lateral modulus of subgrade reaction, k_h, can be derived e.g. according to Baguelin (1997).

$$k_h = \frac{0.65E_s}{1-v^2}\left[\frac{E_sD^4}{E_pI_p}\right]^{\frac{1}{12}} = 0.867E_s\left[\frac{E_s64}{E_p\pi}\right]^{\frac{1}{12}} \tag{18}$$

If the modulus of elasticity is taken as $E=50c_u$, where c_u is the cohesion the lateral modulus of subgrade reaction can be written:

$$k_h = \frac{k_0 c_u}{b} \qquad 157 \le k_0 \le 242 \tag{19}$$

where b is the width of the pile and c_u the cohesion.

For long term loading the creep effect must be considered. This is done approximately by reducing the lateral soil stiffness:

$$k_h = \frac{50c_u}{b} \tag{20}$$

The pressure p is limited to a value p_u that for drained conditions can be calculated by:

$$p_u = N_c c_u \tag{21}$$

where N_c is a constant that varies between 8-12 for deep soil layers (<3b) and decreases to 2 for layers closer to the surface. For short term loading $N_c=9$ can be used and for long term loading the creep is considered by a lower value of $N_c=6$.

To describe the non-linear behaviour of soft clays in a more nuanced way, Matlock (1970) suggested a load-displacement relationshp that, besides the limit displacement value for the soil pressure against the piles as described earlier, also the displacement at half the limit pressure should be calculated according to Skempton (1951):

$$y_{50} = 2.5\varepsilon_{50}b \tag{22}$$

where ε_{50} is the strain at half the ultimate shear stress according to Skempton (1951) and b is the width of the pile. The strain ε_{50} is not a parameter that is routinely measured during the geotechnical assessment before the bridge is built but the Table 6 can be used as a guide for choosing the value from the known cohesion, c_u.

The load-displacement curve can then be written as:

$$p = \frac{1}{2}\left(\frac{y_{tot}}{y_{50}}\right)^{\frac{1}{3}} \; ; p \le p_u \tag{23}$$

where y_{tot} is the pile displacement relative the soil.

The elasto-plastic model will reach the limit pressure at smaller pile displacements than what the model suggested by Matlock (1970) will and this difference is large for softer clays.

Table 6 Guidance to choose value for ε₅₀ (Svahn et. al. 1996).

c_u [kN/m^2]	ε_{50}
10-25	20
25-50	10
50-100	7
100-200	5
200-400	4

3.7.4 Cohesion-less soil (friction soil)

In the following section, three methods for determining the load-displacement curve of a typical cohesion-less soil are considered and the results presented in Figure 20.

For cohesion-less soils there is no unambiguous expression that describes the relation between the lateral modulus of subgrade reaction and the strength parameter ϕ'. The relationship between lateral displacement and soil pressure against the pile is therefore based on suggested empirical load-displacement curves based on experimental data. There are numerous suggestions on different load-displacement curves among them are Reese (1974). The load-displacement curves are non-linear.

To calculate the limit pressure that can occur when a pile deflects in soil Reese et al. (1974) suggested following expressions that are derived with a wedge-like failure mode and Mohr-Coulumb failure criterion.

$$p_u = \gamma z \left[\frac{K_0 z \tan(\emptyset)\sin(\beta)}{\tan(\beta - \emptyset)\cos(\alpha)} + \frac{\tan(\beta)}{\tan(\beta - \emptyset)}\left(D + z\tan(\beta)\tan(\alpha)\right) \right. \tag{24}$$
$$\left. + zK_0\tan(\beta)\left(\tan(\beta)\sin(\beta) - \tan(\alpha)\right) - K_a D \right]$$

where ϕ, β and α are soil parameters for cohesion and γ is the unit weght of the soil.

For soil under the water table the submerged unit weight γ' should be used.

At some depth below the soil surface, the soil will flow around the pile and instead of a wedge like failure mode a shear failure of surfaces in the soil are formed so that blocks of soils can move around the displaced pile, for this mode the following expression was derived by Reese et al. (1974) for this case:

$$p_u = DK_a\gamma z(\tan^8(\beta) - 1) + DK_0\gamma z\,\tan(\emptyset)\tan^4(\beta) \tag{25}$$

At the depth where expressions (24) and (25) are identical there is a transition: expression (24) is valid above this point and (25) under this point.

3. Literature review

When tests where made to verify the theoretical model shown above by Cox et al. (1974) a poor correlation was found and correction factor was developed, as shown in Figure 16. As can be seen in the figure, the discrepancies are smaller for cyclic loads and decreases with depth.
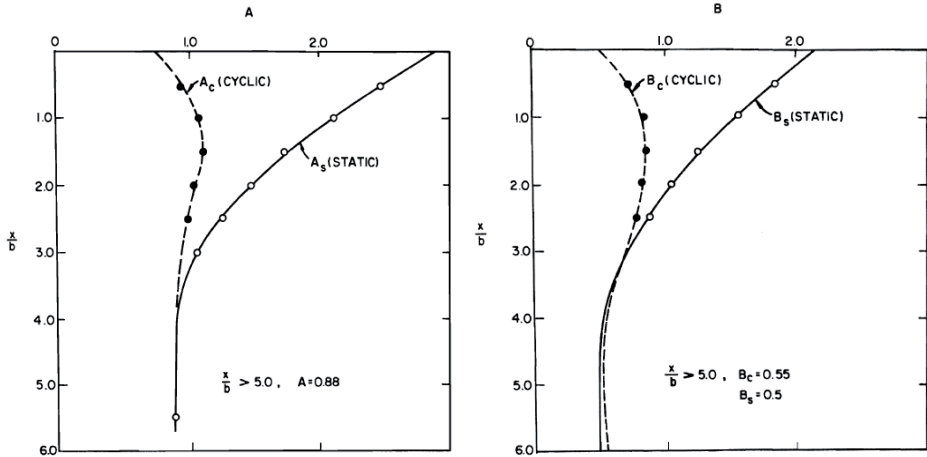

Figure 16 Correction factors vs. depth of slender piles (Reese et. al. 1974).

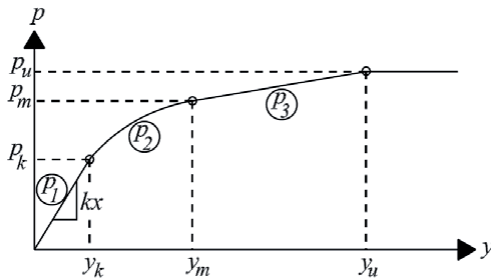The load-displacement curve for cohesion-less soils can be described with three parts as shown in Figure 17.

Figure 17 Typical load-displacement curve for cohesionless soil (Reese et. al. 1974).

The first part is linear with the modulus of subgrade reaction derived from Figure 19 or Table 7. The third part is also linear between the points of *(y=D/60, p=Bp_u)* and *(y=3D/80,p=Ap_u)*. In these expressions *A* and *B* are the corrections factors shown in Figure 16 The second part between the linear parts is non-linear and described by the equation:

$$p = Cy^{\frac{1}{n}}$$

(26)

$$n = \frac{BP_u}{m\, D/60} \tag{27}$$

$$C = \frac{BP_u}{\left(\dfrac{D}{60}\right)^{\frac{1}{n}}} \tag{28}$$

$$m = \frac{240P_u(A - B)}{5D} \tag{29}$$

Table 7 Values for the constant k_s for lateral modulus of subgrade reaction according to Reese et. al. (1994).

	Water saturated sand [MN/m³]	Sand above water table [MN/m³]
Loose sand	5	7
Medium dense sand	16	24
Dense sand	34	61

The procedure of obtaining load-displacement curves as described above is very tedious and it is based on very few tests and it is questionable whether it is suitable for design purpose for integral abutment bridges.

O'Neill and Murchison (1983) proposed a simplified method for sand load-displacemenet curves that are approximated using the dimensionless parameters C_1, C_2 and C_3. The maximum pressure against the deflected pile in the upper part where a wedge like soil failure is likely to take place is calculated by:

$$p_u = \gamma z(C_1 z + C_2 D) \tag{30}$$

And at some depth where the soil will flow around the pile and the soil failure is in the form of shear planes the maximal pressure is calculated with following expression:

$$p_u = \gamma z C_3 D \tag{31}$$

The results from expression (30) and (31) will give the same results as expression (24) and (25).
And the load-displacement curve can be calculated with the expression:

$$p = A\, p_u \tan\left(\frac{n_h z}{A p_u} y\right) \tag{32}$$

and for calculating A the following simplified expression can be used:

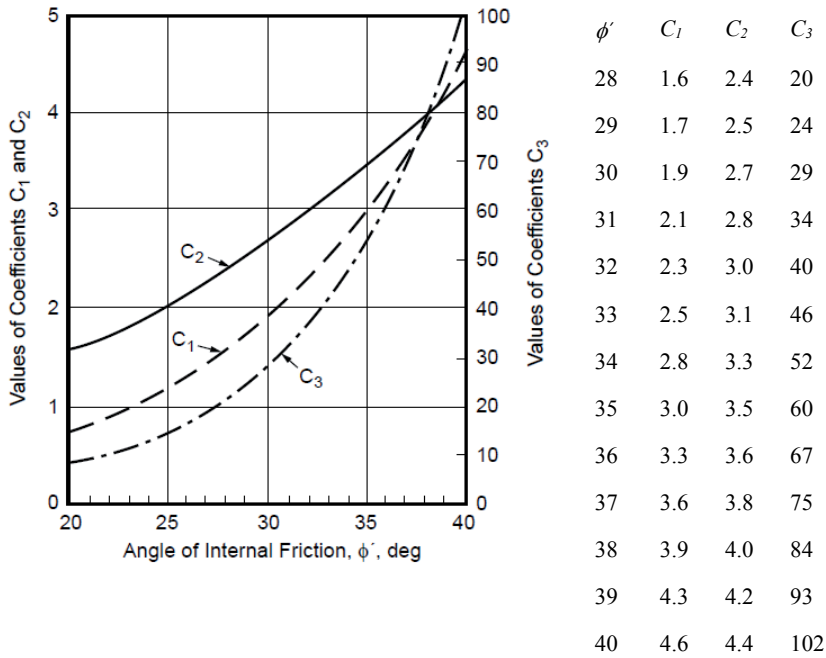| ϕ'	C_1	C_2	C_3
28	1.6	2.4	20
29	1.7	2.5	24
30	1.9	2.7	29
31	2.1	2.8	34
32	2.3	3.0	40
33	2.5	3.1	46
34	2.8	3.3	52
35	3.0	3.5	60
36	3.3	3.6	67
37	3.6	3.8	75
38	3.9	4.0	84
39	4.3	4.2	93
40	4.6	4.4	102

Figure 18 Coefficients as function of angle internal friction.
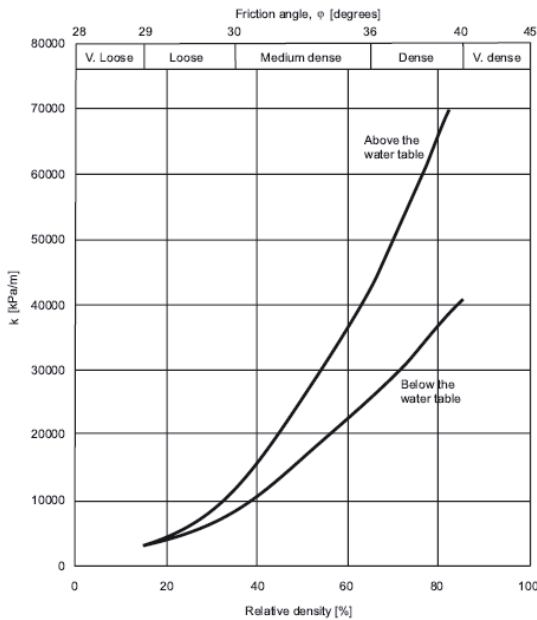
Figure 19 Variation of initial modulus of subgrade reaction n_h as function of relative density, API (1993).

$$A = 3 - 0.8\frac{z}{D} \geq 0.9 \tag{33}$$

For cyclic load $A=0.9$ can be used in all cases. The expression (33) will not give the exact same A as if Figure 16 is used and thus the maximal horizontal pressure against the pile will not be the same with the two methods.

A soil model with linear curve based the initial slope of the load-displacement curve according to Reese et. al.(1994) is suggested by Svahn et. al. (1996). To account for the non-linear response of soil the lateral modulus of subgrade reaction is suggested to be half of the initial modulus according to Reese et. al.(1994) and is expressed as follows:

$$k_h = \frac{1}{2}k_s z \tag{34}$$

where k_s is given in Table 7 and z is the depth under the surface of the soil. As can be seen by the expression the width of the piles do not affect the size of the modulus.

The maximal pressure acting on the pile is calculated with the following expression:

$$p_u = 3K_p \gamma z D \tag{35}$$

where $N_\phi = 3K_p$ and γ should be substituted with γ' if the pile is situated under the water table. Creep is not considered for friction soils.

The three different methods yields different load-displacement curves as can be seen in Figure 20. With the two methods described first (Reese et al. 1974 and O'Neill et. al. 1983) the ultimate soil pressure will be reached at different pile displacements (constant with depth for the method suggested by Reese et al. 1974 but increases linearly with depth in the method suggested by O'Neill et. al. 1983). As the loading is of cyclic nature for piles in integral abutments it is logical to choose the factor A accordingly. In the method suggested by Svahn et. al. (1996) the ultimate soil pressure against the pile increases linearly with the depth as does the modulus of subgrade reaction but y_u remains constant with depth.

As seen by the load-displacement curves shown in Figure 20 the ultimate pressure against a pile is reached at very small displacements if the piles are slender as is the case in the example.

It is assumed that the largest displacements take place near the pile head and thus the largest soil pressure against the pile also is at the upper part of the pile. As soon as the limit value, p_u, of the soil pressure is obtained the lateral modulus of subgrade reaction will behave plastically at further displacement of the pile. The pile will behave elastically until a plastic hinge is formed somewhere along the pile and then the pile resistance is reached at the ultimate limit state. To reach this state the pile must be ductile and belong to Class 1 cross-section according to EN 1993-1-1 (CEN 2008). For the serviceability limit state the resistance is reached as soon as the

stresses in the pile reaches the yield point, this is of course at a lower load level than ULS.

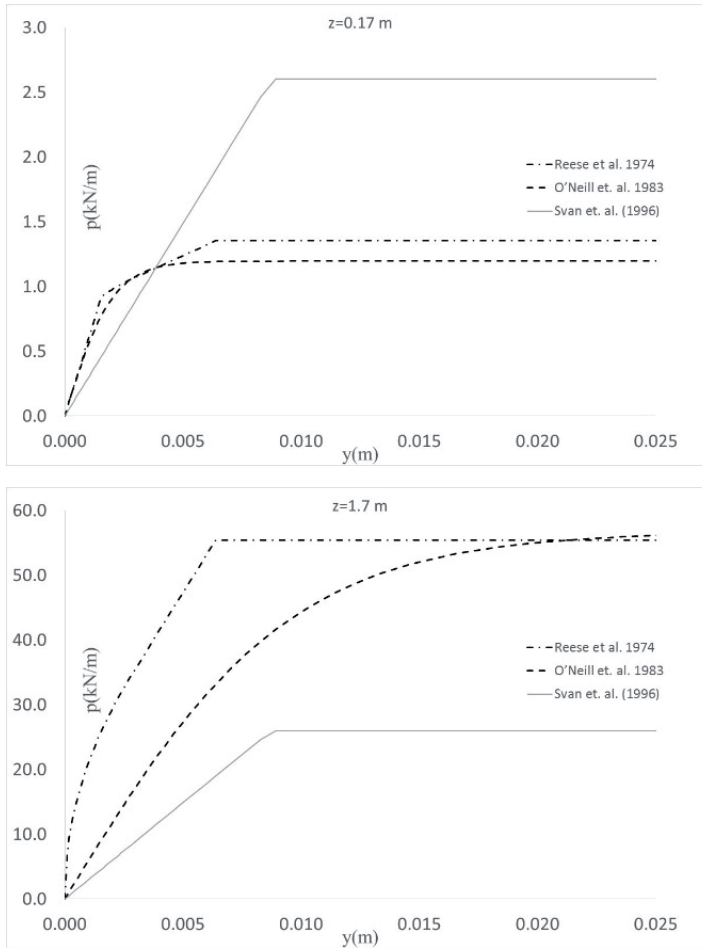*Figure 20 Example of load-displacement curves by the three different methods that are described. The input used to create these curves are $\phi=30°$, $K_0=0.4$), $\gamma=10$ kN/m^3, $n_h=3.5$ MN/m^3 and only the pile diameter is differ , D=0.17 m (top) and 1.7 m (bottom). Cyclic conditions are assumed.*

The procedure to calculate the moments and shear forces along the pile considering second order effects and in-elastic material behaviour is an iterative process that is preferably done with computer programs.

3.8 Piles supporting integral abutments

3.8.1 Introduction

Research concerning piles in integral abutment bridges has been conducted in USA since the 1980s (Greimann et. al 1988, Moulton et. al. 1985 and Wolde-T et. al. 1988).

Oesterle, et al. (1999) presented four pile-design options to improve the ductility for a pile where the calculated horizontal displacements at the top exceeds the code limits. The first option was to increase the size of the pile cross section, the second option was to re-orientate the pile for strong-axis bending. For either of these options the pile-displacement limit will increase for a pile. However, these researchers noted that the increased flexural stiffness of the pile will cause a larger moment to be induced at the top of the pile when the bridge superstructure is subjected to temperature changes. Based on the recommendations by Yang, et al. (1985), Oesterle, et al. suggested a third option that involved the use of a pre-bored hole for each abutment pile. Prior to casting the abutment-pile cap, these holes should be filled with loose sand to increase the flexibility of the pile for lateral displacements of the pile head. A fourth option was to use semi-integral abutments rather than integral abutments. Two types of semi-integral abutments were suggested. The first type of abutment has a pinned pile-head condition. The second type of an abutment permits horizontal translation between the abutment and the pile cap, which eliminates lateral displacement at the top of an abutment pile. These researchers noted that both types of semi-integral abutments will increase the cost of the bridge construction compared to other types of abutments. Also, Oesterle, et al. commented that these types of semi-integral abutments may require future costs to maintain.

A design example for HP250 x63 piles in a 130 m long, three-span, integral abutment bridge with steel girders was presented by Wasserman (2001). The pile behaviour was modelled using a computer program that accounts for the elastic-plastic soil-structure interaction to establish the point of inflection in a pile. Regarding the pile orientation, Wasserman stated that weak-axis bending (induced by pile-head displacement) provides the least resistance to lateral displacement. These strength-behavioural models for combined loading were established for typical beam-column members in structural frames, which have specific effective lengths for flexural buckling and unbraced lengths for lateral-torsional buckling.

Ingram, et al. (2004) performed field tests on five, HP250x63 piles that were driven about 11.6 m into soil. A pre-bored hole was not used for either pile. The first pile was driven into a compacted fill, and the second pile was driven into virgin clay. Each pile had a reinforced concrete abutment that was cast around the top of the pile. The pile tests were monitored using strain gages along the length of the piles, load cells, and displacement transducers. Vertical and horizontal loads were applied to the test piles. From these field tests, axial load and bending moment resistances were

experimentally established for the test piles. To analytically predict axial load versus bending moment, interaction relationships for the test piles, Ingram, et al. (2003) applied the AASHTO Standard Specification (1996); AISC LRFD Specification (1998); and a plastic-limit-strength criterion, which neglected any member length effects on axial load and bending moment resistances. These researchers graphically illustrated the three interaction relationships for the test piles and showed experimental data points on the same graphs. The experimentally determined pile resistances were more closely predicted by the plastic limit- strength criteria than by the AASHTO or AISC member-resistance models. Ingram, et al. concluded that the AASHTO and AISC interaction-design equations, which consider member length effects, do not accurately model the behaviour of a pile in soil.

Greimann et. al. (1988) presented a design model for piles in joint-less bridges. The simplified design method is based on two failure modes:

1) the pile slips through the soil as a result of the load exceeding the resistance of the soil and

2) a lateral mechanism where the pile fails due to a combination of buckling and plastic collapse caused by axial force and lateral displacement .

The model consists of only one pile and lateral group effects can be ignored if the spacing between the piles are greater than 3D. The pile is idealised as a beam column with elastic-perfectly plastic material properties. The piles are considered to be pinned or fixed at the pile top. The soil is modelled with three sets of springs: horizontal springs, vertical springs along the pile and a point vertical spring at the pile tip. For the slip mechanism, the load bearing resistance is the sum of the maximum load carried by the tip and by friction along the pile. For the lateral mechanism following relationsship based on the Rankine formula can be used to check if the resistance of the pile is sufficient:

$$\frac{N_d}{N_{cr}} + \frac{N_d}{N_{pl}} \leq 1.0 \qquad (36)$$

where N_d is the axial design load, N_p plastic resistance and N_{cr}, the critical buckling load. The critical buckling load, N_{cr}, for the pile is calculated using the following expressions developed for straight piles:

$$N_{cr} = U'\sqrt{k_h EI} \qquad (37)$$

for piles where the lateral stiffness off the soil is constant and:

$$N_{cr} = V' n_h^{\frac{2}{5}} (EI)^{\frac{3}{5}} \qquad (38)$$

for piles in soil with linearly increasing soil stiffness. The non-dimensional buckling coefficients U' and V' are given in Table 8.

The plastic resistance for piles in integral abutments with lateral displacement are given by these expressions:

$$N_{pl} = \frac{2M_p'}{y} \tag{39}$$

for piles with pinned connection and:

$$N_{pl} = \frac{4M_p'}{y} \tag{40}$$

where M_p' is the plastic moment resistance reduced because of the simultaneous axial load, N_d, in the pile. The method gives conservative results for the ultimate load bearing resistance of piles and FE-simulations were done to prove this point.

Table 8 Values of non-dimensional buckling coefficients.

	Pinned pile connection	**Fixed pile connection**
U'	2.0	2.5
V'	2.3	4.2

The University of Knoxville did two sets of field tests to evaluate design criteria used by Tennessee Department of Transportation (Burdette et. al. 2004). The first set of tests were done on five steel H-piles (HP 250×63) supporting a concrete abutment and the second on four pre-stressed concrete piles (356 mm square). Piles were driven into residual red clay soil. Concrete abutments were built on top of the piles to simulate the behaviour of actual integral abutments and the slab was integrally connected to a slab.

The test abutments were displaced horizontally by a horizontal force. First the force was applied to displace the abutments to the limits of the design criteria used by Tennessee department of Transportation and then far beyond that. It was concluded that with steel piles the limit displacement was governed by the cracking of the abutment. No specific recommendation was formulated by the researchers but a value of as much as 38 mm seemed reasonable for concrete piles and more for steel piles according to the authors. FE-models were also made to investigate other soil parameters than those on the test site (Ingram et. al. 2004). It was concluded from the analysis that design of piles in integral abutments with typical beam-column equations can be extremely conservative as the lateral support provided by the soil prevents pile buckling in most practical cases.
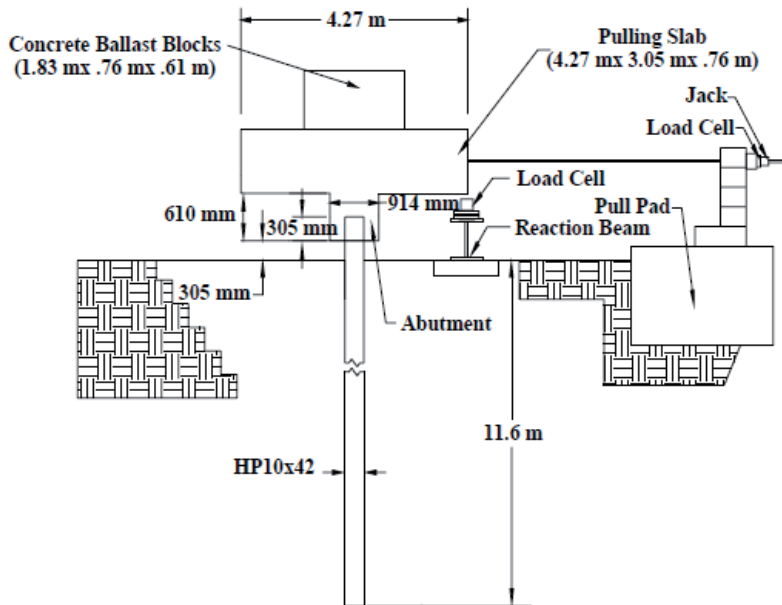
Figure 21 The test set up (Burdette et. al. 2004).

3.8.2 Cantilever method

In Iowa, a design procedure was developed for thermally-induced lateral translation and applied vertical loads (Greimann, et al. 1987 and 1988 and Abendroth and Greimann 2005). The pile-soil interaction is modelled with three equivalent-cantilever lengths and the abutment piles are replaced by equivalent cantilevers. These equivalent lengths, which are based on the flexural buckling, bending moment and horizontal stiffness of a pile in soil, were developed to design the piles as a steel beam-column. Two different methods were suggested. The first one does not permit plastic redistribution of internal forces and is quite conservative. In the second, plastic redistribution is permitted to occur in an abutment pile. To use the second one, the pile cross section must have sufficient, inelastic-rotation capacity before local buckling occurs in an element of the cross section. A continuation of the integral-abutment research at Iowa State University was performed by Girton, et al. (1989 and 1991). This research provided additional confirmation of the design procedures for the piles in an integral abutment.

Chen (1997a and 1997b) investigated the effective lengths of piles in integral abutments analysed with the equivalent cantilever method and compared approximate methods that are commonly used in design with more precise analytic methods. It was shown that the approximate methods did not always display result that where on the safe side. A numerical procedure was proposed to calculate the effective length of laterally-loaded piles and Chen presented design tables for the

effective-pile length for the bending moment, horizontal stiffness, and buckling of steel HP-piles of various dimensions surrounded by different soils. Chen recommends to provide at least a 3 m predrilled hole with loose sand to limit the stress in the pile during and after installation. The lateral support of the pre-drilled hole can be questionable and should be regarded as unsupported in the analysis according to Chen (1997b).

3.8.3 Design of piles according to Massachusetts Department of Transportation

Massachusetts Highway Department has developed a simplified methodology to ensure adequate strength for piles in integral abutments that are subjected to inelastic deformations (Conboy et. al. (2005). This methodology uses the cantilever approach developed by Greiman et. al. (1987) at Iowa State University and is valid for steel H-piles HP10×85 and HP12×125 placed in one row under each abutment and of steel with f_y=345 MPa. Integral abutment piles are considered to be sufficiently braced to prevent lateral torsional buckling and Euler buckling. The methodology builds on the fact that compact sections are Class 1 (according to EN 1993-1-1 CEN 2008) capable of between 3 to 5 times the rotation capacity beyond the rotation at which a plastic hinge first forms assuming fully elastic behaviour up to full plastic moment. The designer of a bridge only needs to calculate the axial force in the in the pile at the ultimit limit state and compare it with the maximum axial load given in tables in the LRFD Bridge Manual if all the following criteria are fulfilled (cited from the LRFD Bridge Manual, Massachusetts Department of Transportation, (2013)):

1. Total bridge lengths shall be limited to 42.6 m for steel bridges and 61.0 m for concrete bridges. These maximum span lengths restrict the pile heads lateral displacement to approximately 25 mm in each direction.

2. Skew angles shall be limited to 30°.

3. The structure shall be a straight bridge or a curved bridge with straight beams that are parallel with each other.

4. Horizontal curvature shall be limited to a 5° subtended central angle.

5. The difference in the profile grade elevation at each of the abutments shall not exceed 5% of the bridge length.

6. Abutment heights, measured from the deck surface to the bottom of the cap, shall not exceed 4.57 m.

7. The bridge shall sit upon parallel abutments and piers.

8. The bridge shall have abutments with parallel wingwalls (U-wingwalls).

9. The top of bedrock, as per Geotechnical Report, shall be located lower than the established pile tip elevation.

10. The abutments of the bridge shall not be scour susceptible.

The values of the maximum axial factored pile load that are given in the tables are based the following expression:

$$\frac{N_u}{0.70A_sf_y} = \frac{8.0}{9.0}\left(\frac{M_y}{1.75Z_yf_y} + \frac{M_x}{1.75Z_xf_y}\right) \tag{41}$$

where M_y and M_x are the factored bending moments round the piles respective axis.

In the expression the plastic section modulus, Z, is used. The expression is valid for the compacted gravel backfill used by Massachusetts Department of Transportation.

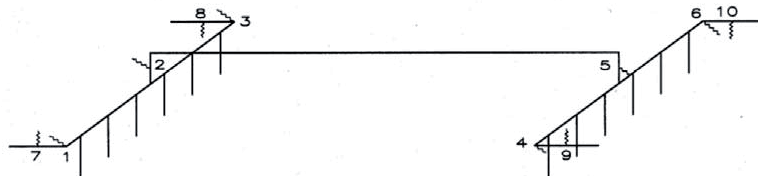The maximum factored axial pile loads at the ultimit limit state is given in Table 9 and Figure 22 The model of an integral abutment bridge should look like this according to Massachusetts DOT (Massachusetts DOT LRFD Bridge Manual Part 1).

Table 10 along with minimum pile lengths. As a comparison $A \cdot f_y = 3.8$ MN and 5.6 MN for piles HP 250×85 and HP 310×125 respectively if $f_y = 355$ MPa.

Table 9 Maximum factored axial pile load in ultimiate limit state, N_u, and minimum pile length, L_f for HP 250×85

	N_u (MN)				L_f(m)
Skew	**10°**	**20°**	**30°**	**40°**	
Dry loose sand	1.87	1.76	1.68	1.41	6.69
Wet loose sand	1.91	1.81	1.62	1.34	6.69
Dry dense sand	1.63	1.46	1.73	1.36	4.86
Wet dense sand	1.68	1.52	1.68	1.24	5.17
Wet stiff clay	1.69	1.48	1.34	1.91	4.26
Wet soft clay	2.10	1.98	1.27	1.86	6.69

Figure 22 The model of an integral abutment bridge should look like this according to Massachusetts DOT (Massachusetts DOT LRFD Bridge Manual Part 1).

Design of Steel Piles for Integral Abutment Bridges

Table 10 Maximum factored axial pile load in ultimate limit state, N_u, and minimum pile length, L_f for HP 310×125

Skew	N_u (MN)				L_f (m)
	10°	20°	30°	40°	
Dry loose sand	2.85	2.71	2.61	2.54	7.60
Wet loose sand	2.91	2.78	2.69	2.62	7.90
Dry dense sand	2.50	2.26	2.10	2.01	5.47
Wet dense sand	2.58	2.36	2.22	2.13	5.78
Wet stiff clay	2.59	2.30	2.15	2.06	4.86
Wet soft clay	3.17	3.02	2.94	2.89	7.90

The equivalent length of the piles in integral abutment bridges are given in a table in the LRFD Bridge Manual that is reproduced in Table 11

Table 11 Equivalent lengths according to Massachusetts DOT LRFD Bridge Manual Part 1, Table 3.10.11-4.

		L_{equ} (mm)	
		HP 250×85	HP 310×125
1	Dry Loose Sand	2530	2896
2	Wet Loose Sand	2591	2987
3	Dry Dense Sand	2225	2530
4	Wet Dense Sand	2286	2591
5	Wet Stiff Clay	2286	2591
6	Wet Soft Clay	3048	3505

The bridges should be modelled as a 3D space frame as a minimum, including abutments, wing walls, piers (if any), piles and soils springs. The model shall be representative of the geometry, including skew (see Figure 22). The springs representing the soil pressure against abutment and wing walls are compression only springs that can be calculated with the soil pressure coefficient, K, expressed as a function of the displacement of the abutment due to temperature change, δ_t, and the height of the abutment, H.

$$K = 0.43 + 5.7\left(1 - e^{-190\left(\frac{\delta_T}{H}\right)}\right) \tag{42}$$

The expression is valid for the compacted gravel backfill used by Massachusetts Department of Transportation.

3.9 Low cycle fatigue

Piles in long integral abutment bridges will experience strains that exceeds the yield limit due to the annual temperature variations. According to the Eurocodes it is possible to model plastic behaviour by elastic-plastic analysis with plastic section modelled as plastic hinges (5.4.3 in CEN 2009b and CEN 2008). To be able to make a plastic global analysis the cross section has to have sufficient rotation capacity and the stability of the members at plastic hinges must be assured. This means that class 1 cross sections are required. Where plastic global analysis is used for ultimate limit state, plastic redistribution of forces and moments at the serviceability limit state may occur and the effect should be considered (7.1 (4) in CEN 2008). But for bridges, stresses at the serviceability limit state should come from linear elastic analysis and the nominal stress range should be limited to *1.5f_y*. This will of course limit the length of integral abutment bridges that can be built and designed according to the Eurocodes.

Because of the limited number of temperature cycles over the life span of a bridge, high stress ranges in the serviceability limit state can be regarded as a low cycle fatigue problem. Low-cycle fatigue is characterized by repeated inelastic strains leading to material failure that occurs within a low number of cycles (less than 1000). For the calculation of number of load reversals to crack initiation, *2N_f*, for most metallic materials, strain life approach and corresponding Coffin-Manson expression

$$\frac{\Delta\varepsilon}{2} = \frac{\Delta\varepsilon_e}{2} + \frac{\Delta\varepsilon_p}{2} = \frac{\sigma_f'}{E}\left(2N_f\right)^b + \varepsilon_f'\left(2N_f\right)^c \tag{43}$$

are widely used due to their practicality and the existence of an extensive knowledge base. The most accurate way to obtain the necessary Coffin-Manson fatigue parameters σ_f', *b*, ε_f' and *c* is to perform tests with the material of interest but because of the complexity and high costs of cyclic experiments it is attractive to find ways to determine the parameters from cheaper monotonic tension tests (Basan et. al. (2011). Meggiolaro et. al. (2004) presented an extensive statistical evaluation of the existing Coffin–Manson parameter estimates based on monotonic tensile and uniaxial fatigue properties of 845 different metals, including 724 steels. It was found that results from tensile tests did not correlate well with the Coffin-Manson fatigue parameters. Better life predictions are obtained simply from constant estimates of the parameters *b, c,* σ_f'/σ_u and ε_f' such as in the medians method, which combines good average life predictions with one of the lowest standard deviations. The medians for the Basquin-Coffin-Manson fatigue parameters, according to Meggiolaro et. al. (2004), are as follows:

$$b = -0.09 \tag{44}$$

$$c = -0.59 \tag{45}$$

$$\sigma_f' = 1.50\sigma_u \tag{46}$$

$$\varepsilon_f' = 0.51 \tag{47}$$

and the Coffin-Manson expression thus takes the following form:

$$\frac{\Delta\varepsilon}{2} = \frac{\Delta\varepsilon_e}{2} + \frac{\Delta\varepsilon_p}{2} = \frac{1.5\sigma_u}{E}\left(2N_f\right)^{-0.09} + 0.51\left(2N_f\right)^{-0.59} \tag{48}$$

The expression can be viewed in Figure 23 with the test described in Paper V visualised as four dots in the diagram at 0.017 strain. The tests are made by bending a steel pipe and the steel did not have a constant strain range through the loading cycles. The response of the tested pipe became softer during the tests due to softening of concrete and to some extent the steel. Therefore it is questionable to compare the results with fatigue tests made on coupons subjected to constant strain amplitudes. But the comparison is made to see if a conservative design assumption can be found. When designing bridges the designer is assuming fixed (or hinged) conditions and it resembles the situation at the beginning, before any softening occurs. The strain ranges at the beginning of the tests have been used. The Coffin-Manson expression with the coefficients and exponents used in (48) can be non-conservative and should not be used for design without proper safety coefficients. According to Meggiolaro et. al. (2004) the coefficient of variation of the stress amplitude for 10^3 cycles is 18 %. If the same coefficient of variation can be assumed for low cycle fatigue this can be used to derive a design curve.

Razmi et. al. (2012) investigated and proposed a guideline for the determination of fatigue life of piles in integral abutment bridges. The process was illustrated with a case study where the length of an integral abutment bridge was varied to evaluate effect of the daily and seasonal temperature variation. The authors concluded that an exponential reduction of the fatigue life will take place if the length of an integral abutment bridge is increased and found that the daily temperature variations gave much more damage than the annual temperature variations because of the larger number of cycles. The contribution of the seasonal temperature variation were negligible according to the authors. Razmi et. al. (2012) used a FE-model with non-linear material to calculate the strains in the structure. The von Mises yield criterion was used to determine when plastic strains were present. In the paper the amplitude of the daily temperature variations were assumed to be 15.3° C and the annual 30.5° C. This is a very large ratio (50 %) and explains why the seasonal variations have so little influence over the fatigue life in the study. Other authors have suggested 25 %. And though the maximum amplitude of the daily temperature changes can be large the mean daily temperature change is much less, as can be seen in Table 1 for Stockholm. The fatigue life was calculated by Razmi using an expression proposed by Koh et. al. (1991).

$$\varepsilon_a = \varepsilon'_f \left(2N_f\right)^c = 0.0795\left(2N_f\right)^{-0.448} \tag{49}$$

The validity of the model was proven by the good correlation with experiments presented by Mander et. al. (1994). The experiments conducted by Mander et. al. (1994) was made with reinforcement bars with patterned surfaces at it would seem likely that the fatigue life of a reinforcing bar is shorter than that of a pile with a smooth surface.

In the off-shore industry, fatigue assessment is a vital part of the design process and low cycle fatigue can occur in places where the stress concentration factor is high and there are a few cycles in the form of high waves in storms with limited duration. According to DNV (2010 the way to handle low cycle fatigue is to use one of the SN-curves that are used for high cycle fatigue (the particular curve that is used in the low cycle fatigue region is called B1) and regard the strains as stresses where $\Delta\varepsilon{\cdot}E{=}\Delta\sigma$. The number of cycles to failure can be calculated as follows:

$$logN = log\overline{a} - m\log(\Delta\varepsilon{\cdot}E) \tag{50}$$

and with m=4 and $log\overline{a}$=15.117 the number of cycles to failure is given by:

$$logN = 15.117 - 4\,log(\Delta\varepsilon{\cdot}E) \tag{51}$$

In the same way it is possible to use the SN-curves from Eurocodes and with the detail category C=160 MPa (Detail nr 3 in Table 8.1 in CEN 2009a), which is appropriate for un-welded piles, with m=3 and $log\overline{a}$=12.913. The expression then becomes:

$$logN = 12.913 - 3\,log(\Delta\varepsilon E) \tag{52}$$

For pipe piles with longitudinal welds a lower detail category must be chosen, C=140 MPa (Detail nr 11 in Table 8.2 in CEN 2009a) and with m=3 the expression becomes:

$$logN = 12.739 - 3\,log(\Delta\varepsilon E) \tag{53}$$

In Figure 23 some of the models discussed above have been plotted in a diagram together with test results from Mander et. al. (2004), Duschika et. al. (2007) and Chakraborti et. al. (2006).
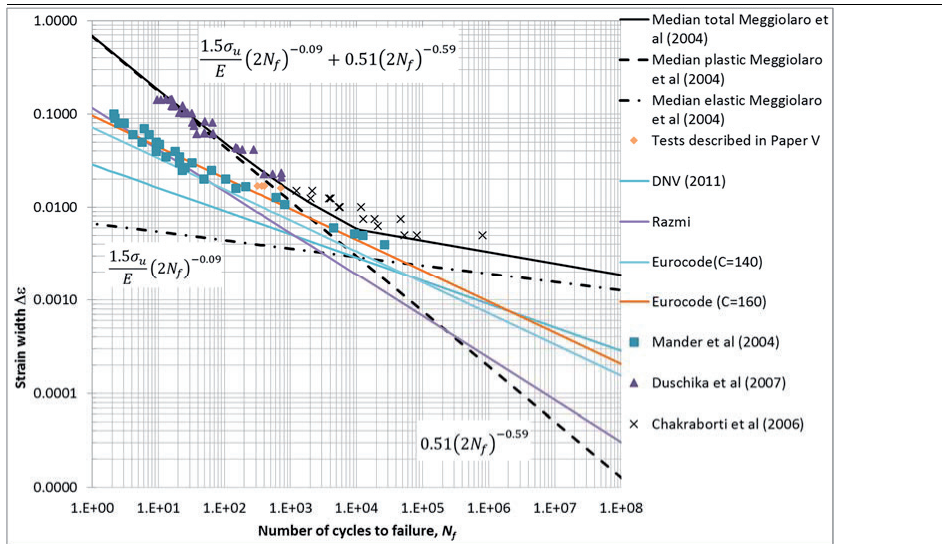
Figure 23 Low-cycle fatigue tests (dots) and different expressions (lines) that can be used to calculate the low cycle fatigue life of steels.

As seen in Figure 24 the curves derived from Eurocodes are conservative for the two number of cycles 120 and 43800 that corresponds to yearly and daily temperature cycles for 120 years. If strains caused by other loads than temperature cannot be neglected a damage according to the Palmgren-Miner rule can be calculated.
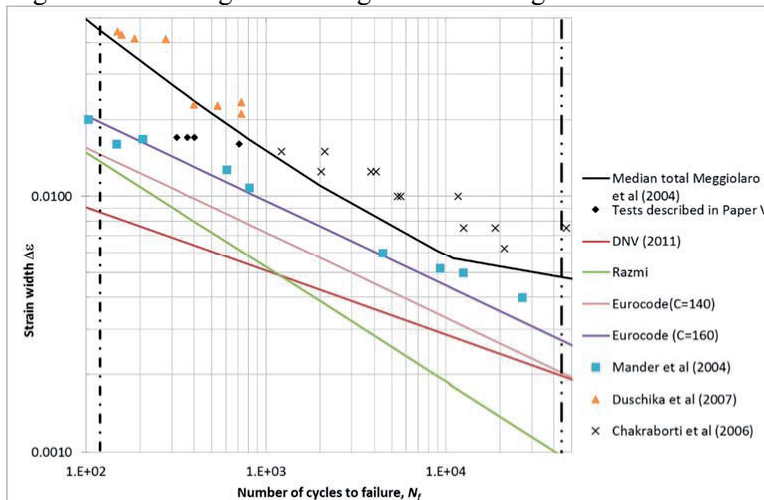

Figure 24 The area between 100 cycles and 100 000 cycles of Figure 23 is enlarged in this figure.

For example if the strain range due to the serviceabilty limit state value of annual temperature changes is 1.0 % and the strain range of daily temperature variations is 0.1 % the damage according to the Palmgren-Miner rule would be 5%.

It has been shown in Paper V that steel piles can withstand more than 300 cycles of rotation with initial strain range exceeding 16 000 µstrain before the first fatigue crack occurred. It is suggested that a conservative value of 10 000 µstrain (1 %) is used as a design limit for a service life of 120 years (120 cycles). This is under the assumption that the bridge is subjected to one large temperature cycle every year.

3.10   Initial imperfections and second order moments

When designing piles, second order effects should be taken into consideration if:

$$\frac{N_{cr}}{N_d} < 15 \tag{54}$$

where N_{cr} is the critical buckling load and N_d the design load (EN 1993-1-1 CEN 2009c).

The initial shape of the pile is assumed to be the same as the buckling shape.

The initial imperfection, e_0, of the pile as a function of the critical buckling length, l_c, can be assumed to be according to Table 5.1 in EN 1993-1-1 (CEN 2008) and is:

$$\frac{e_0}{l_c} = \frac{1}{200} \tag{55}$$

for steel pipe piles that are cold formed. For piles with H-profile the value is 1/300 for strong axis bending and 1/250 for weak axis bending. By using these values the effect of geometrical imperfections, structural imperfections due to fabrication, residual stresses and variation in yield strength over the cross section are taken into account as long as the appropriate execution standards are followed during construction. This is done by increasing the first order moments along the pile

4 Case study Bridge over Leduån

In 2005 a RFSC project, called "Economic and Durable Design of Composite Bridges with Integral Abutments" or just INTAB, was launched. One outcome from the project was data from monitoring of an integral abutment bridge. The bridge is a composite road bridge with one lane and one span of 40 m and was designed and built at the beginning of the project, early 2006. The bridge crosses the small river Leduån in the north of Sweden. The monitoring of the bridge over Leduån is described in Nilsson (2008) and in Papers III and IV in this thesis. Most of the construction work was done from January to July 2006 and in August 2006 the work was completed. In September 2006 the instrumentation of the bridge was completed and the monitoring started.

4.1 Short term monitoring

Short term monitoring was done at four different times during the period between January 2007 and January 2008. The tests were done by loading the bridge with a lorry that stopped at 22 different location along the bridge while data from gauges were collected and stored.
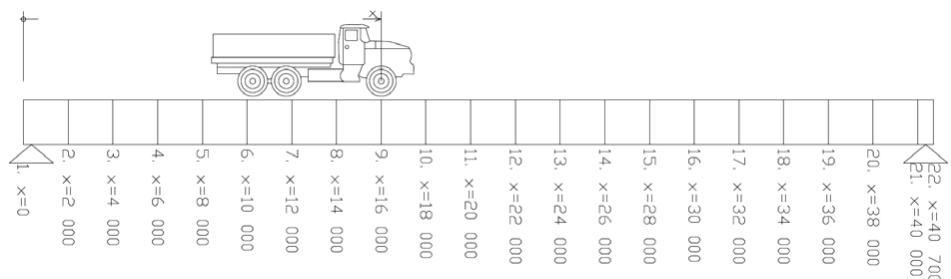
Figure 25 During the short term monitoring a lorry entered the bridge and stopped at 22 location along the bridge as shown in the figure and one stop at the location that gives maximal rotation of the abutment.

The test set-up and the result from the short term monitoring is presented in Nilsson (2008) and Papers III and IV.

4.2 Long term monitoring

The bridge was monitored in the period from 2006-10-19 until 2008-01-08. The results from 351 days of monitoring were obtained. The results below are not presented elsewhere but might be included in a future paper on the long term monitoring.

The temperatures were measured at three locations (Nilsson 2008) on the bridge, in the concrete slab and in both flanges of the eastern girder. All gauges were placed in mid-span. The measured temperatures, over the whole period, are is shown in Figure 26 and Figure 27. Results for the warmest and coldest weeks during this period are presented in Figure 28 and Figure 29.

The coldest bridge temperature during the measured time was -19.2°C , -17.0°C and -22.9 °C (concrete, upper flange and lower flange respectively). The coldest ambient temperature was -22.9 °C expressed as 8h mean, -22.5 °C as 12h mean and -19.6 °C as 24 h mean. The 24 h mean seems to give a good estimate of the coldest effective bridge temperature (EBT).

The highest bridge temperature during the measured time was 26.0°C , 25.0°C and 26.7 °C (concrete, upper flange and lower flange respectively). The warmest ambient temperature was 25.3 °C expressed as a 8h mean 24.8 °C as 12h mean and 22.1 °C as 24 h mean. For the warmer days an ambient mean temperature over a shorter time seems to give a better estimate of EBT. But the EBT is also affected by solar radiation, wind speed and rain. It is therefore thought to be a good estimate to use the 8h mean temperature and add a solar increment to get the highest EBT. According to figure 6.1 in EN 1993-1-5 (CEN 2009e) the design value for the EBT is 3-5 °C above the extreme ambient 1h mean temperature for composite bridges. The monitoring of Leduån does not seem to support this increase of the design value. The highest 1h mean temperature during the measurement was 26.2 °C.

Figure 26 Minimum 24 h temperatures during monitoring.
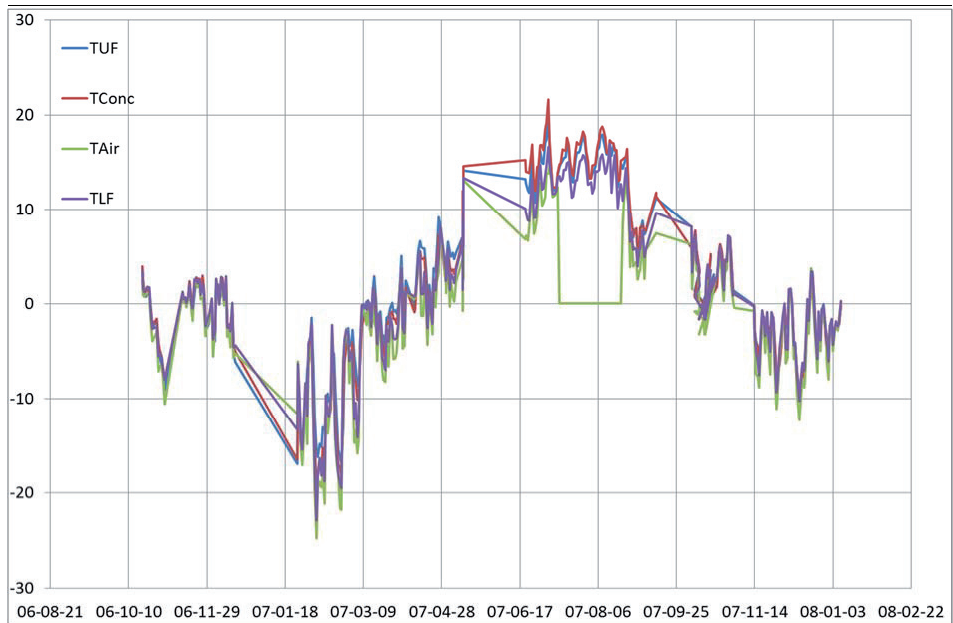

Figure 27 Maximal 24 h temperatures during monitoring.
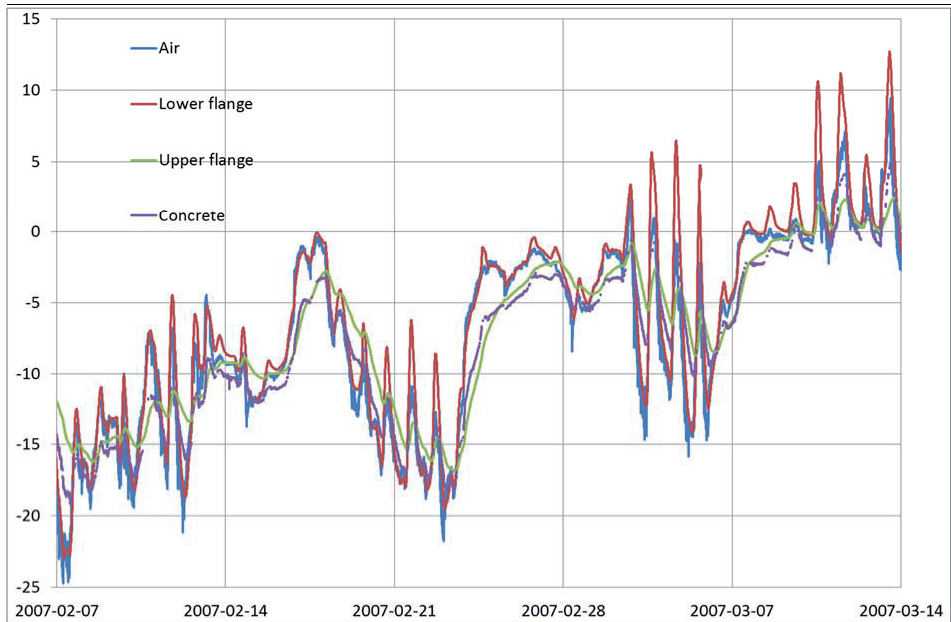
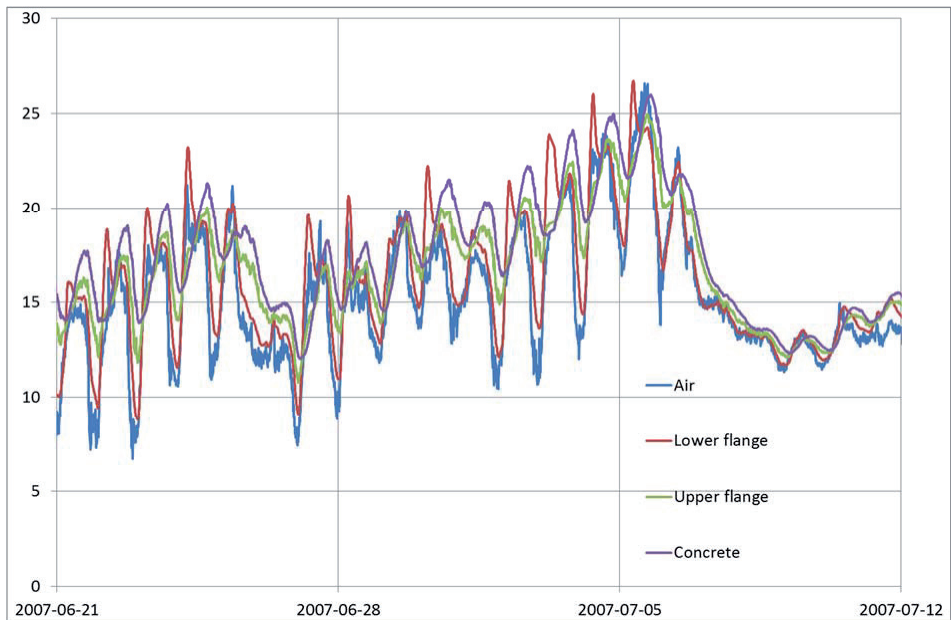*Figure 28 Temperatures during the coldest period.*

Figure 29 Temperatures during the warmest period.

The daily temperature changes are of interest as they are much more frequent than the larger annual temperature changes and they might cause fatigue damage. In

Figure 30 the daily temperature changes for each day during the measurement is shown in a bar graph where each bar represents the number of days that the temperature variation was within 0-1 °C, 1-2 °C etc. The mean ambient daily temperature range is 5.9 °C with a standard deviation of 4.0 °C and the mean daily EBT range is 3.1 °C with a standard deviation of 1.8 °C.
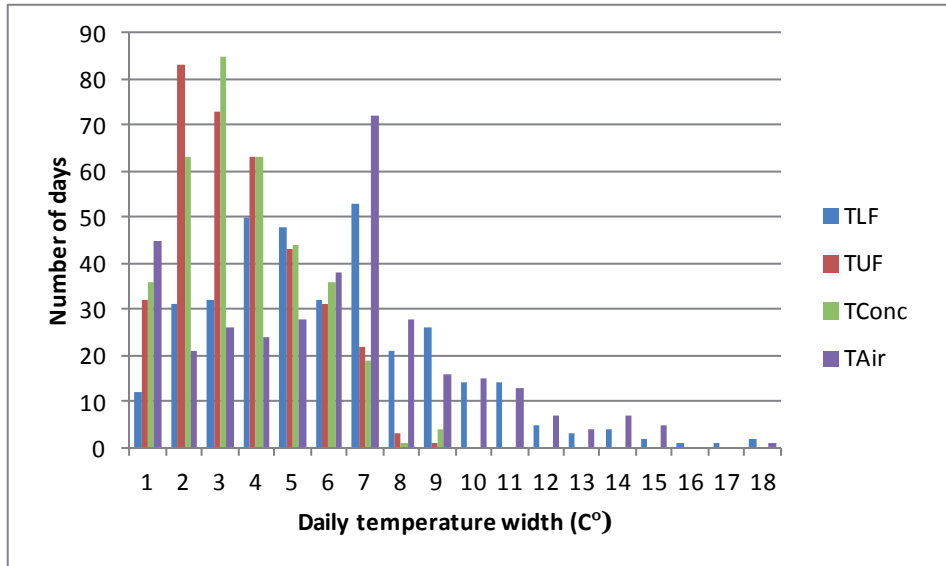
Figure 30 The charts shows the number of days with different temperature rangess.

Table 12 The table shows the maximum, minimum and range of measured temperature during the monitoring of Leduån.

		T_{LF}	T_{UF}	T_{Conc}	T_{Air}
Max	(°C)	27	25	26	27
Min	(°C)	-23	-17	-19	-25
Range	(°C)	50	42	45	52

5 Suggested design method

5.1 General

In the following section a method to design integral abutment bridges is suggested. The method is based on the Eurocodes as far as possible. The assumptions that are made are supported by studies described earlier in the thesis.

The design methods used to design the piles of integral abutment bridges differ, depending on which design rules are used and on the experience of the designer, as well as on chosen structural details. If every possible situation were to be analysed the design work would become very time consuming. To identify the key situations that would control the design, the following should be considered:

- Different load cases. Piles should be designed for situations that includes that for the largest axial force as well as the largest moment that is induced by translation and rotation at the pile top.

- Corrosion of the steel piles will reduce the cross section with time, as material is lost. The initial pile will be stiffer and thus larger moments will come from the displacement of the pile, while the corroded pile at the end of the life span of the bridge will have larger stresses from axial forces and a lower buckling resistance. Both situations should be considered if this is a likely possibility.

- The geotechnical parameters of the soil are often uncertain and cases for both stiff and soft soil around piles should be considered.

- The stiffness of the embankment behind the abutment can differ at opposite ends of the bridge. This can lead to larger pile displacement at one abutment than at the other when the bridge expands in the summer. Stiff soil at one abutment and less stiff on the other should be considered if this is a likely possibility.

- The bridge should be analysed in elongated state, with passive earth pressure from the embankment, and contracted state with active earth pressure from the abutment.

This leads to a number of load cases and multiple analysis models.

Integral abutment bridges should generally be designed based on one of two different concepts:

1. Low flexural stiffness of piles/low degree of restraint. If the integral abutment is supported by one row of flexible piles, the superstructure can be analysed as a beam with hinged supports. For this concept the soil-structure interaction is vital.

2. High flexural stiffness of piles/high degree of restraint. If the integral abutment is supported on stiff piles or spread footings, the rotation of the superstructure, and to some extent the displacement, will be restrained and a large support moment will be introduced in the superstructure.

For this concept the connection between the abutment and the superstructure needs to be stronger and more robust but the sagging moment of the superstructure is reduced in the spans adjacent to the abutment, and a more slender superstructure can be used. If the piles are relatively short and stiff enough the structure acts like a frame and the soil-bridge interaction is not as vital as in bridges with more slender piles. The concept with short and stiff piles is not discussed further in detail here.

5.2 Conceptual design

The design method described below is for an integral bridge on slender steel piles with small stiffness; steel piles with a small area moment of inertia should be used. The piles are encased in the concrete abutment so that the section where the piles are restrained by the abutment is placed as near the neutral axis of the main beams as possible (i.e. a shallow abutment is created).

The piles should be placed in one row to minimise restraint while the superstructure expands. The embankment material should be well graded gravel or blast rock that is well compacted so that as much as possible of the superstructure rotation will be restrained and pile rotation can be minimised. Thorough compactation of the embankment will also ensure that settlement will be as small as possible. To avoid pile rotation caused by permanent loads, as much as possible of the deadweight should be placed before the piles are rotationally locked to the superstructure.

5.3 Soil parameters, site investigation

The design of the foundation of a bridge requires knowledge of the nature of the soil in the area where the abutments are being placed. The soil on site must be investigated to derive the soil parameters necessary to design the piles. The site investigation should result in a geotechnical report where the soil conditions are stated so that the modulus of sub-grade reaction can be determined (e.g. using the guidance in section 3.7.3 or 3.7.4 for clays or sands respectively). For the engineer

to be able to analyse the bending that is caused by the abutments displacements and rotation, only the soil down to a certain depth is of interest for the analysis. Lateral displacements of the pile will be negligible below that depth. The displacement along the lower part along the pile will oscillate back and forth. The length of the analysed pile is sufficient if the analysis shows that there are at least two points of contraflexure near the bottom end of the analysed pile. The solution will in that case be the same as if the full length of the pile was analysed.

5.4 Global analysis

To calculate the forces for the design of piles in an integral abutment, a global analysis should be performed.

One of the major parameters that influences the calculated pile stresses is the stiffness of the backfill behind the abutment. The rotation of the abutment will decrease with increased soil pressure against the back wall of the abutment. In summer, when the bridge elongates, the pressure can be calculated with the passive coefficient K_p. A low value should be used as stiffer soil means less rotation of the abutment and thus lower stresses in the piles. In the winter, when the bridge shortens, an active soil pressure could be expected. But for traffic load at frozen conditions it has been shown that the response of the bridge is stiffer than in summer (see Chapter 4 as well as Table 5-7 in Paper IV).

The author's suggestion is the following:

- A 3D-model should be made of the bridge. The superstructure can be modelled with beam elements. The important thing is that it is possible to model both vertical forces and displacements in a reasonably accurate way. The model should include a hinge between the superstructure and lower part of the abutment to properly model the loads that are introduced before the piles and superstructure are rigidly connected. The hinges must then be replaced with a stiff connection for loads introduced after the piles and superstructure are rigidly connected.

- The soil around the piles can be modelled with discrete springs. The spacing between the springs should be short enough so that the shape of the pile deflection can be modelled in a realistic way (a distance of 1 D between springs is sufficient). The spring stiffness can be calculated using expression (19), (20) or (34). The soil springs are linear and correspond to the initial stiffness of the soil. The soil response will be softer as displacement of the pile increases and makes this calculation overestimate the pile stresses. The characteristic values of the soil parameters should be used.

- The earth pressure against the abutment and the wing walls should be included as loads. The at-rest earth pressure acts as a permanent load and the

passive earth pressure acts as a live load. The passive earth pressure only occurs in load situations with loads that cause displacement where the structural part moves against the soil. One third of fully passive earth pressure can be used as an initial load in load cases that cause passive earth pressure (see 3.3.5 and Kerokoski 2006). Characteristic values should be used.

5.5 Serviceability limit state

As noted in section 1.1, many codes (e.g. EN 1993-2 CEN 2009b) states that the stresses in steel parts shall not exceed the yield limit f_y. It was concluded that as the bending of the piles is restricted by the imposed displacement and rotation of the superstructures ratcheting should not be a problem in piles of integral abutment bridge. It is the authors' opinion that no checks concerning the piles need to be made at the serviceability limit state. The fatigue limit checks (section 5.6) are sufficient to ensure that the strains do not cause any cracks in the piles. No additional displacement of the superstructure will occur because of yielding in the piles as long as the pile is slender.

5.6 Fatigue limit state

For piles in integral abutments bridges, low cycle fatigue should be considered. At the fatigue limit state the actual strains have to be assessed to evaluate the adequacy against fatigue failure. To calculate the damage caused by the traffic a relevant fatigue spectrum and detail category should be used. In the case of a pile without welded details C=160 MPa is used (Detail nr 3, Table 8.1 in EN 1993-1-9, CEN 2009a). For automatically welded pipe piles, without start/stop positions, the detail category for the weld is C=140 MPa if t≤12.5 mm and C=125 MPa if t > 12.5 mm (Detail nr 11, Table 8.2 in EN 1993-1-9, CEN 2009a). If the damage that the traffic causes is less than 10% according to Palmgren-Miner rule, as the case can be for longer bridges, the damage caused by traffic can be neglected.

To calculate the strains from temperature variations it is suggested that 80 % of the range of the uniform bridge temperature (see equation (1)). One cycle per year is used in the calculation. Every year is not as severe during the lifespan of a bridge and using the max value is too conservative.

If the calculated strain range in the pile top, based on ideal conditions with rigid connection between abutment and pile top, is less then $3f_{yk}/E$ the pile can be regarded as elastic. The reason why it is possible to have strain ranges exceeding $2f_{yk}/E,$ which correspond to yield strain in summer as well as in winter is the following:

- The strain hardening of the steel increases the yield strain in the pile.

- The concrete surrounding the pile softens considerably with cyclic loading, which leads to lower shear force, moment and strain at a certain displacement.

As can be seen in Figure 31, the behaviour softens rapidly during the first load cycles and is from cycle two softer than that of a clamped connection.

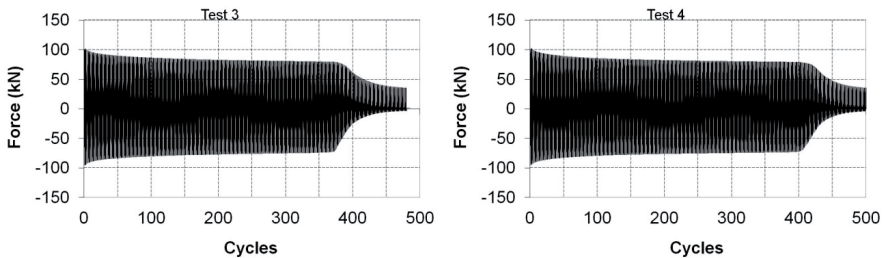If the strain range is larger than $3f_{yk}/E$ the plastic strain should be calculated. The strain range may be reduced by a factor of 1.5 because of strain hardening and softening of concrete.

Figure 31 Changes in force applied over time during each test. Figure taken from Paper V.
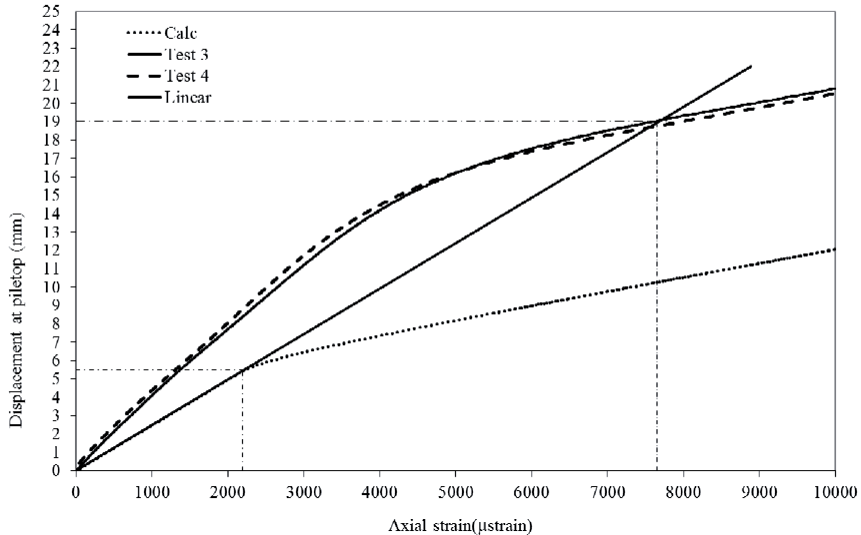
Figure 32 The figure shows the difference between the ideal elasto-plastic behaviour of a cantilever and behaviour of a pile encased in concrete as was measured in the tests described in Paper V.

It has been shown that the test piles could withstand more than 300 cycles, before the first fatigue crack occurred, at constant displacement range that creates initial strain

ranges exceeding 16000 µstrain. It is thus safe to suggest that a conservative value of 10 000 µstrain (1 %) is used as a strain limit for a service life of 120 years years for strains calculated according to the previous paragraphs caused by temperature. If traffic is not negligible a damage calculation according to Palmgren-Miner is performed.

5.7 Ultimate limit state

As a first check at the ultimate limit state the internal forces and moment taken from the global analysis (with partial factors appropriate for the ultimate limit state) are compared with the resistance calculated by a relevant code (e.g. EN 1993-2, CEN 2009d). If the verification is unsuccessful, as it will be for bridges that are not very short and with yield strains in the piles, a more thorough check will have to be done as described below.

The cross sections of the piles must be in Class I according to Eurocode (EN 1993-1-1 CEN 2008) to be able to form a plastic hinge. For H-shaped steel piles the flanges should comply with the following expression:

$$\frac{c}{t} \leq 9\sqrt{\frac{235}{f_y}} \tag{56}$$

and the web should comply with the following expression:

$$\frac{c}{t} \leq 72\sqrt{\frac{235}{f_y}} \tag{57}$$

where c is the outstanding flange or the web depth excluding the fillet radius and t the thickness of the flange. For a circular pile the expression becomes:

$$\frac{D}{t} \leq 50\sqrt{\frac{235}{f_y}} \tag{58}$$

where D is the outer diameter and t the thickness of the pile.

The analysis at the ultimit limit state is preferably done for a single pile. Group pile effects are negligible if the spacing between piles exceeds $3D$ (Svahn et. al. 2006) perpendicular to the lateral load. The piles are placed in one row so there are no group effects in the longitudinal direction of the bridge. For forces acting in the lateral direction of the bridge group effects are not nessecary if the spacing between adjacent piles exceeds $8D$.

The pile will be subjected to a imposed moment at the pile top due to the fact that it is clamped to the abutment. The moment cannot exceed the plastic moment

resistance (with axial force considered as explained below). To calculate the resistance at the ultimit limit state the following model can be used:

- The pile model is pinned at the top. The calculation is performed with initial imperfections (see section 3.10) if relationsship (54) holds.

- Linear springs are placed along the pile with at a distance $1D$ between springs. The spring stiffnesses, calculated for the global analysis (Section 5.4), are multiplied by relevant coefficient.

- The pile is loaded at the pile top with three simultaneous loads; 1) design axial force, 2) forced displacement and 3) a moment as large as full plastic moment. The full plastic moment is calculated taking into account the axial force that is present at the same time by subtracting the area N_d/f_y from the cross-section. The axial force and the imposed displacement are collected from the global analysis. The rotations and shear forces from the global analysis are not used.

- If the calculated soil pressure is larger than the ultimate soil pressure, p_u, anywhere along the pile, the spring stiffnesses are reduced at those locations. This is an iteration that is done until the calculated soil pressure equals p_u.

- The second order moment for sections below the pile top are calculated and checked. The moment for any section along the pile should be smaller than the plastic moment that acts on the pile top.

6 Conclusions

6.1 General conclusions

The purpose of this thesis is to give suggestions for the way that steel piles in integral abutments should be designed. In such bridges the pile tops are assumed to be encased in concrete. The following conclusions are based on the studies of steel piles with an imposed displacement (Paper I), the different ways to construct integral abutment bridges (Paper II), the measurement of the behaviour of one bridge (Paper III and Paper IV), the laboratory tests simulating low cycle fatigue (Paper V) and the simulation of temperature variations and traffic loads (Paper VI).

As noted in Paper II, bridges with integral abutments are built in different ways around the world. In North America, slender steel piles seem to be preferred by many bridge owners. In Europe, on the other hand in situ cast concrete piles with large diameter (typically 1 m) are preferred in countries such as Germany and Austria. In China the concept of integral abutments has not been reported but activities are taking place and many integral abutment bridges are going to be built there in the coming years. Despite the different solutions, most bridge owners seem to be satisfied with the perfomance of integral abutment bridges. As long as bridge owners continue to share their experiences, of the successes and the failures, the use of integral abutment bridges will continue to improve and provide an even more durable and cost effective solution for the future.

Research question 1: *Do integral bridges perform as expected under load and will the stresses/strains in the piles be as large in reality as expected according to the design codes?*

There have been many projects that have included monitoring of bridges with integral abutments and some of them are discussed in chapter 3. The problems that have been reported are mostly concerning development of passive pressures behind the abutment due to the cyclic loading of the soil during thermal movement of the superstructure and the void that forms at the embankment adjacent to the bridge.

The monitoring of the bridge over Leduån showed measured strains that were lower than calculated. The reason is believed to be 1) lower temperature range due to short

measuring period, 2) the piles not being rigidly attached to the concrete abutment and 3) uncertainties in soil properties. The design assumptions seemed to be reasonable.

The field measurements that the author has looked into all come to the conclusion that pile strains are lower than calculated ones. But the measurements are all done for a short period of time compared to the design life of the bridges. Part of the problem with integral abutment bridges is that, for all their simplicity of construction, they are complicated structural systems. To thoroughly analyse a given structure, the designer must not only design for primary loads (dead load, live load, wind load, etc.) but must also accurately account for secondary loads (creep, shrinkage, settlements, temperature effects, etc.). To further complicate the analysis, the response of the structure to a given set of forces is strongly dependent on the geometry, materials, configuration, soil interaction and construction details of the individual system.

In order to avoid complicated analysis, integral abutment bridges should typically be designed by using conservative methods and by building on field experience.

Research question 2: *How do the yearly temperature variations influence the static load-carrying resistance of the piles?*

The top of the piles in an integral abutment will have almost the same horizontal displacement and rotation as the abutment, as they are cast integrally with the abutment. It has been shown (Paper I) that a limited displacement does not decrease the load carrying resistance. The pile axial load bearing resistance is limited by the geotechnical considerations and plastic axial resistance will be far from fully utilized. In many recommendations a horizontal displacement of 25 mm (1 inch) is considered to be some kind of limit under which the load bearing resistance of the pile is not affected. This of course depends on a number of parameters as pile size and soil properties but for most commercially available slender steel piles it is safe to say that as long as the yearly temperature variations leads to displacements that are smaller than 25 mm it will have a minor influence on the load bearing resistance of the pile.

Research question 3: *Is it possible to allow strains exceeding the yield point in steel piles and still have a safe design for 120 years?*

It is shown by the experiment described in Paper V that steel piles can withstand hundreds of constant displacement cycles causing initial strain ranges exceeding six times the yield limit before any cracks will occur. The strain ranges will decrease with time as the concrete surrounding the piles will degrade and crack. This will cause the connection to behave more softly than a clamped connection which is normally assumed in design.

The sum of the calculated stresses from moments and normal forces can exceed the yield limit in a pile. There will be no additional stresses caused by imposed rotation beyond the point when yield strains are reached.

It is thus possible to allow strains exceeding the yield limit in steel piles supporting integral abutments but low-cycle fatigue will need to be checked at the servicability limit state.

Research question 4: W*hat fatigue spectra can steel piles in integral abutment bridges be expected to experience, during their lifetime? What design criteria should be used for the piles?*

The strains in the piles vary with time. The cyclic nature of the loads that cause the strain variation in the pile and the time that the piles are designed for will change. The response will differ for the same load when the bridge is new and when 120 years have passed. The lateral reaction from the soil, the connection between the pile and the abutment, the yield stress of the pile (due to hardening) and the cross section of the pile (due to corrosion) will all change over time. A conservative assumption is to calculate the strains with properties based on the initial conditions.

Three design criteria need to be fulfilled. First the piles need to have the rotation capacity enabling a moment redistribution. Second the moment and axial force at the notional plastic hinges, described in Chapter 5, must be less than or equal to the resistance of the pile. Third the buckling resistance of the pile needs to be sufficient taking into to account the lateral support by the soil and the displacement of the pile.

Research question 5: *If yielding is allowed,* w*hat model should be used to analyse strains in piles, to verify the adequacy against low cycle fatigue?*

To use the detail categories from Eurocode 3-1-9 (CEN 2009) and treat the plastic strains as stresses by multiplying them with modulus of elasticity, E, will be a conservative approach that is rational for bridge design. More accurate models can of course be used if needed but this will require more knowledge from the designer.

The plastic strains caused by annual temperature variations can be used to calculate a damage with the Palmgren-Miner rule where the limit of the strain range is 10 000 μstrain (1 %) for a service life of 120 years (the damage equals unity if $365 \cdot 120$ strain cycles of the magnitude 1 % occurs). The annual temperature variation to be used in the damage calculation is 80 % of the characteristic value calculated according to the Eurocode (CEN 2003b).

6.2 Further research

- The concrete around the pile top softens because of the cyclic nature of the loading and this influences the strains in the piles a great deal. Future investigations should be carried out to find a model for calculating the stresses and also recommend suitable details to minimize the stresses at the pile tops.

- Monitoring of more bridges with integral abutment would be useful as each bridge site is unique.

- More research regarding the lateral behaviour of steel piles is needed. The models that the load-displacement curves in section 3.7.3 and 3.7.4are constructed from are based on few observations and all effects are not fully investigated. Among the research that would be beneficial is full scale tests in slopes, correlation between in-situ measurements and load-displacement curves, response of piles to displacements in transverse direction.

References

Abendroth R. E. and Greimann Lowell F., (2005), *Field Testing of Integral Abutments-Final Report*, Center for Transportation Research and Education Iowa State University, Report. no. HR-399

Ahn J., Yoon J., Kim J. and Kim S., (2011),*Evaluation on the behavior of abutment–pile connection in integral abutment bridge,* Journal of Constructional Steel Research, 67, pp. 1134–1148

Al-Emrani M. and Mustafa A., *Fatigue design of steel and composite bridges,* Report 2014:10, Chalmers University Of Technology

Alampalli S. and Yannotti A. P, (1998), *In-Service Performance of Integral Bridges and Jointless Decks*, Transportation Research Record 1624, TRB, National Research Council, Washington, D.C., 1-7

Arockiasamy M., Narongrit B., and Sivakumar M., (2004) *State-of-the-Art of Integral Abutment Bridges: Design and Practice*, Journal Of Bridge Engineering ASCE, Vol. 10, No. 3

Arockiasamy M., (2005), *Time-Dependent Behavior of Continuous Composite Integral Abutment Bridges*, Practice Periodical On Structural Design And Construction

Arsoy S., Duncan J. M. Hon M., Barker R. M (2004), *Behavior of a Semiintegral Bridge Abutment under Static and Temperature-Induced Cyclic Loading*, Journal of Bridge Engineering, 2004.9:193-199.

Banks J., Bloodworth A., Knight T. and Young J., (2008), *Integral Bridges – Development of a Constitutive Soil Model for Soil Structure Interaction*, ASCE Structures Congress 2008

Basan R., Franulovic M., Prebil I. and Crnjaric-Zic N., (2011), *Analysis of strain-life fatigue parameters and behaviour of different groups of metallic materials*, International Journal of Fatigue 33 484–491

Baugelin F., Frank R. and Said Y. H., (1977), *Theoretical Study of Lateral Reaction Mechanism of Piles*, Geotechnique, Vol. 3, pp. 405-434

Bonczar C., Breña S. F. S.,Civjan S., DeJong J. and Crovo D., *Field Data and FEM Modeling of the Orange-Wendell, Bridge, 2005, Integral Abutments and Jointless Bridges (IAJB 2005)*, The 2005 – FHWA Conference, Federal

Highway Administration, (FHWA)/Constructed Facilities Center (CFC) at West Virginia University

Braun, A., Seidel, G. and Weizenegger, M., (2006), *Rahmentragwerke im Brückenbau*, Beton- und Stahlbetonbau 101

Breña S. F., Bonczar C. H., Civjan S. A., DeJong J. T. and Crovo D. S., (2007), *Evaluation of Seasonal and Yearly Behavior of an Integral Abutment Bridge*, Journal of Bridge Engineering, Vol. 12, No. 3, ISSN 1084-0702/2007/3-296–305

Broms B., (1964), *Lateral Resistance of Piles in Cohesionless Soils*, Journal of the Soil Mechanics and Foundations Division, ASCE, 90. 27-63.

Burdette Edwin G. and Goodpasture David W., (1982), *Thermal Movements of Continuous Concrete and Steel Structures*, The University of Tennessee, Research Project No. 77-27-2

Burdette Edwin G., Howard Samuel C., Tidwell Brandon J., Wasserman Edward P., Ingram Earl E., Deatherage Harold J., Goodpasture David W., (2004), *Lateral Loas Tests on Prestressed Concrete Piles Supporting Integral Abutments*, PCI Journal September-October 2004, pp 70-77

CEN, (2010), EN 1990, *Eurocode − Basis of structural design*, European committee for standardization

CEN, (2009c), EN 1991-1-1, *Eurocode 1: Actions on structures - Part 1-1: General actions − Densities, self-weight, imposed loads for buildings,* European committee for standardization

CEN, (2003a), EN 1991-1-4:2005, *Eurocode 1: Actions on structures - Actions on structures – Part 1-4: General actions – Wind actions*, , European committee for standardization

CEN, (2003b), EN 1991-1-5:2003, *Eurocode 1: Actions on structures - Part 1-5: General actions -Thermal actions*, European committee for standardization

CEN, (2005a), EN 1991-1-6:2005, *Eurocode 1: Actions on structures - Part 1-6: General actions – Actions during execution*, European committee for standardization

CEN, (2005b), EN 1991-2:2005, *Eurocode 1: Actions on structures - Part 2: Traffic loads on bridges*, European committee for standardization

CEN, (2008), EN 1993-1-1:2005, *Eurocode 3: Design of steel structures –Part 1-1: General rules and rules for buildings,* European committee for standardization

CEN, (2009a), EN 1993-9:2005 E, *Eurocode 3: Design of steel structures –Part 1-9: Fatigue*, European committee for standardization

CEN, (2009b), EN 1993-2:2006, *Eurocode 3: Design of steel structures –Part 2: Steel Briges,* European committee for standardization

CEN, (2009d), EN 1993-2:2006, *Eurocode 7: Geotechnical design −Part 1: General rules*, European committee for standardization

Chacón R., Mirambell E. and Real E., (2013), *Strength and ductility of concrete-filled tubular piers of integral bridges*, Engineering Structures 46, pp. 234–246

Chakraborti P.C. and Mitra M.K., (2006) , *Microstructural response on the room temperature low cycle fatigue behaviour of two high strength duplex ferrite–martensite steels and a normalised ferrite–pearlite steel*, International Journal of Fatigue, No. 28, pp. 194–202

Chen Y. (1997a), *Assessment on Pile Effective Lengths and Their Effects on Design-I. Assessment*, Computers & Structures Vol. 62, No. 2, pp. 265-286

Chen Y. (1997b), *Assessment on Pile Effective Lengths and Their Effects on Design-II. Practical Applications*, Computers & Structures Vol. 62, No. 2. pp. 287-312.

Civjan S. A., Bonczar C. , Breña S., DeJong J. and Daniel C., (2007), *Integral Abutment Bridge Behavior: Parametric Analysis of a Massachusetts Bridge*, Journal of Bridge Engineering, Vol. 12, No. 1, ISSN 1084-0702/2007/1-64–71

Collin P., Veljkovic M. and Petursson H., (2006), *International Workshop on Bridges with Integral Abutments-Topics of relevance for the INTAB project,* Luleå University of Technology, 2006:14

Conboy D. W. and Stoothoff E. J., (2005), *Integral Abutment Design and Construction: The New England Experience*, Integral Abutments and Jointless Bridges (IAJB 2005), The 2005 – FHWA Conference, Federal Highway Administration, (FHWA)/Constructed Facilities Center (CFC) at West Virginia University

Cox W. R., Reese L. C., and Grubbs B. R., (1974), *Field Testing of Laterally Loaded Piles in Sand*, Proceedings of the Sixth Annual Offshore Technology Conference, Houston, Texas, paper no. OTC 2079.

DeJong J., Howey D. S., Civjan S. A., Breña S., Butler S. D., Daniel S. C., Hourani N. and Connors P. (2004), *Influence of Daily and Annual Thermal Variations on Integral Abutment Performance*, ASCE Geotechnical Engineering for Transportation Projects, GeoTrans 2004

Dicleli M., Eng P. and Albhaisi S. M., (2004), Maximum Length of Integral Bridges Based on the Performance of Steel H-Piles at the Abutments, Canadian Journal of Civil Engineering, 32 , pp 726-738

Dicleli M. and Albhaisi S. M., (2005), *Analytical formulation of maximum length limits of integral bridges on cohesive soil*, Canadian Journal of Civil Engineering, 32 , pp 726-738

Dicleli M. and Erhan S., (2010), *Effect of soil-bridge interaction on the magnitude of internal forces in integral abutment bridge components due to live load effects*, Engineering Structures 32, 129-145

DNV, (2013), *Design of Offshore Wind Turbine Structures*,Offshore Standard DNV-Os-J101, https://exchange.dnv.com/publishing/codes/docs/2014-05/Os-J101.pdf

Dreier D., Burdet O. and Muttoni A., (2011), *Transition Slabs of Integral Abutment Bridges*, Structural Engineering International, Vol. 21, No. 2, pp. 144-150

Drinkwater L. J., (2007), *Analysis of the Sunniberg Bridge*, Proceedings of Bridge Engineering 2 Conference, University of Bath, Bath, UK

Dunker K. F. and Ahmad A.-H., (2005), *Expanding the Use of Integral Abutments in Iowa*, Proceedings of the 2005 Mid-Continent Transportation Research Symposium, Ames, Iowa, August 2005.

Dunker K. F. and Liu D., (2007), *Foundations for Integral Abutments*, Practice Periodical on Structural Design and Construction, Vol. 12, No. 1, ISSN 1084-0680/2007/1-22–30

Dupont B. and Allen D. L., (2002), *Movement and Settlements of Highway Bridge Approaches*, Research Report KTC-02-18/SPR-220-00-1F, Kentucky Transportation Center, University of Kentucky

Dusicka P., Itanib A. M. and Buckleb I. G., (2007), *Cyclic response of plate steels under large inelastic strains*, Journal of Constructional Steel Research 63 156–164

Emerson, M. (1977). *Temperature differences in bridges: basis ofdesign requirements,* TRRL Laboratory Report 765, Transport and Road Research Laboratory, Crowthorne, Berkshire, pp. 39.

England G. L, David B. I. and Tsang, N. C. M. (2000). *Integral Bridges: A Fundamental Approach to the Time-Temperature Loading Problem*. Thomas Telford Ltd, ISBN 0 7277 2845 8.

Erhan S. and Dicleli M., (2009), *Live Load Distribution Equations for Integral Bridge Substructures*, Engineering Structures 31, Volume 31, Issue 5, pp-1250–1264

Faraji B. S., Ting J. M., Crovo D. S. and Ernst ., (2001), *Nonlinear Analysis Of Integral Bridges: Finite-Element Model*, Journal of Geotechnical and Geoenvironmental Engineering, Vol. 127, No. 5, ISSN 1090-0241/01/ 0005-0454–0461

Finnra, 2002, *Supplementary Bridge Design Instructions*, Finnish Road Administration

Feldmann, M., Naumes, J., Pak, D., Veljkovic, M., Nilsson, M., Eriksen, J., et al. (2010). *Economic and durable design of composite bridges with integral abutments*, Final Report EUR24224. Luxembourg (L): European Commission, Research Fund for Coal and Steel Unit (RFCS).

Fennema J. L., Laman J. A. and Linzell D. G., (2005), Predicted and Measured Response of an Integral Abutment Bridge, Journal of Bridge Engineering, Vol. 10, No. 6, November 1, ISSN 1084-0702/2005/6-666–677

Fu H. C., Ng S. F., and Cheung M. S., (1990), *Thermal Behavior Of Composite Bridges*, Journal of Structural Engineering, Vol. 116, No. 12, pp. 3302-3323

Girton D. D., Hawkinson T. R., L. F. Greimann, Bergenson K., Ndon U. and Abendroth R. E., (1989), *Validation of Design Recommendations for Integral-Abutment Piles*, Iowa DOT Project HR-292

Girton D. D., Hawkinson T. R. and L. F. Greimann (1991), *Validation of Design Recommendations for Integral-Abutment Bridges*, J. Struct. Eng. 1991.117:2117-2134.

Greimann L. F., Abendroth, R. E., Johnson D. E. and Ebner P. B., (1987), Pile *Design and Tests for Integral Abutment Bridges-Final Report*, College of Enginerring Iowa State University, Iowa DOT project HR-273, ISU-ERI-Ames-88060

Greimann L. F., Pe-Shen Y. and Wolde-Tinsae A. M.,(1991*), Nonlinear Analysis of Integral Abutment Bridges*, J. Struct. Eng. 1986.112:2263-2280

Greimann L. and . Wolde-Tinsae A. M.,(1988), *Design Model for Piles In Jointless Bridges*, Journal of Structural Engineering, Vol. 114, pp. 1354-1371

Harvey D. I., Kennedy D. W. and and Ruffo Gordon W., (2001) Integral Abutment Bridges-Design and Constructibility

Hassiotis S. and Xiong K., (2007), *Field Measurements of Passive Pressures Behind an Integral Abutment Bridge*, Seventh International Symposium on Field Measurements in Geomechanics

Huang J., French C. and Shield C., (2004), *Behavior of Concrete Integral Abutment Bridges Final Report 1996-2004*, Report no. MN/RC - 2004-43, University of Minnesota, pp 349, http://www.lrrb.org/PDF/200443.pdf

Huang J., Shield C. and French C., (2008), *Parametric Study of Concrete Integral Abutment Bridges*, Journal of Bridge Engineering, Vol. 13, No. 5

Huckabee P, (2005), *Plastic Design of Steel HP-Piles for Integral Abutment Bridges*, Integral Abutments and Jointless Bridges (IAJB 2005), The 2005 – FHWA Conference, Federal Highway Administration, (FHWA)/Constructed Facilities Center (CFC) at West Virginia University

Husain I and Farago B, (1993), *Integral Abutment bridges*, Report SO-93-01, Ontario Ministry Of Transportation Structural Office Design Section

Husain I. and Bagnariol D., (1999a), *Semi-Integral Abutment bridges*, Report BO-99-03, Ontario Ministry Of Transportation Bridge Office, ISBN 0-7778-8859-9

Husain I. and Bagnariol D., (1999b), *Performance of Integral Abutment bridges*, Report BO-99-04, Ontario Ministry Of Transportation Bridge Office, ISBN 0-7778-9265-0

Iles D., (2005), *Integral Steel Bridges: A Summary of Current Practice in Design and Construction*, SCI Publication

Ingram E. E., Burdette E. G., Goodpasture, D. W. and Deatherage H. J., (2003). *Evaluation of Applicability of Typical Column Design Equations to Steel H-Piles Supporting Integral Abutments*, Engineering Journal, American Institute of Steel Construction, 40 (1), 50-58.

Ingram E. E., Burdette E. G., Goodpasture D. W., Deatherage J. H. and Bennett R. M.,(2004), *Behavior of Steel H-piles Supporting Integral Abutments,Proceedings of the 2004 Structures Congress*, Nashville, Tennessee, May 22-26, 2004

Jin-Hee A., Ji-Hyun Y., Jong-Hak K., Sang-Hyo K., (2011), *Evaluation on the behavior of abutment–pile connection in integral abutment Bridge*, Journal of Constructional Steel Research 67 1134–1148

Kaufmann W. and Alvarez M., *Swiss Federal Roads Office Guidelines for Integral Bridges,* Structural Engineering International, Vol. 21, No. 2, pp. 189-194

Kalayci E., Civjan S. A. and Breña S. F., (2012), *Curved Integral Abutment Bridges – Thermal Response Predictions Through Finite Element Analysis*, Engineering Structures 43, pp. 129–138

Kalayci E., Civjan S. A., Breña S. F. and Allen C. A., (2012), *Load testing and Modeling of Two Integral Abutment Bridges in Vermont, US*, Structural Engineering International, Vol. 21, No. 2, pp. 181-188

Kauffman W. and Alvarez M., (2012), *Swiss Federal Roads Office guidlines for integral bridges*, Structural Engineering International, Volume 21, Number 2, (pp. 189-194)May 2011

Kerokoski O., (2006), *Soil Structure Interaction of Long Jointless Bridges with Integral Abutments*, Tampere University of Technology, Publication 605

Khodair Y. A., (2004), *Numerical and Experimental Analysis of Integral Abutment Bridge*, PhD thesis, Faculty of Stevens Intitute of Technology

Kim W. S. and Laman J. A., (2010a), *Integral abutment bridge response under thermal loading*, Engineering Structures 32, pp 1495-1508

Kim W. S. and Laman J. A., (2010b), *Numerical analysis method for long-term behavior of integral abutment bridges*, Engineering Structures 32, pp 2247-2257

Kim W. S. and Laman J. A.,(2012), *Seven-Year Field Monitoring of Four Integral Abutment Bridges*, Journal of Performance of Constructed Facilities, Vol. 26, No. 1, February 1, ISSN 0887-3828/2012/1-54–64

Kim S. H., Yoon J. H., Jun K. H., Choi W. J. and Ahn J. H., (2011), *Evaluation On The Behavior Of Abutment–Pile Connection In Integral Abutment Bridge*, Journal of Constructional Steel Research 67 (2011) 1134–1148

Kirupakaran K., Hanlon B., Muraleetharan K. K. and Gerald A. M., (2012), *Field-Measured Response of an Integral Abutment Bridge*, ASCE GSP 225 Proceedings of GeoCongress 2012 held in Oakland, California, March 25-29, 2012, pp 2157-2166

Koch, E., 2006, *Eisenbahnbrücken bei der Deutschen Bahn* AG

Koh, S.K., and Stephens, R.I., (1991), *Mean Stress Effects on Low Cycle Fatigue for a High Strength Steel*, Fatigue Fracture of Engineering Material and Structures, Vol. 14, No. 4, pp. 413-428.

Krizek J., (2011), *Soil-Structure Interaction of Integral Bridges*, Structural Engineering International, Vol. 21, No. 2, pp. 169-174

Kunin J., Alampalli S., (1999), *Integral Abutment Bridges: Current Practice in the United States and Canada*, Report FHWA/NY/SR-99/132

Laaksonen A., (2011), *Structural Behaviour of Long Concrete Integral Bridges*, Ph.D. thesis, Tampere University of Technology, Publication 978

Mander J. B., Panthaki F. D. and Kasalanati A., (1984), *Low-Cycle Fatigue Behavior of Reinforcing Steel*, Journal of Materials in Civil Engineering, No. 6, pp. 453-468

Martin R. and Kang T., (2012), *Structural Design and Construction Issues of Approach Slabs*, Practice Periodical on Structural Design and Construction. Submitted January 23, 2011; accepted July 16, 2012; posted ahead of print November 3, 2012. doi:10.1061/(ASCE)SC.1943-5576.0000133

Maruri R. and Petro S., (2005), *Integral Abutments and Jointless Bridges (IAJB) 2004 Survey Summary*, Federal Highway Administration, (FHWA)/Constructed Facilities Center (CFC) at West Virginia University

May I. M. and Gordon S. R., (2006), *Development of in situ joints for pre-cast bridge deck units*, Bridge Engineering; 159(1), pp. 17-30.

Massachusetts Department of Transportation, (2013), *LRFD Bridge Manual Part I and Part II 2013 Edition*, https://www.massdot.state.ma.us/highway/DoingBusinessWithUs/ManualsPublicationsForms/LRFDBridgeManual2013Edition.aspx

Matlock, H., (1970). *Correlation for design of laterally loaded piles in soft clays,* 2nd Offshore Technology Conference, Houston, Texas, 577-594.

Meggiolaro M.A. and Castro J.T.P., (2004), *Statistical evaluation of strain-life fatigue crack initiation predictions*, International Journal of Fatigue 26 (2004) 463–476

Meyer B. J. and Reese L. C., (1979), *Analysis of Single Piles Under Lateral Loading*, Research Report 244-1, Center of Transport Research, University of Texas, Austin

Moberg A., Bergström H., Ruiz Krigsman J. and Svanered O., (2002*), Daily air temperature and pressure series for Stockholm (1756-1998*). Climatic Change 53: 171-212, temperature series available at http://www.smhi.se/klimatdata/meteorologi/temperatur/stockholms-temperaturserie-1.2847

Moorty S. and Roeder C.W., (1992), *Temperature-Dependent Bridge Movements,* Journal of Structural Engineering, Vol. 118, No. 4, pp. 1090-1105

Moulton L. K., GangaRao H. V. S. and Halvorsen G. T., (1985), *Tolerable Movement Criteria for Highway Bridges*, U.S. Department of Transportation Federal Hghway Administration , Report no. FHWA/RD- 85/107

Mourad S. and Tabsh S. W., (1998), *Pile Forces in Integral Abutment Bridges Subjected to Truck Loads*, Transportation Research Record 1633, Paper No. 98-0197

Mourad S. and Tabsh S. W., (1999), *Deck Slab Stresses In Integral Abutment Bridges*, Journal Of Bridge Engineering, 1999.4, p.p. 125-130

Nilsson M. (2001) *Samverkansbroar ur ett samhällsekonomiskt perspektiv*, Master Thesis, Luleå University of Technology, Sweden (in Swedish)

Nilsson M.,(2008), *Evaluation of In-situ Measurements of Composite Bridge with Integral Abutment*, Licentiate Thesis 2008:2 ,Lulea University of Technology

NYSDOT, (2005), *Bridge Manual –3rd Edition*, New York State Department of Transportation, Section 11.5.1.6

O'Neill M. W., (1985), *An Evaluation of the Behavior and Analysis of Laterally Loaded Pile Groups*, API, PRAC 84-52, University of Houston, University Park, Department of Civil Engineering, Research Report No. UHCE 85-11

Oesterle, R. G. and Tabatabai, H., (2014), *Design Considerations for Integral Abutment/ Jointless Bridges in the USA,* Civil and Environmental Engineering Faculty Articles. Paper 1. http://dc.uwm.edu/cee_facart/1

Pak D., Naumes J., Veljkovic M. , Nilsson M. ,Collin P ,Petursson H., Kerokoski O., Vroomen C. , Verstraete M., Haller M. and Hechler O., (2008), INTAB-*Economic and durable design of composite bridges with integral abutments*, Final Report RFSR-CT-2005-00041, European Commission, Research Fund for Coal and Steel Unit (RFCS).

Pak D., (2012), *Zu St*ahl-*Verbundbrücken mit integralen Widerlagern* (Ph.D. thesis in German), Heft 74, RWTH Aachen University, Shaker Verlag, ISBN 978-3-8440-0362-8

Pétursson H., (2000), *Bridges with Integral Abutment* (in Swedish), Lulea University of Technology

Phillip S. K. O., Xiaobin L., and Harold S. H., (2010), *Field Behavior of an Integral Abutment Bridge Supported on Drilled Shafts*, Journal of Bridge Engineering, Vol. 4, No. 2, May 1999, pp. 125-130

Potgieter I. C. and Gamble, W. L. (1983). *Nonlinear temperature distributions in bridges at different locations in the United States*, PCI Journal, Precast/Prestressed Concrete Institute, JulyAug 1983, pp. 80-103.

Poulus H. G. and Davis E. H., *Elastic Solutions for Soil and Rock Mechanics* (Soil Engineering),

Pugasap K., Kim W. and Laman J. A., (2009), *Long-Term Response Prediction of Integral Abutment Bridges*, Journal of Bridge Engineering, No. 14, pp. 129-139

Razmi J., Ladani L. and Aggour M.S., (2012), *Fatigue life of piles in integral abutment bridges, a case study*, Journal of Bridge Engineering, No. 18(10), pp. 1105–1117.

Rankine, W., (1857), *On the stability of loose earth*. Philosophical Transactions of the Royal Society of London, Vol. 147.

Reese L. C., Cox W. R., Koop F. D., (1974), *Analysis of Laterally Loaded Piles in Sand*, Offshore Technology Conference, Houston, Paper. No. OTC 2080

Shoukry S. N., William G. W. and Riad M. Y., (2008), *Response of an Integral Abutment Bridge to Temperature Variations*, Proceedings of the 2008 Structures Congress held in Vancouver, British Columbia, Canada, April 24-26

Skempton A.W, (1951), *The Bearing Capacity of Clays*, Building Research Congress, Division 1, Part 3, London

Svahn P.O. and Alén C., (2006), *Laterally Loaded Pile,s* Report 101 (In Swedish), Commission on Pile Resaerch, ISSN 0347-1047, www.palkommissionen.se

Thippeswamy H. K., GangaRao H. V. S., and Franco J. M., (2002), *Performance Evaluation of Jointless Bridges*, Journal of Bridge Engineering, Vol. 7, No. 5, ISSN 1084-0702/2002/5-276

Timoshenko S.P.,(1963), *Theory of Elastic Stability-second edition*, McGraw-Hill, ISBN 0-07-085821-7

TRVFS,(2011), *Swedish Road Administration regulations concerning amendments to regulations (VVFS 2004:43) on the application of European,* In Swedish, http://www20.vv.se/vvfs/pdf/2011nr012.pdf

Wasserman E. P., (2001), *Design of Integral Abutments for Jointless Bridges, Structure,* National Council of Structural Engineers, Council of American Structural Engineers and Structural Engineering Institute, 24-33.

Winkler, E., (1867), *Die Lehre Von Elasticitaet Und Festigkeit*, 1st Edn., H. Dominicus, Prague

White, H., (2007*), Integral Abutment Bridges: Comparison of Current Practice Between European Countries and the United States of America*., Special Report 152, Transportation Research and Development Bureau, New York State Department of Transportation

White, H., (2008), W*ingwall Type Selection for Integral Abutment Bridges: Survey of Current Practice in the United States of America*, Special Report 154, Transportation Research and Development Bureau, New York State Department of Transportation

Wolde-T. A. M., Greimann L. and Yang P. S., (1988a), *End-Bearing Piles In Jointless Bridges*, Journal of Structural Engineering, Vol. 114, No. 8, pp. 1870-1884

Wolde-T. A. M., Klinger J. E. and Elmer J. W., (1988b), *End-Bearing Piles In Jointless Bridges, Journal of Performance of Constructed Facilities,* 1988.2, pp 11-125

Xu M., Bloodworth A. G. and Clayton C. R. I., (2007), *Behavior of a Stiff Clay behind Embedded Integral Abutments*, Journal of Geotechnical and

Geoenvironmental Engineering, Vol. 133, No. 6, ISSN 1090-0241/2007/6-721–730

Xue J., (2013), *Retrofit of Existing Bridges wiith Concept of Integral Abuytment Bridge- Static and Dynamic Parametric Analyses*, PhD Thesis, University of Trento, Università IUAV di Venezia.

Zhuang Y., Chen B., Briseghella B. and Xue J. (2014), *Design and Practise of Jointless bridges in China,* Proceedings of 1st International Workshop of Integral Abutment/Jointless Bridges, 8-12 March, Fozhou University

Paper I

Innovative Solutions for Integral Abutments

Hans Pétursson and Peter Collin

This paper is based on tests planned and evaluated by Pétursson, who also has been the author of this paper. Collin has contributed with his experiences, views and opinions through the whole process.

Innovative Solutions for Integral Abutments

Hans Pètursson[a] & Peter Collin[b]

[a] M. Sc, Tekn.Lic, Ramböll Sverige AB, Luleå, Sweden

[b] Prof. Luleå Univ of Techn/Ramböll Sverige AB, Luleå, Sweden

Summary

The cost of maintenance is an ever-growing problem for road administrations around the world, and bridges are no exception to the rule. One way to reduce the need for future maintenance, as well as the investment cost, is to make bridges without transition joints. In order to investigate if the cross-shaped steel pile commonly used in Sweden is suitable for use in integral abutments, two full-scale laboratory tests were carried out. Experience from the United States shows that bridges with integrated abutments are increasingly outclassing the traditional bridges with joints, the former being not only less expensive to maintain, but also more affordable to build. In the following, two analytical methods are described that can be used to calculate the capacity of piles based on plastic design.

Keywords: composite bridges, integral abutments, steel piles.

1) Introduction

In some parts of USA, bridges with integral abutments have been built since the 1960's.

In Iowa bridges with integral abutments have been showing satisfying performance since 1964. The longest bridge measures approximately 100 m.

Featuring more than 2,400 bridges with integrated abutments, Tennessee is probably the state with the widest experience of this type of bridge. Over the years, the Department of Transportation has gradually extended the limits for the length of bridges with integral abutments to the current maximal 120 m for steel bridges and 240 m for concrete bridges. The limits are based on the expected movement at the bridge ends, which shall be less than 100 mm (50 mm at each end). The longest concrete bridge with integral abutments is 352 m and the longest in steel is 152 m.

Each year, New York State spends $7 million on replacements and repair of bridge joints [2]. In the beginning of the 1980's, the first integral abutment bridge was built. By 1996, 155 bridges with integral abutments had been built in the state. When a bridge is built today, the New York State Department of Transportation always tries to eliminate joints whenever possible.

In order to understand the mechanisms of an integrated abutment, it is necessary to study the effect that movement in the abutment has on the stresses in the pile. The bridge length varies with the structure's temperature. Movements in the piles are also induced by rotations of the superstructure.

Analysing the load carrying capacity of piles subjected to lateral movements is complex as it contains two codependent elements; the flexural pile and the soil. To further complicate matters, soils are often inhomogeneous. Analytical solutions are only possible to obtain for simple cases where the stiffness of the soil is constant along the pile and the materials feature elastic behaviour. Expressions for the case with constant soil stiffness are given by theories for beam on an elastic foundation [3]. To handle more complex cases where soil stiffness varies with depth, an equivalent stiffness can be assumed.

Although a section in a steel pile may reach yield stresses, this does not imply that the ultimate load is reached. The moment along the pile can be re-distributed and further load increase is possible. If elastic theory is used to calculate the moment distribution along the pile, the re-distribution effect is not accounted for. Analytical methods have been developed to calculate the capacity of piles based on plastic design.

2) Testing of steel piles restrained by elastic springs

The purpose of the tests described in this section was to detect the decrease of load carrying capacity of an elastically restrained steel pile, when the pile top is subjected to deflections arising from the traffic load. The piles tested were X130· 16 mm, delivered from Fundia AB.

One end of the pile was embedded in a concrete block to 500 mm. The concrete block was supposed to mimic the back wall of a bridge. The dimensions of the concrete block were 1.0· 0.75· 0.75 m.. Springs were attached to the pile at 1 m spacing. The springs would then respond to any pile movement in a manner resembling that of the soilaround a bridge pile. After moving the concrete block 25 mm transversely relative the pile, the latter was subsequently loaded through the concrete block until failure. The result shows that the load carrying capacity was substantial even after the transverse deformation.

The configuration of the testing can be seen in Fig. 1. The pile top was deflected 25 mm perpendicular to the pile length axis.
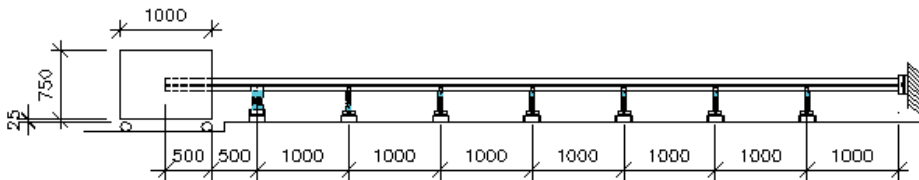
Fig. 1 The test set-up.

The yield stress of the steel in the piles was 310 MPa according to the manufacturer and it was proven by tensile tests of the steel (see Table 1).

Table 1 Results from tensile tests of steel in piles.

	fy (MPa)	fu (MPa)	E (GPa)	A5
Test pile 1 coupon 1	325	513	225	0,346
Test pile 1 coupon 2	321	509	218	0,367
Test pile 2 coupon 1	320	504	197	0,350
Test pile 2 coupon 2	317	506	215	0,252

The results of the tests showed that the piles capacity was 73% and 79% of the theoretical capacity of a perfectly straight pile. The piles tests were also simulated with the FE-program DIANA. The results from the FE-simulations showed good agreement with the pile tests (within 5%). This made it possible to simulate the ultimate load for a variety of conditions to verify the proposed design method. The FE-analysis is described in more detail in [1].
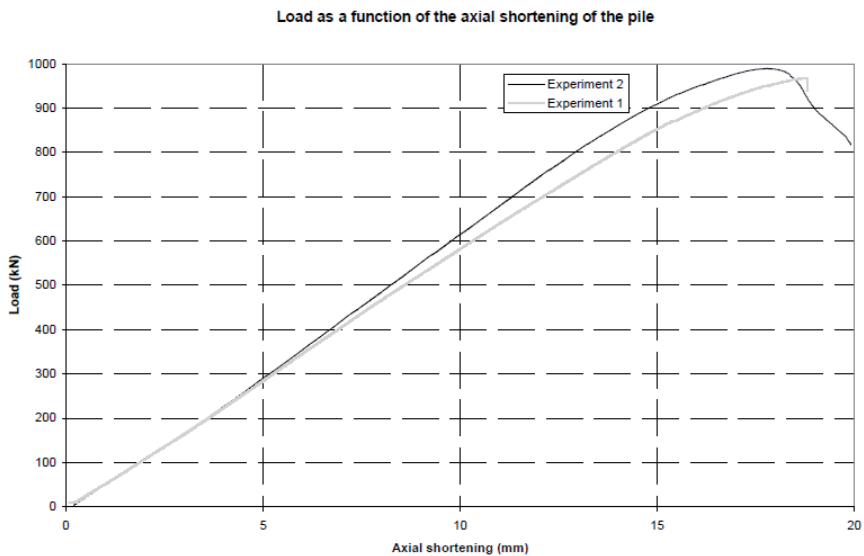
Fig. 2 Results from pile testing.

Table 2 Results from pile testing.

	Ultimate load test (kN)	Ultimate load (fyk· A)	Ultimate load	FE (kN)
Test 1	967	0	73	1005
Test 2	990	0	79	1007

3) Pilot Project

3.1 Bridge over Fjällån

Fig. 3 Bridge over Fjällån after completion

In the 1980's a few bridges with integral abutments were built in Sweden. Most of the short to medium span bridges in Sweden are semi-integral, meaning that there are no joints on the road surface but that the bridge rests on bearings. In a project at Lulea University of Technology it was investigated if the cross-shaped piles were suitable for integral bridges. Within the project a bridge was built in the Swedish province of Västerbotten, completed in September 2000. The bridge was a single span composite bridge with a span length of 37.15 m.

In order to minimise the bending stresses arising from the deflection of the bridge, the work was carried out in the following way:

1) Eight piles, X180· 24 mm, were used for each abutment. The piles were rotated 45 degrees from the line of support, minimising the bending stresses from the traffic load, (see Fig. 5.)

2) The side wings and the lower parts of back walls were cast.

3) The steel girders were erected on steel bearings on top of the lower part of the back wall as seen in Fig.

4. On safe-hand side, the girders were designed as simply supported girders, not taking the restraint from the embankment into account.

4) The formwork for the side wings was removed, giving the steel piles a rotation in the opposite direction of the one arising from the traffic. In other words, the piles were pre-stressed.

5) The upper parts of the back walls were cast together with the concrete deck of the bridge.

6) The embankment behind the back walls was filled up, and the pavement as well as the side rails was placed on the bridge.
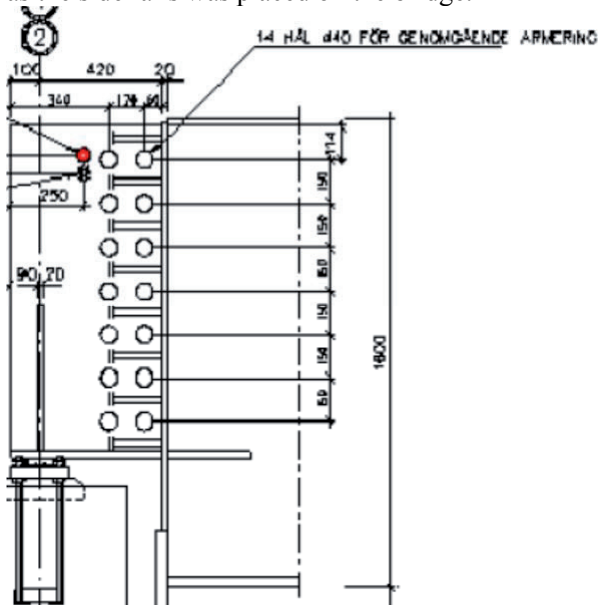
Fig. 4 Detail of the connection between the steel beam and abutment.

One of the main reasons why integral abutment bridges have not yet become common in Sweden is the difficulty to analyse them.
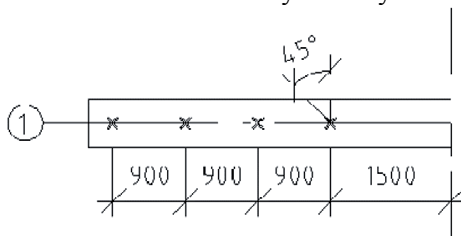
Fig. 5 Pile configuration.

3.2 Bridge crossing the Hökvik River.

The bridge crossing the Hökvik River is located in the central part of Sweden outside the city of Falun. The bridge is a two lane arch bridge with span 42 m and will replace an old concrete arch bridge. The time schedule for the construction of the bridge is very tight. The Swedish road administration (Vägverket) bought the construction work in February 2004 and the bridge is scheduled to be finished in September 2004. The foundation of the old bridge will be left in place and the piles of the integral

abutment will be driven just behind the old abutment. The backfill behind the old abutment will be removed and the piles will be driven from a level 3.65 m below where the lower edge of the back wall will be. Then steel tubes will be placed over the piles and sand will be filled around the piles. The soil where the piles are to be driven consists of dense sand.

The sand will be loosely packed and therefore the pressure against the piles will be minimised when he piles deforms due to abutment translation and rotation. Then the bank will be filled up to the level of the lower side of the back wall. One part of the back wall can then be cast toact as support to the steel arch. The steel arch is built before the old bridge is removed and can be used during the removal work. After the removal of the old bridge the concrete road way can be cast between the two steel arches.

The superstructure is a steel arc with inclined hangers. The inclined hangers will substantially stiffen the superstructure compared to vertical hangers, especially for unsymmetrical loading.

The piles that are used are cross shaped steel piles with 200 mm width and 30 mm thickness. Eight piles are placed under each support and the outermost piles are inclined 4:1 to take care of transverse horizontal loading as wind and transverse component of vehicle brake forces.

Integral abutments were chosen for this bridge merely for the economical benefits. Money and time was saved because old abutments did not have to be removed.
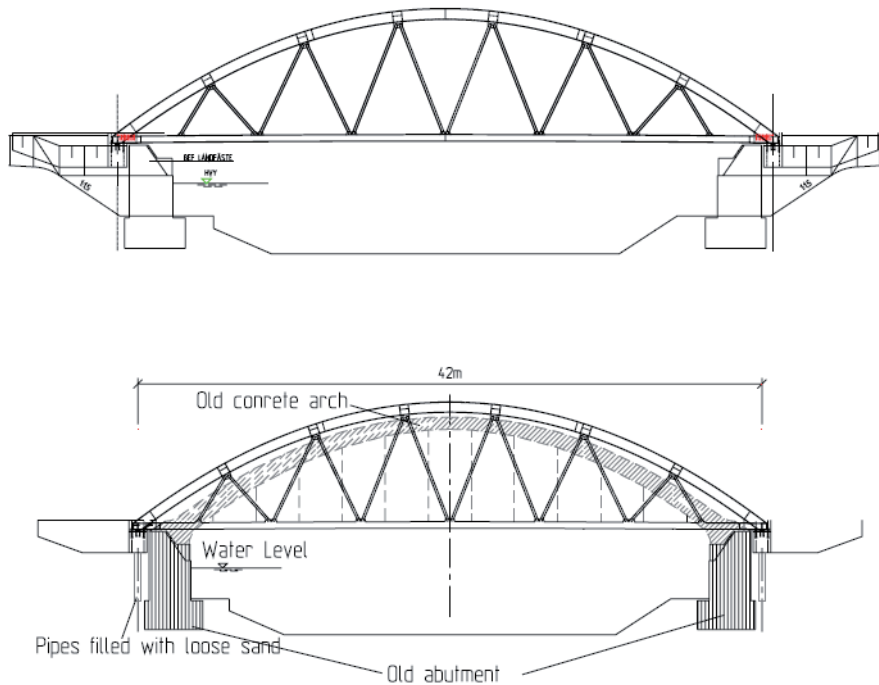
Fig. 6 Sketch showing bridge over the Hökvik River.

4) Design Method Proposal

4.1 Global analysis

The global analysis can be carried out in a number of ways. To be competitive, bridges with integral abutments need to be designed in a rational manner. With computer programs it is possible to model the interaction between piles and bridge deck in a realistic manner. The ultimate strength of the piles can be calculated with FEM where the non-linear behaviour of the steel piles and earth surrounding the piles are modelled in a realistic way. Stresses in serviceability state for piles in soils where properties vary with depth are also convenient to calculate with FEM. Non-linear FE-calculations are often time consuming and not wide spread among bridge engineers. And even if designers have the necessary tools to make an advanced un-linear FE-analysis there is a need for a simpler method

The global analysis is often made with a 2D computer program with beam elements. This can also be done for a bridge with integral abutments. The connection between the back-wall and the piles can be regarded as pinned and the girder can be assumed to expand and extract without resistance. The stiffness of the piles is low and can be neglected compared to the stiffness of the girder. To include the normal force and moment of the earth pressure against the back wall spring elements can be used. The

springs should have different properties in tension and compression to account for passive and active earth pressure.

4.2 Serviceability Limit State

Usually the calculated stress in a steel component shall not exceed characteristic value of the yield stress in the serviceability limit state. In reality residual stresses from manufacturing are added to the calculated stresses. Welded beams have residual stresses around the welds that can be as high as the yield stress even before the beams are loaded. One argument for having the yield strength as a limit in serviceability limit state is to prevent plastic deformation from accumulating and thus giving a bent impression of the structure. In an integral abutment accumulated plastic deformation in the piles will not affect the bridge deck due to the difference in stiffness.

Another argument is that the accumulated deformations also accelerate the strains and finally cause a collapse. The loads that can cause repeated yielding in the piles are traffic and temperature. The moments that are induced by these loads are interacting when the temperature is high.

Assume that a pile is subjected to a great number of load cycles with stochastic varying magnitude. In the worst case the stress in the pile reaches yield stress in compression in one edge and is then unloaded elastically. If the magnitude of the next load cycle is exactly the same the stress will reach the yield stress but no additional plastic deformations will occur. If the magnitude of the load is less in the second cycle than the first the stress will not reach the yield stress.

In reality the weight of the trucks that passes over a bridge will vary and there will not be two identical load cycles. As the number of trucks increases the risk of additional plastic deformation decreases. Thus the number of cycles that cause plastic deformation will be limited.

If the load amplitude of the cycles are varying in a stochastic manner the chance of all time high stress in the pile is:

For load cycle 1: 100%

For load cycle 2: 50%

For load cycle 3: 33% etc.

The total number of cycles that causes all time high stress in the pile can be written as the sum of 1/x were x goes from 1 to total number of load cycle. Integration gives a value that for 400 000 load cycles gives

$$\int_{0.5}^{400,000} \frac{1}{n} dn = \ln(400,000) - \ln(0.5) = 14 \text{ load cycles} \qquad (1)$$

This does not mean that all 14 cycles will give plastic deformation.

The traffic loads in most design codes are of a magnitude that most trucks do not reach. The worst case when the temperature in the structure reaches the design value

only occurs for a limited numbers of days every year. The conclusion is that plastic deformations will only occur a few times even if the calculated stresses will exceed the yield stress

If yield stresses shall be allowed in steel piles the restriction is that low cycle fatigue should be avoided. This can be done with Whöler diagrams. The strain width that is calculated in the piles is substituted by stress width. The stress width is calculated as strain times $E = 210\ GPa$. The number of cycles that can be permitted with the strain width ε can be written as:

$$n_t = \left(\frac{C}{E \cdot \varepsilon \cdot 1.1 \cdot 1.2}\right)^3 \cdot 2 \cdot 10^6 \text{where} \tag{2}$$

C = detail category according to Euro code 3, 112 MPa.

E = elastic Young's modulus

ε = strain width.

If the yield strength in the pile is 355 MPa and the strain width in the serviceability is 6·355/210000=1,0 %

the number of cycles before fatigue limit is reached:

$$n_t = \left(\frac{112}{6 \cdot 355 \cdot 1.1 \cdot 1.2}\right)^3 \cdot 2 \cdot 10^6 = 127 \tag{3}$$

If it is assumed that the design values for traffic and temperature are reached once every year each in a stochastic manner the probability that they occur simultaneously is one in 133 000. It is highly unlikely that temperature and traffic load will occur at the same time during the 100 years that a bridge is supposed to be in service, if the assumptions above are true There are however loads of a smaller magnitude that will cause fatigue damage to the pile.

There are a number of parameters that influence the magnitude of the strains in a pile, such as temperature variation, numbers of trucks that pass the bridge and their weight, span length, stiffness of soil surrounding the pile, stiffness of the bridge deck and the height of the abutment wall. It is thus difficult to suggest design rules that are valid for all bridges with integral abutments. An attempt to quantify the strains than can beexpected in a bridge with integral abutments is described in [1].

The moment that acts on a pile due to temperature change in the bridge deck is:

$$M_0 = \frac{\Delta \cdot k_h \cdot L^2}{2} = \frac{\Delta \cdot k_h \cdot \sqrt{\frac{4 \cdot E \cdot I}{k_h}}}{2} = \Delta \cdot \sqrt{k_h \cdot E \cdot I} \tag{4}$$

If the stress reaches yield the moment can be expressed as:

$$M_0 = \frac{2 \cdot f_y \cdot I}{b} \tag{5}$$

If the two expressions above are equal then the soil stiffness is:

$$k_h = \frac{4 \cdot f_y^{\,2} \cdot I}{\Delta^2 \cdot b^2 \cdot E} \tag{6}$$

The strains caused by traffic depend on a number of parameters. If both the steel pile and soil are elastic the strain is:

$$\varepsilon = \frac{N}{A \cdot E} + \frac{b}{I \cdot E} \cdot \frac{\Delta \cdot k_h \cdot L^2 + \alpha \cdot k_h \cdot L^3}{4} \tag{7}$$

If the traffic load is added when the pile top have obtained yield stress the strains will be higher. The rotation is assumed to take place in a region of the pile that has a length twice the size of the width of the pile and the plastic region acts like a frictionless hinge where the strain will be:

$$\varepsilon = \varepsilon_N + \frac{\Delta}{2 \cdot L} = \varepsilon_N + \frac{\Delta}{2 \cdot \sqrt[4]{\dfrac{4 \cdot E \cdot I}{k_h}}} + \frac{\varphi}{2} \tag{8}$$

It is reasonable to design the pile as a pile with hinged connection at the top in the serviceability stage. This way the stresses in the pile will be limited and a plastic hinge is allowed to form in the pile top. The design can then be done with conventional methods. An analysis can have the following steps:

The global analysis gives the axial force N, horizontal displacement Δ_D and rotation α with appropriate partial load factors γ_l. The horizontal displacement at the piles:

$$\Delta = \Delta_ö + \alpha \cdot e \tag{9}$$

where e is the vertical distance from the centre of the bridge deck to the pile top. The horizontal displacement Δ should not exceed 25 mm in the serviceability limit state.

The stress in the pile is calculated as:

$$\sigma = \frac{N}{A} + \frac{b}{A} \cdot \frac{\Delta \cdot k_h \cdot L^2}{4} \tag{10}$$

and shall not exceed f_{yk}.

4.3 Ultimate limit state

The capacity in the ultimate limit state is limited by buckling and by moment/rotational capacity as illustrated in. The load capacity in the ultimate limit state is according to Granholm [5].

$$\frac{N_u}{N_{cr}} + \frac{N_u}{N_P} = 1.0 \tag{11}$$

N_p = plastic capacity (see b)

N_{cr} = elastic buckling load (see a.)
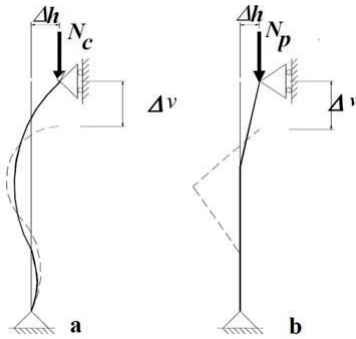
Fig. 7 Failure modes for compressed piles.

To calculate the buckling load the following equation can be used for pile with hinged top and were the stiffness of the soil is constant [4]:

$$N_{cr} = 2.0 \cdot \sqrt{k_h \cdot E \cdot I} \tag{12}$$

If the pile top is fixed the buckling load is [4]:

$$N_{cr} = 2.5 \cdot \sqrt{k_h \cdot E \cdot I} \tag{13}$$

For soils with linearly varying stiffness with depth and pinned top the buckling load is [4]:

$$N_{cr} = 2.3 \cdot (E \cdot I)^{\frac{7}{5}} \cdot \sqrt{n_h} \tag{14}$$

For soils with linearly varying stiffness with depth and fixed top the buckling load is [4]:

$$N_{cr} = 4.2 \cdot (E \cdot I)^{\frac{7}{5}} \cdot \sqrt{n_h} \tag{15}$$

If the soil stiffness varies in a more complicated way equivalent soil stiffness is calculated and the formulas above can be used. The plastic capacity of the pile is for hinged pile top [4]

$$N_p = \frac{2 \cdot M_p'}{\Delta} \tag{16}$$

and for fixed pile top [4]

$$N_p = \frac{4 \cdot M_p'}{\Delta} \qquad (16)$$

When the buckling and plastic capacity of the pile have been calculated the normal force N horizontal displacement ΔD and the rotation α are taken from the global analysis. The horizontal displacement of the pile top can be calculated as $\Delta D + \alpha \cdot e$ where e is the distance between the gravity centre of the composite section and the pile top.

5) Comparison to other foundation methods

In the masters thesis of Anna Nilsson and Kristoffer Torén[6], the economical aspects of 15 different bridges in northern Sweden were investigated. For four of those bridges, the cost for five optional foundations were studied, namely;

A Bridge founded above ground water level

B Bridge founded under ground water level, concrete cast in the water

C Sheet pile wall and unreinforced bottom layer of concrete preventing water intrusion

D Elevated foundation

E Integral abutments

A geotechnical expert at the road authorities was designing the optional foundations with respect to geometri etc. A contractor calculated the total prices for the bridges.

The four bridges studied were built in concrete, with the span 15.9, 21.4, 18.1 and 16.0 m span, respectively. The free width was 7 m for the first three bridges, and 9 m for the last. The prices indicated in fig. 8 are the mean values for those four bridges.
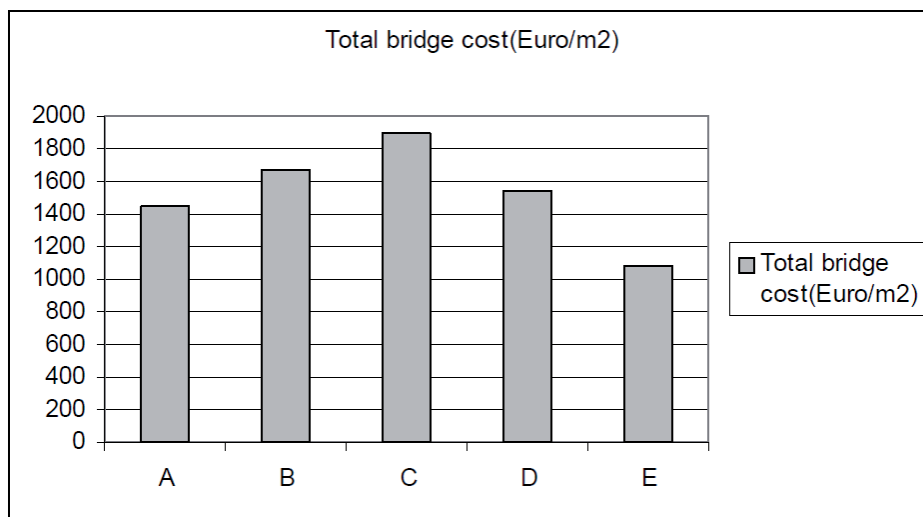
Fig. 8 Bridge costs for different bridges.

6) Conclusions

The concept of bridges with integrated abutments has several advantages such as minimised maintenance costs and the removal of joints and bearings at end supports of a bridge. The concept has been proved to be competitive in the USA, and is believed to be so in most countries, if only given the chance by contractors and the authorities. In Sweden the concept can save much effort, as no work has to be carried out under the water level. Laboratory tests as well as computer simulations indicate that the decrease in load capacity due to rotations and translations of the pile top should be no problem. A full scale in situ test of such a bridge, with respects to the stresses the piles, should be worth carrying out, to verify the tests and simulations mentioned above.

In the bridges carried out so far, the critical section for the piles have been at the pile top, since the bending moments from translation and are concentrated here. The stresses from bending moments are normally of the same magnitude as those from the vertical load itself. This implies that a modified design with respect to the restraint of the pile top might very make the concept even more competitive, if those bending stresses could be reduced. One solution could be to use spherical steel bearings on the pile tops, and surround the upper parts of the piles with a very soft material.

7) References

[1] Pétursson Hans, Bridges with integral abutments, Licentiate thesis / 2000:32 (2000), Lulea University of Technology, Dept. of Steel Structures

[2] Alampalli, Sreenivas and Yannotti P Arthur,- In Service Performance of Integral Bridges and Jointless Decks-Transportation Research Record 1624-pp. 1-7

[3] Theory of Elastic Stability, Timoshenko S.P., McGraw-Hill

[4] Greimann L F and Wolde-Tinsae A M, Design Model For Piles In Jointless Bridges(1988), Journal of Structural Engineering, Vol. 114, No 6, pp 1354-1371, ISSN 0733-9445/88/0006-1354

[5] Granholm H, On the Elastic of Piles Surrounded by a Suporting Medium, Centraltryckeriet Stockholm, 1929

[6] Anna Nilsson, Kristoffer Torén, Foundation methods for small span bridges, Masters Thesis 2001:122, Luleå University of Technology (in Swedish).

Paper II

Integral Abutment Bridges: The European Way

Harry White II, Hans Pétursson and Peter Collin

<u>Published in:</u>

Practice Periodical On Structural Design And Construction, Practice Periodical on Structural Design and Construction, Vol. 15, No. 3, August 2010, pp. 201-208.

Paper II presents results from a European survey that was conducted by Pétursson and Collin in early 2007 to illustrate the design criteria used by different countries for Integral Abutment Bridges . The paper is written by Pétursson based on a report written by White. White and Collin have read and suggested improvements on drafts of the paper.

Integral Abutment Bridges: The European Way

H. White II[1]; H. Pétursson[2]; and P. Collin[3]

Abstract: Integral abutment bridges are becoming more popular in Europe, but the traditions differ from country to country. This leads to different technical solutions for the same problem in each country. A European survey was conducted in early 2007 to illustrate the design criteria used by each different country for integral abutment bridges. The survey requested information useful to a designer comparing the design requirements and restrictions of various European countries. As an added measure of comparison, these results were compared to some recently conducted surveys of state agencies within the United States. When looking at the results of the European survey responses and past surveys of U.S. transportation agencies, it is clear that there are many similarities in design assumptions and construction practices. Yet, there are also significant differences.

Introduction

Integral abutment bridges (IABs) are structures where the superstructure and substructure move together to accommodate the required translation and rotation. There are no bridge expansion joints and in the case of fully IABs (FIABs), there are no bearings. In the United States, there are more than 9,000 FIAB and 4,000 semi-IABs (SIABs) (Maruri and Petro 2005). The IAB have proven themselves to be less expensive to construct, easier to maintain, and more economical to own over their life span (Maruri and Petro 2005). The European experience with IAB is significantly less, but what experience has been gained has been positive. As a result, the trend is toward making IAB a larger percentage of all newly constructed bridges across Europe (Fig. 1).

As an example, in 1999 the German Federal Ministry of Transport, Building, and Urban Affairs (BMVBS) published a list of 10 single span prototype bridges and recommended their use to the authorities (Bundesministerium für Verkehr, Bau- und Wohnungswesen 1999). Eight of these 10 bridges were FIAB with a maximum span of up to 150 ft. (45 m). In 2003, many of the BMVBS recommendations were replaced by the Eurocode-based DIN Fachbericht 101 to 104, which contained no specific rules concerning IAB. Given the lack of governing standards or guidelines for IAB in Germany, designers must rely only on their experi-

ence. The result is that only a small group of engineering companies have specialized in frame bridges and IAB, respectively.

To broaden the knowledge base for IAB design and construction, the International Workshop on IABs was held in Stockholm, Sweden in May of 2006. Designers and researchers from eight different countries participated in the workshop. The goal of the workshop was to share the experiences of the participants and to further the understanding of the design, construction, and maintenance of IAB.

During the workshop, it became clear that each country represented a slightly different approach to the design of IAB. In spite of the different viewpoints, each representative indicated that their designs were successful and stated that they would be constructing additional IAB in the future (Collin et al. 2006).

European Survey

As a follow-up to the information obtained from the workshop, a European survey (White 2007) was conducted in January of 2007 to illustrate the design criteria used by European countries for IAB. The survey was sent to representatives of every European country where IAB had been constructed. Of those countries that were contacted, bridge designers from England, Finland, France, Ireland, Luxembourg, Germany, and Sweden responded to the survey. The answers from France and Luxembourg were not included in the final results. France uses a great number of three-sided reinforced concrete fixed frame structures, but no true IAB as described above. Luxemburg had limited input to the survey due to its limited bridge population.

The survey requested information that would be useful to a designer when comparing the design requirements and restrictions of various countries. A summary of the responses to the survey may be found in Table 1. Each country that responded to the European survey indicated that IABs are permitted as a design option. In fact, the U.K. and Ireland requires that all bridges less than 200 ft. (60 m) and with a skew less than 30° be constructed as an IAB unless there are overriding reasons.

It is important to note that the responses obtained are from practicing bridge engineers of their respective countries. These

[1]Professional Engineer, New York State Dept. of Transportation, POD 3-4, 50 Wolf Rd., Albany, NY (corresponding author). E-mail: HWhite@dot.state.ny.us

[2]Licensed Engineer, Swedish Rail Administration, 781 85 Borlänge, Sweden. E-mail: hans.petursson@banverket.se

[3]Professor of Technology, Dept. of Civil, Mining and Environmental Engineering, Luleaa Univ. of Technology, LTU SE-971 87 Lulea, Sweden. E-mail: Peter.Collin@ramboll.se

PRACTICE PERIODICAL ON STRUCTURAL DESIGN AND CONSTRUCTION © ASCE / AUGUST 2010 / **201**

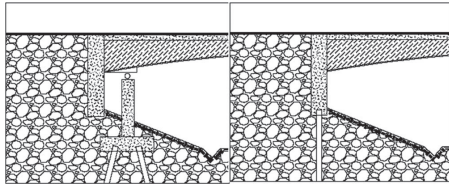Pract. Period. Struct. Des. Constr. 2010.15:201-208.

101

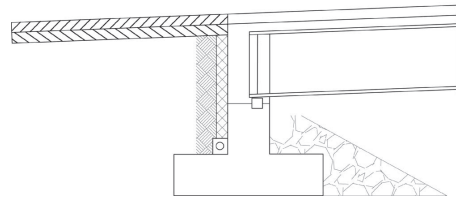**Fig. 1.** Examples of a SIAB to the left and FIAB to the right

Fig. 2. Example of an IAB on spread footing used in the U.K. (Iles 2005, with permission from SCI)

engineers work for government agencies, consulting firms, technical universities, or a combination of the above. In many cases, the engineers design structures in countries besides their own. These varied experiences give them a unique viewpoint on the issue of IAB design.

Since IAB are a relatively new concept in Europe, the codes are rapidly changing to keep pace with new information. The survey responses are accurate as of the time of the European survey, but may be changed at any time. A unified Eurocode for bridge design has been adopted by most European countries. The old bridge codes are being phased out and should be completely replaced by 2011. However, national rules for items such as bridge detailing will still exist. As an added measure of comparison, the results of the European survey were compared to some recently conducted surveys of state agencies within the United States in an effort to provide a frame of reference to the reader.

Foundation Requirements

IAB are still quite new in most European countries. There are few standards. The experiences from other bridge foundations types

are the starting point from which engineers in Europe apply the concept of integral abutments.

Pile foundations are not always required in Europe for FIAB. This is in direct contradiction to many U.S. agency requirements. Many U.S. agencies require the piles to be placed in a single row (Maruri and Petro 2005) on the belief that the single row permits the abutment stem to translate into and out of the soil while also permitting rotation of the abutment stem. Spread footings, by their very nature, restrain the rotation of the abutment stem (Fig. 2). In the U.K., however, spread footings are the preferred foundation for FIAB on the belief that the bridge and the approach pavement will settle equally. There have not been any reported problems related to the restrained abutment rotations.

Despite the success in the U.K., most European countries use a pile supported foundation for their FIAB. The European Survey indicates that designers account for the bending forces in the piles. In most European countries, empirical design is not permitted, and the function of the bridge must be verified by calculations. Although there are no requirements for the procedure, designers typically create a computer finite-element model using

Table 1. Summary of Selected Criteria Used by European Respondents

Criteria	England	Finland	Ireland	Germany	Sweden
Use fully IABs?	Yes	Yes	Yes	Yes	Yes
Maximum skew angle?	30°+	30°	30°+	None	None
Steel pile foundation used?	Yes	Yes	Yes	Rarely	Yes
Steel pipe pile filled with reinforced concrete?	Rarely	Yes	Yes	Rarely	Yes
Reinforced concrete pile foundation used?	Yes	Rarely	Yes	Yes	No
PS piles used?	Rarely	No	Rarely	No	Yes
Spread footing used?	Yes	No	Yes	Yes	Yes
Use active soil pressure, full passive soil pressure, or other requirement?	Other requirement	Depends on span length	Other requirement	Passive	Depends on span length
Approach slabs recommended?	No	Yes	No	Yes	Varies
Wingwalls permitted to be cast rigidly with abutment stem?	Yes	Yes	Yes	Yes	Yes
Use SIABs?	Yes	Yes	Yes	No	Yes
Maximum skew angle?	30°+	30°	30°+	—	None
Steel pile foundation used?	Yes	Yes	Yes	—	Yes
Steel pipe pile filled with reinforced concrete?	Rarely	Yes	Yes	—	Yes
Reinforced concrete pile foundation used?	Yes	Rarely	Yes	—	—
PS piles used?	Rarely	No	Rarely	—	Yes
Spread footing used?	Yes	Yes	Yes	—	Yes
Use active soil pressure, full passive soil pressure, or other requirement?	Other requirement	Depends on span length	Other requirement	—	Depends on span length
Approach slabs recommended?	No	Yes	No	—	Varies
Wingwalls permitted to be cast rigidly with abutment stem?	Yes	Yes	Yes	—	Yes

Fig. 3. H-piles in corrugated polythene pipe sleeves (Iles 2005, with permission from SCI)

Fig. 5. Swedish IAB detail with small diameter steel pipe piles

theoretical springs to represent the soil supporting the pile along its length, as well as the fill behind the back wall.

The design philosophy varies between different countries and that is reflected in their choice of pile. Some countries strive to make the piles stiff to resist the stresses induced from the abutment translation and rotation while others choose slender piles in an attempt to lessen the impact of the piles on the overall structure. For example, England, Ireland, and Sweden use sleeves around the piles to prevent soil from restraining the free bending of the piles during superstructure translation (Figs. 3 and 4). This theoretically distributes any longitudinal translation and rotation along a greater length of the pile, thereby reducing the moment induced in the pile. Without the soil to prevent the buckling of the pile, this method of construction may require stronger piles to accommodate the unsupported length.

The following is a listing of the various pile types that are used with FIAB in Europe.

• X-piles. Cross-shaped steel piles, also called X-piles, have been used to support integral bridges in Sweden (Pétursson 2000). The X-shaped piles are driven vertically and rotated 45° in order to minimize the bending stresses (Collin et al. 2006). This pile type is being discontinued by the manufacturer, thus it will not be used in the future.

• H-piles. H-piles are not commonly used in Europe. This practice is quite different from the United States, where more than 70% of State agencies reported (Maruri and Petro 2005) using steel H-piles for a majority of their IAB. Of the agencies that use steel H-piles, 33% required the orientation of the strong axis of the pile perpendicular to the bridge expansion, while 46% required orientating the weak axis perpendicular to the bridge expansion. The remaining percentages either had no

requirement or always used symmetrical piles. When they use piles, England and Ireland use steel H-piles with the strong axis perpendicular to the bridge expansion.

• Small diameter pipe piles. Small diameter pipe piles are not commonly used for FIAB in Europe or the United States. Small diameter pipe piles may be drilled or driven. In rocky soil, it is best to predrill for the piles when precise location is important (Fig. 5).

• Large diameter steel pipe piles. Large diameter steel pipe piles filled with reinforced concrete are the most common pile type used in Europe. In Finland, more than 1,000 jointless bridges have been built in the last 10 years (Kerokoski 2006), and a large percentage of them rest on reinforced concrete filled steel pipe piles. These steel pipe piles are typically 2.25 ft. (700 mm) in diameter but can be up to 4.0 ft. (1.2 m) in diameter (Fig. 6). If the distance to the bedrock is short, pipe piles can be used (Fig. 7). In this case, the design usually assumes that the large diameter piles provide fixity at the beam ends, and the beam's midspan moments decrease while the end moments increase.

Fig. 6. Finnish FIAB with large diameter steel pipe piles during construction [picture by Anssi Laaksonen, Haavistonjoki Bridge Monitoring, Tampere University of Technology, with permission (Kerokoski 2006)]

Fig. 4. Reinforced concrete piles inside concrete manhole rings (picture by David Price of Mott MacDonald Ltd., with permission)

Fig. 7. Short steel pipe piles on rock as used in Sweden

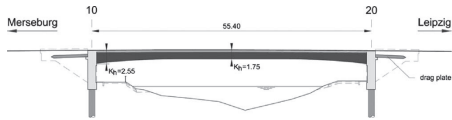# Design of steel piles for integral abutment bridges

Fig. 8. Sketch of a German bridge with reinforced cast-in-place concrete piles (SSF Ingenieure, Germany, with permission)

- Cast-in-place reinforced concrete piles. Cast-in-place concrete piles are used in some European countries. In Germany, large diameter cast-in-place piles are used to constrain end rotation and lower the midspan beam moments (Fig. 8). These piles typically have a diameter of 3.0 ft. (900 mm). The desired constraint could also be obtained by using wide spread footings.
- Precast (PC) and prestressed (PS) concrete piles. PC and PS concrete piles are not commonly used in Europe, with the exception of Sweden. In Sweden, PC/PS concrete piles are common in all bridge types, including FIAB, due to their low cost and ready availability.
- Steel core piles. Although not common, steel core pipe piles have been used for FIAB in Europe. The pile system consists of a cover pipe, injected concrete, and a core steel pile (Fig. 9). Drilling is performed down to the bedrock. The cover pipe is
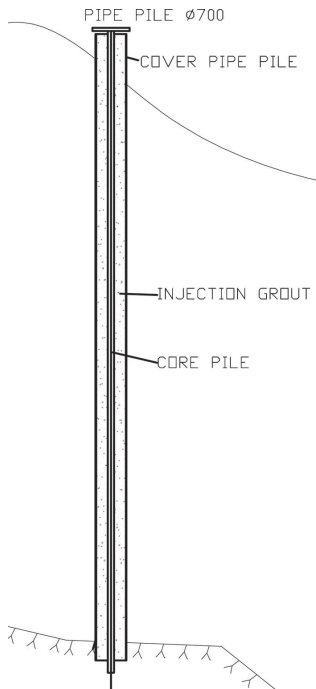
drilled 12 in. (300 mm) into bedrock and the pile is drilled 20 in. (500 mm). When the cover pipe is placed in the hole, the interior is rinsed and then injected with concrete. The steel core is then installed. After inspection and driving pile to refusal, the pile is cut to the right length. A pressure distribution plate is then fit to the top of the pile. In this way the very slender steel pile can be used and the concrete stabilizes the pile from buckling. A few FIAB have been built in Sweden with steel core piles.

Backfill

The most common backfill material used by European countries is well-compacted gravel or sand. In the United States (Maruri and Petro 2005), 69% of the responding states require well-compacted granular backfill, while 15% require the backfill to be left loose in an effort to reduce forces on the moving abutment stem.

Some European countries require that the backfilling operations are conducted evenly on both sides of the structure to reduce any undue lateral forces on the structure. Other countries have no requirements at all for backfilling procedures.

None of the countries require the use of an elastic "cushioning" material behind the abutments. In the United States, 23% of the respondents use some sort of compressible material behind the abutment stem to lessen the soil pressure on the abutment stem (Maruri and Petro 2005).

When questioned about the design soil pressure behind the abutment stem, there was little agreement among the European countries. Germany uses full passive pressure. Ireland and England have formulas in their design codes that estimate the soil pressure behind an IAB as typically being between the classical "at rest" pressure and full "passive" pressure (*BA 42/96* 2003). The same goes for Sweden, where full passive pressure is used only if the movement is more than 0.005 times the height of the abutment stem. In Finland, the type of soil and the horizontal displacement of the abutment stem into that soil dictate when full passive pressure is applied (Finnish Road Administration 2002). In the United States, 59% of the states surveyed accounted for full passive pressure. The remaining states used either minimum mandated loadings, active or at rest pressures, or did not consider lateral loads (Maruri and Petro 2005).

Approach Slabs

According to the European survey, approach slabs are not required for bridges with integral abutments. However, most countries indicated that approach slabs were desirable and that their length range from 10–25 ft. (3.0–8.0 m). European approach slabs are most commonly buried beneath the roadway surface. One end is connected to the back of the abutment stem and moves horizontally along with the bridge abutment. The other end of the slab is buried at least 20 in. (500 mm) under the road surface (Fig. 10). Most states in the United States require the use of approach slabs to reduce impact forces that are caused by vehicles when axles move from the relatively soft embankment to the stiff bridge. Almost half (46%) of those states report (Maruri and Petro 2005) that settlement of the approach slab is a maintenance problem. Use of a buried approach slab or "drag plate" makes settlement of the approach slab more easily repairable and may eliminate this concern.
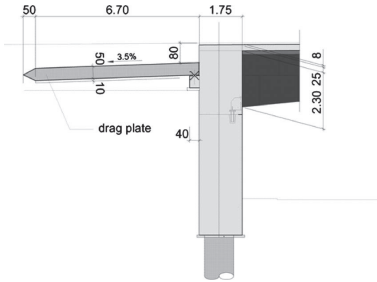

Fig. 9. Sketch of a steel core pile as used in Sweden

104

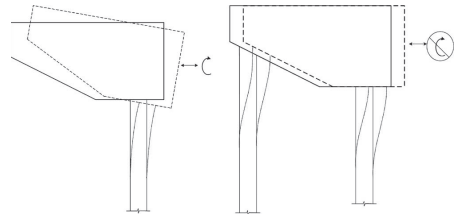**Fig. 10.** Example of a German drag plate approach slab (SSF Ingenieure, Germany, with permission)

Fig. 12. Movement and rotation of an FIAB with cantilevered U-wingwalls with and without piles beneath the wingwall

Wingwalls

A wingwall is defined as the retaining walls adjacent to the abutment stem which retain the fills behind the abutments and ensure the slope stability of the approach roadway. The European survey respondents indicated that there are no restrictions on the use of U-wingwalls (wingwalls that are perpendicular to the abutment stem, Fig. 11). Typically, the U-wingwalls are rigidly cast with, and are cantilevered off of, the rear of the abutment stem. Although it is not common, some permit the use of piles beneath the U-wingwalls. Having multiple piles in the line of rotation provides a moment coupling force that restrains rotation of the abutment stem and may induce forces into the structure that were not accounted for in the design (Fig. 12). In the United States, 81% of surveyed states (White 2008) permit the use of U-wingwalls but do not typically permit piles to be placed beneath them in order to allow the entire abutment to translate and rotate.

The European survey also indicates that other wingwall types, such as flared wingwalls (Fig. 13) and in-line wingwalls (Fig. 14), are also permitted. Each of the countries permit, and in fact encourage, the wingwalls to be rigidly cast with the abutment stem so that they move into and out of the retained soil. There are no established maximum lengths before the wingwalls are required to be placed on an independent foundation.

In the United States, 32% of state agencies permit the use of flared wingwalls, while 65% permit the use of in-line wingwalls

(White 2008). Maximum length limit on when the wingwalls must be placed on a foundation separate from the abutment stem are not consistent from state to state.

Beam Design

According to the European survey, the bridge beams are designed using a number of methodologies. For small skews, most countries permit use of line-girder analysis techniques, although the beams are analyzed twice. First, the beams are analyzed for the "no end restraint" or "simple span" condition. This indicates the
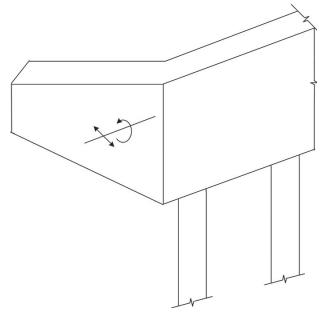

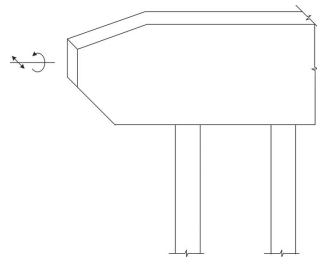**Fig. 13.** Sample diagram of an FIAB with a cantilevered flared wingwall

Fig. 14. Sample diagram of an FIAB with a cantilevered in-line wingwall

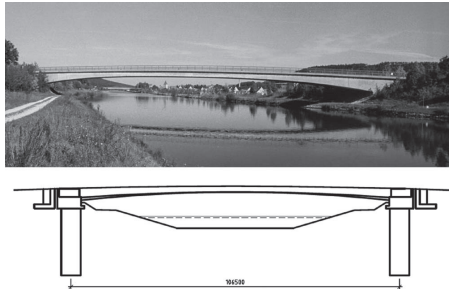

Fig. 11. Sample diagram of an FIAB with a cantilevered U-wingwall

105

Fig. 15. Southern Viaduct Berching, Germany (picture and longitudinal section by SSF Ingenieure, Germany, with permission)
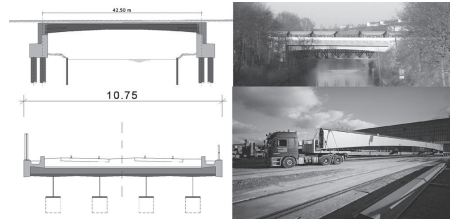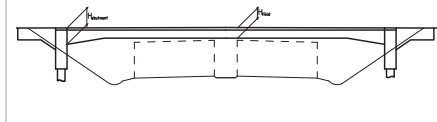

Fig. 16. Teltowkanal Bridge: engineering sketches and photos from fabrication shop (picture by SSF Ingenieure, Germany, with permission)

maximum positive moment that could be induced in the beam at midspan. Next, the beams are analyzed as "fully restrained" or "fixed" to determine the maximum end moments that may be induced in the abutment. Sweden permits the use of 50% of the calculated passive pressure behind the abutment to lessen the midspan positive moments on the bridge beams.

In England, it is strongly recommended that computer models be used for all FIAB (Iles 2005). Germany indicated that three-dimensional (3D) modeling is only used for large skews or complicated framing arrangements, while Sweden indicated that 3D computer modeling is becoming more commonplace for all IAB. In the United States, state agencies are split between using line-girder techniques and 3D modeling (Kunin and Alampalli 1999), with the decision depending on structure specifics.

A common practice in Germany is the use of vaulted-tapered girders and beams, which allows for an easier transfer of the bending moments at the frame edge and leads to a very winsome shape of the bridge. In combination with very rigid foundations, quite long single span bridges can be realized, compared to conventional bridges (Fig. 15). The usual beam slenderness of German road and railway frame bridges can be summarized as given in Table 2 (Braun et al. 2006).

Fig. 16 shows details of a composite railway bridge with integral abutments. Prefabricated elements were used during the construction of the bridge. As expected for a structure of this type, the main focus of the design and detailing is the engineering of the frame edge (Koch 2006).

Steel Beams

The European survey indicates that steel beams are permitted for IABs, but are seldom used. When steel box girders are used, only one box girder is permitted in the cross section. The minimum number of I-beams in cross section is two. Only Finland reported a limit on maximum individual span length or total bridge span length at 230 ft. (70 m). In other countries, the lengths are limited by resulting pile stresses or other design criteria. Of those European countries that indicated a limit on the bridge skew angle, the maximum allowable reported skew angle is 30°.

Only Sweden indicated a maximum roadway grade (4%). No European country reported a maximum bridge width. To compare, U.S. agencies report (Maruri and Petro 2005) maximum individual spans for steel girder bridges using integral abutments of 213–985 ft (65–300 m) with a maximum overall bridge length of 500–2,000 ft (150–650 m). Maximum skew angle limits range from 15°–70°. New York State limits the roadway grade to 5% (New York State DOT 2005).

Cast-In-Place Concrete Beams

The European survey indicates that cast-in-place reinforced concrete beams are permitted for bridges with integral abutments, but are seldom used except for short span three-sided frame structures. The maximum allowable skew angle reported is 30°. Shrinkage of the concrete is typically accounted for in the design. New three-sided cast-in-place frames are seldom constructed in the United States. PC/PS concrete frames are far more common due to their ready availability, ease of construction, and relative cost. The requirements of these frames vary from one agency to another, and will not be discussed here.

PC/PS Concrete Beams

The European survey indicates that PC/PS concrete beams are the predominant beam used for FIAB. When PC/PS box girders are used, only one box girder is permitted in the cross section. The

Table 2. Usual Slenderness (L/h) of FIAB in Germany (adapted from Braun et al. 2006, with permission of SSF Ingenieure, Germany)

Bridge Type	$h_{abutment}$	h_{field}	Without Taper
Road bridge			
Concrete	12-18	20-25	18-21
Prestressed concrete	15-19	24-30	20-25
Composite	15-19	25-35	21-25
Railway bridge			
concrete	10-15	20-25	16-18
Prestressed concrete	Not common	---	---
Composite	15-18	25-30	18-21

Fig. 17. Sunniberg Bridge in Switzerland (courtesy of Dr. Ana M. Ruiz-Teran)

minimum number of PC/PS concrete I-beams in cross section is two. The same rules for length, skew, width and grade apply as for steel beams. To compare, U.S. agencies report (Maruri and Petro 2005) maximum individual spans for PS/PC concrete IABs ranging from 20–650 ft (6–200 m). Maximum allowable total bridge lengths range from 500–3,800 ft (150–1,175 m).

Curved Geometry

Horizontally curved alignments are advantageous for IAB. Constraints due to temperature and shrinkage can be considerably reduced by horizontal "relaxation" (movement) of the superstructure. In this way, complicated concrete technology and complicated on-site construction procedures can be avoided to decrease cracking and reduce overall cost. Additionally, the resulting slender structure offers an improved aesthetic. The Sunniberg Bridge in Switzerland is 1,725 ft (526 m) long and does not use any expansion joints or bearings (Fig. 17). In the United States, maximum allowable degree of curvature ranges from 0°–10° (Maruri and Petro 2005).

Conclusions

It is worth repeating that the European Survey was completed by practicing bridge engineers and, therefore, the responses are based on their experience and individual understanding of the governing design codes. As such, the survey responses should not be taken as policy statements of their respective countries. Even with this caveat, the compiled responses are useful as they reflect the current application of the bridge design codes on structures that are actually being designed and built.

When looking at the results of the European survey responses and past surveys of U.S. transportation agencies, it is clear that there are many similarities between design assumptions and construction practices. Yet, there are also significant differences.

Design parameters that are considered fundamental by one

agency are completely ignored by another. In one country, an FIAB may require piles to be driven in the ground and be of a minimum length. In another country, the same bridge may be required to use piles, but they must be placed in preaugered holes and within pipe casings to prevent soil interaction near the pile top. In still another country, that same bridge would be built on spread footings to reduce differential settlements. Based solely on field performance, it is difficult to determine which methods are better than the others.

Part of the problem is that IAB, for all their simplicity of construction, are complicated structural systems. To thoroughly analyze a given structure the designer must not only design for primary loads (dead, live, wind, etc.) but must also accurately account for secondary loads (creep, shrinkage, settlement, temperature effects, etc.). To further complicate the analysis, the response of the structure to a given set of forces is very dependant on the geometry, materials, configuration, soil interaction, and construction details of the individual system.

It seems unlikely that there will come a time when every agency across the world will agree on every detail of what makes the best IAB. In the meantime, the differences in design philosophy between agencies are less important than the fact that IAB are more economical to build and to own than traditional bridges. As long as agencies continue to share their experiences, of the successes and the failures, IAB will continue to improve and provide an even more durable and cost effective solution for the future.

References

BA 42/96. (2003). "Amendment No. 1, highway structures: Approved procedures and general design, Section 3.5." The Stationary Office, London.

Braun, A., Seidel, G., and Weizenegger, M. (2006). "Rahmentragwerke im Brückenbau, Konstruktion, Berechung und Volkswirtschaftliche Betrachtung." *Beton-und Stahlbetonbau*, 101(3), 187–197.

Bundesministerium für Verkehr, Bau- und Wohnungswesen. (1999). "Stahlverbundbau—Musterentwürfe für einfeldrige Verbundüberbauten zur Überführung eines Wirtschaftsweges und eines Straßenquerschnittes RQ 10,5." *Allgemeines Rundschreiben Straßenbau 23/1999*, Vers. Nr. 11/99, Verkehrsblatt-Verlag, Dortmund, Germany, S 1050.

Collin, P., Veljkovic, M., and Petursson, H. (2006). *International Workshop on Bridges with Integral Abutments*, Lulea Univ. of Technology, Lulea, Sweden.

Finnish Road Administration (Finnra). (2002). "Sillansuunnittelun täydentävät ohjeet (supplementary bridge design instructions)." *Vaasa*, Multiprint Oy, Helsinki, Finland (in Finnish).

Iles, D. (2005). *Integral steel bridges: a summary of current practice in design and construction*, SCI Publication, Berkshire.

Kerokoski, O. (2006). "Soil structure interaction of long jointless bridges with integral abutments." Ph.D. thesis, Tampere Univ. of Technology, Tampere, Finland.

Koch, E. (2006). "Eisenbahnbrücken bei der Deutschen Bahn AG." *Stahlbau*, 75(10), 786–790.

Kunin, J., and Alampalli, S. (1999). "Integral abutment bridges: Current practice in the United States and Canada." *Rep. No. FHWA/NY/SR-99/132*, NYSDOT, Albany, N.Y., 8–9.

Maruri, R. F., and Petro, S. H. (2005). "Integral abutments and jointless bridges (IAJB) 2004 survey summary." *Proc., FHWA Conf. on Integral Abutments and Jointless Bridges (IAJB)*, Federal Highway Administration (FHWA)/Constructed Facilities Center (CFC) at West Virginia Univ., Morgantown, W.Va.

New York State DOT. (2005). *NYSDOT Bridge Manual*, 3rd Ed., Section 11.5.1.6, Albany, N.Y.

Pétursson, H. (2000). "Broar med integrerade landfästen (bridges with

107

integral abutment).” Lulea Univ. of Technology, Lulea, Sweden (in Swedish).

White, H. (2007). “Integral abutment bridges: Comparison of current practice between European countries and the United States of America.” *Special Rep. No. 152*, Transportation Research and Devel-

opment Bureau, New York State DOT, Albany, N.Y.

White, H. (2008). “Wingwall type selection for integral abutment bridges: Survey of current practice in the United States of America.” *Special Rep. No. 154*, Transportation Research and Development Bureau, New York State DOT, Albany, N.Y.

Paper III-Monitoring and Analysis of Abutment-Soil Interaction of Two Integral
Bridges

Paper III

Paper III is divided into two parts. The first part is about field tests of two joint-less
   bridges, focusing on the magnitude and significance of earth pressure behind the
   abutments. This part is written by Olli Kerokoski. The second part describes
   some of the measurements done on the bridge over the Leduån and is written by
   Pétursson.

Paper III-Monitoring and Analysis of Abutment-Soil Interaction of Two Integral Bridges

Monitoring and Analysis of Abutment-Soil Interaction of Two Integral Bridges

H. Pétursson[1] and O. Kerokoski[2]

Abstract: Field tests of two jointless bridges are presented, focusing on the magnitude and significance of earth pressure behind the abutments. The Haavistonjoki Bridge is a 56-m-long, continuous three-span bridge. Instrumentation was used to measure the horizontal displacement of an abutment, abutment rotation, abutment pile strains, earth pressures behind the abutments, superstructure displacements, frost depth, and air temperature. The measured earth pressures were compared with pressures that had been calculated on the basis of Nordic codes of practice and the Eurocodes pertaining to bridges. The bridge over the Leduån is a single-span composite bridge with a cast-in-place concrete deck on top of two steel beams. This bridge, spanning 40 m, is slender, with a 1.7-m-high superstructure. The bridge was fitted with strain and displacement gauges and short-term measurements were made using a loaded truck. The field test results for this bridge were verified with calculations based on an abutment rotation stiffness calculation model developed during the research presented in this paper. **DOI:** 10.1061/(ASCE)BE.1943-5592.0000314. *© 2013 American Society of Civil Engineers*.

CE Database subject headings: Bridges; Tests; Earth pressure; Bridge abutments; Soil-structure interactions; Monitoring.

Author keywords: Integral bridge; Bridge tests; Bridge abutments; Soil-structure interaction; Earth pressure.

Introduction

Integral bridges are defined as bridges with no expansion joints between the superstructure and the supporting abutments (Kerokoski 2006). Use of such structures was first considered after observing the successful performance of old bridges with inoperative joints [e.g., Mourad and Tabsh (1999)]. If the bridge has no bearings, it is often referred to as a fully integral bridge. One commonly discussed problem regarding integral bridges is the influence of longitudinal elongation of the superstructure that occurs because of seasonal temperature variations and the earth pressure against the abutment. In addition, live loads move the abutment in relation to the embankment and cause variation in the earth pressure against the abutment.

The superstructure of integral bridges is cast integrally with their substructure (Lehane et al. 1999). The superstructure is permitted to expand and contract without joints (Horvath 2000). Hence, thermal movements affect the behavior of the substructure and of the soil around intermediate piers and abutments.

An integral bridge designer should take into account the factors that affect bridge performance and displacements, for example, temperature and moisture changes in concrete sections and creep (Card and Carder 1993). The modeling of the abutment-soil interaction has been presented, for example, by Dicleli (2005) and Krizek (2010).

In this context, the background of the present work is twofold. First, the longitudinal thermal response and earth pressure against the abutment of a three-span reinforced-concrete bridge is presented. The results are taken from monitoring the Haavistonjoki Bridge in Finland and are compared with values calculated using three different codes: Finnish (Finnra 1999a), Swedish (Vägverket 2004), and Eurocodes (European Committee for Standardization 2004).

Second, a simple model is presented that attempts to predict the rotational stiffness of an integral abutment bridge when such a bridge is subjected to traffic loading. The model is derived from the earth pressure as calculated using Swedish bridge codes. The results are compared with measurements undertaken on a Swedish integral abutment bridge at Leduån. Long-term monitoring was also carried out on this bridge, but these results are not reported in this paper.

Haavistonjoki Bridge, Finland

Superstructure and Substructure

The Haavistonjoki Bridge in Finland is a 56-m-long, continuous-slab bridge. The total length of the three spans is 50 m. The total width of the traffic lanes is 11 m, and the thickness of the deck slab is 860 mm. The bridge is unskewed and jointless. The approach slab, called a transition slab, is located within the approach embankment (see Fig. 1).

Four piers and two abutments support the reinforced-concrete deck as detailed in Figs. 1–3. The supports are designated T1–T4, starting from the western end facing Orivesi. Eight steel pipe piles with a diameter of 710 mm and a wall thickness of 14 mm support the piers and the abutments. These piles were driven through to the bedrock and filled with reinforced concrete.

The connection between the abutment and the 5-m-long transition slab was implemented with vertical dowels on the upper surface of the supporting cantilever as shown in the Finnish-type drawing R15/DL 2 (Finnra 1999b). Steel dowels with a diameter of 25 mm

[1]Steel Bridge Specialist, Swedish Transport Administration, SE 781 89 Borlange, Sweden.
[2]Associate Professor, Tampere Univ. of Technology, Dept. of Civil Engineering, P.O. Box 600, FIN-33101, Tampere, Finland (corresponding author). E-mail: olli.kerokoski@tut.fi

J. Bridge Eng. 2013.18:54-64.

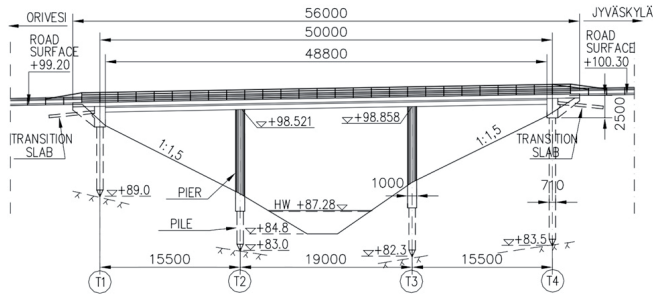# Design of steel piles for integral abutment bridges

Fig. 1. Haavistonjoki Bridge on Highway 9 between Tampere and Jyväskylä [dimensions in mm; Laaksonen (2004) with permission]

Fig. 2. Haavistonjoki Bridge

and a length of 570 mm were installed at 1,000-mm intervals. The recesses for the dowels were made with plastic tubes that had a diameter of 40 mm and were the same length as the thickness of the transition slab. Theoretically, the dowels permitted 8 mm of expansion and 8 mm of contraction in the longitudinal direction of the bridge.

Field Test Program for Haavistonjoki Bridge

The bridge was constructed and fitted with test instruments in the summer of 2003. The test program operated between 2003 and 2010 and used 191 sensors, from which the data logger automatically collected data every 15 min.

Twelve earth pressure cells were installed on the outer surface of the abutments to measure the earth pressures at the interface between the abutment and the embankment. The cells were embedded in the concrete facing outward (see Fig. 4). The eastern abutment was fitted with ten earth pressure cells, and the western abutment was fitted with two.

The 384-mm-wide and 67-mm-thick earth pressure cells were developed, designed, and assembled by Tampere University of Technology. Their structure is shown in Fig. 5, where the cell is pictured without a front plate. They were designed to use strain gauges to measure the strain in the 3-mm-thick inner steel pipe. Each cell was calibrated separately under laboratory conditions before being installed. Based on the test results of the 7-year observation period from 2003 to 2010, the performance of the cell was shown to be reliable.

To check whether there was a gap between the backfill soil and the 1,200-mm-thick abutment, a special manual measuring device was used (see Fig. 6). All six of the devices were installed in the eastern abutment. The inner steel plate of the device could be pushed horizontally against the backfill with a measurement bar to test for the appearance of any gap during wintertime. Grains of soil were prevented from filling the gap between the two plates by means of a textile sheet between the outer plate and the soil.

To measure any changes in bridge length, laser distance meter equipment was installed between opposite abutments. Abutment displacements and rotations were observed using ten 13.5-m-long steel bars installed at three levels through the eastern abutment (see Fig. 7) and at two levels through the western abutment. These bars were anchored to the embankment and did not move. So, the absolute horizontal movement of the abutment could be measured in relation to these anchored bars.

Several temperature gauges were installed to measure temperatures in the concrete, the embankment, and the air.

Soil Properties

The backfill material was well-compacted crushed rock with a grain size of 0−60 mm. The crushed rock was compacted in layers. The friction angle and cohesion values of the backfill were measured under laboratory conditions using samples taken from the bridge site. The results were $\phi = 45°$ and $c = 0$ kPa. Plate bearing tests were performed on the compacted eastern embankment fill prior to the construction of the transition slab. The average values of the two test results were $E_1 = 167$ and $E_2 = 402$ MPa. The results indicated that the crushed rock was a very-dense granular soil (Kerokoski 2006; Finnra 1999a).

The replacement fill area and some site investigation results are illustrated in Fig. 7. The properties of the silt were evaluated based on the results of a weight sounding test (Suomen geoteknillinen yhdistys 1980).

Soil samples were not taken from the western river embankment. The weight sounding test revealed that the soil layers were shallower and that the rock was nearer to the ground surface than at the eastern river embankment.

Field Test Results

The earth pressures measured during the Haavistonjoki Bridge field tests are presented in Figs. 8−10. The results focus on the period in 2004 between February 11 and 15, when the greatest changes in
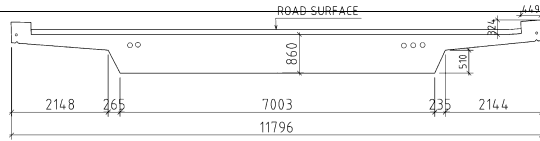
112

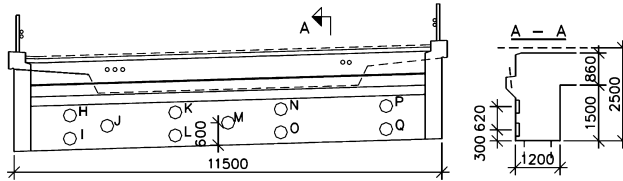**Fig. 3.** Cross section of the Haavistonjoki Bridge concrete deck (dimensions in mm)

Fig. 4. Earth-pressure cells, labeled H−Q, at the eastern bridge abutment (T4; dimensions in mm)

Fig. 5. Earth-pressure cell used for monitoring

bridge behavior took place as a result of a large air temperature increase, and on a 6-month period in 2004 between March 1 and September 1, which serves as an example of long-term bridge behavior.

The height of the vertical part of the abutment under the transition slab is about 1.2 m. Accordingly, there is a point of discontinuity both under the cells and directly above the cells. The bottom of the transition slab support is inclined. The bottom of the transition slab adjacent to the abutment is located at a depth of 0.75 m. Fig. 8 shows the changes in the measured earth pressure for the ten pressure cell locations at the abutment T4, but see also Fig. 9.

The average change in the earth pressures measured by the five cells near the abutment midwidth was 80 kPa. Clearly, the general variation between these five cells was a result of variations in soil density. Observed earth pressures were lower at the cells near the wing walls than near the midwidth of the abutment. Therefore, it can be concluded that the wing walls, being rigid abutment members, transferred part of the stresses and deformations of the bridge into the embankment. Also, generally, the road embankment is less stiff

at its edges in the longitudinal direction because of the shape of the cross section of the road.

During the coldest period, all the earth pressures against the center of abutment T4 were zero because of the contraction of the bridge and the frozen backfill near the abutment. Nonzero earth pressures were measured at abutment T1 and near the wing walls at abutment T4. The most likely reason for the observed lack of earth pressure was that a gap had developed at the abutment-soil interface during the coldest winter days. The presence of the gap was also verified manually using a special measuring device (shown in Fig. 6, consisting of a movable steel bar and plate) positioned through the abutment. The movement of the plate between the soil and the abutment was measureable but not large, that is, less than 1 mm. Consequently, the gap has only minor significance for the behavior of the bridge structure and may be ignored while estimating the stiffness of an integral bridge embankment (see Fig. 11).

Fig. 9 shows changes in the earth pressure and deck temperatures during 2004 between February 10 and 16. During these 6 days, earth pressures changed with the temperatures at abutment T4, increasing as the temperature rose. Fig. 9 also shows the data from cells V and W, which were located at abutment T1.

Both the laser distance meter results and the displacement measurements of the long steel bars through the abutment tracked the average deck temperature changes closely (Laaksonen 2004). The average modulus of lateral subgrade reaction was $k_{s,T4} = (80 \text{ kN/m}^2/5.2 \text{ mm}) = 15 \text{ MN/m}^3$. This figure is based on the average earth pressure change and measured abutment displacement toward the embankment during 2004 from February 11 to 15 at the five earth pressure cells located near the midwidth of abutment T4. This agreed with the results of short-term tests carried out at the Tekemäjärvenoja Railway Bridge, where the same group of researchers measured the modulus of lateral subgrade reaction as having values ranging from 10 to 25 MN/m^3 (Kerokoski 2006). The average modulus of lateral subgrade reaction at abutment T1 was $k_{s,T1} = (57 \text{ kN/m}^2/0.3 \text{ mm}) = 190 \text{ MN/m}^3$, which clearly shows the difference between the stiffness of the two approach embankments. Abutment T1 was extremely rigid because of its close proximity to the rock (see Fig. 1).
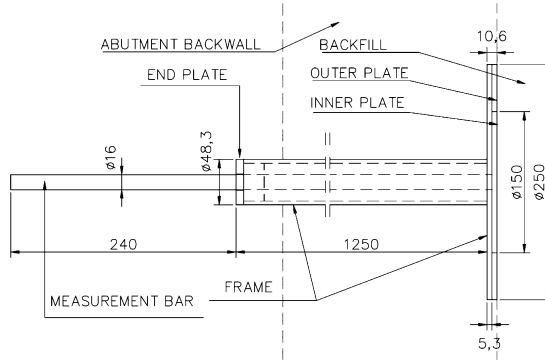
Fig. 6. Gauge-to-measure gap width between the abutment and the backfill [dimensions in mm; Laaksonen (2004) with permission]
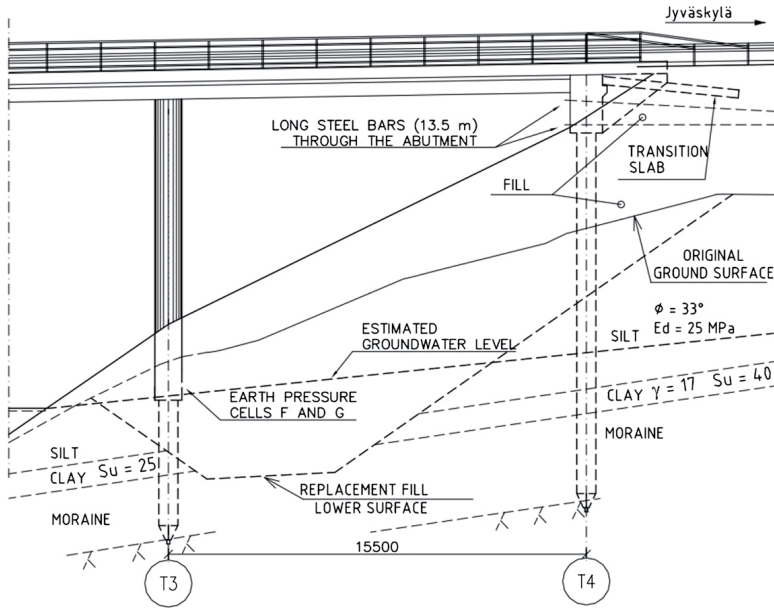

Fig. 7. Basic soil material data for the eastern river embankment (dimensions in mm)

Earth-pressure changes at support T1 remained quite small also between March 1 and August 31 in 2004, and the observed pressure level was quite steady. However, the lateral subgrade reaction coefficient at abutment T1 was large because of the small longitudinal abutment displacement. As shown in Fig. 10, at support T4, after April 1, 2004, the adjacent earth pressure cells L and O, located at the lower center of the abutment, began to parallel each other's measurements. The lowest earth pressures measured during the summertime at support T4 were at the edges of the abutment, that is, at earth pressure cells H, I, P, and Q. The highest earth pressures did not develop as expected in the middle of the summer of 2004 but occurred in May and August in response to deck temperature increases. Even in the middle of March, before the embankment started to warm up and thaw, the pressure was higher than in midsummer.

114

Paper III-Monitoring and Analysis of Abutment-Soil Interaction of Two Integral Bridges

Calculations: Earth Pressure against Abutment Attributable to the Measured Displacement

Earth Pressures

Earth pressure against the abutment, which is moving horizontally toward the embankment, may be estimated using the following equations (Vägverket 2004):

If $\delta = 0$, then $p = p_0$ (1)

If $0 < \delta < \dfrac{h}{200}$, then $p = p_0 + c_1 \cdot \delta \cdot \dfrac{200}{h} \cdot (p_p - p_0)$ (2)

If $\delta > \dfrac{h}{200}$, then $p = p_0 + c_1 \cdot (p_p - p_0)$ (3)

where $c_1 = 1$ in the case of disadvantageous earth pressure (e.g., pressures attributable to forces caused by temperature changes); $c_1 = 0.5$ in the case of advantageous earth pressure (e.g., earth pressure that resists the forces generated by a braking vehicle); $p_0 =$ at-rest pressure; $p_p =$ passive earth pressure; $h =$ abutment height; and $\delta =$ horizontal abutment displacement toward the embankment.
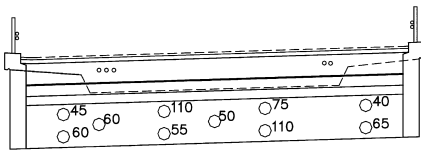
Fig. 8. Maximum changes in the measured earth pressures in 2004 between February 11 and 15, at earth-pressure cells H−Q for bridge abutment T4 [pressures in kPa; Kerokoski (2006) with permission]

At the Haavistonjoki Bridge, the abutment height, h, is about 2,400 mm. Hence, passive earth pressure is at a maximum after the horizontal displacement, δ, reaches $h/200$ or 12 mm.

The measured abutment displacement for abutment T4 between February 11 and 15 in 2004, at a depth of 1.7 m, was 5.4 mm. This displacement corresponds to a ratio of $h/444$, which is less than the ratio $h/200$. Therefore, the earth pressure [Eq. (2)] at this location is expressed as

$$p = 0.55 \cdot p_0 + 0.45 \cdot p_p \qquad (4)$$

The at-rest earth-pressure coefficient, K_0, is 0.34, the passive earth-pressure coefficient, K_p, is 5.83, and for backfill material (crushed rock), the unit weight of the soil, γ, is 18 kN/m^3 (Vägverket 2004). However, for the calculations presented here, we have used a crushed-rock unit weight, γ, of 21 kN/m^3, which is a typical value at the Haavistonjoki Bridge. The calculated pressures on the row of upper and lower Haavistonjoki bridge pressure cells are presented in Table 1.

Using the measurements from the middle five cells shown in Fig. 8, the average measured earth-pressure increase was 80 kN/m^2. Hence, the presented simple equation depicted the relationship between displacement and earth pressure sufficiently accurately, the difference from the average being 18%, which is not considered significant when analyzing soil behavior.

Modulus of Lateral Subgrade Reaction as Described by Various Codes of Practice

Using the Finnish and Swedish codes of practice, the effect of passive earth pressure attributable to displacement of the abutment in dense noncohesive soil has been calculated (see Table 2). The values used for soil density and abutment height were $\gamma = 21$ kN/m^3 and $h = 2.4$ m, respectively. Adhering to Swedish practice, in the calculation, the passive earth-pressure coefficient was taken from European standard EN 1997-1 (European Committee for
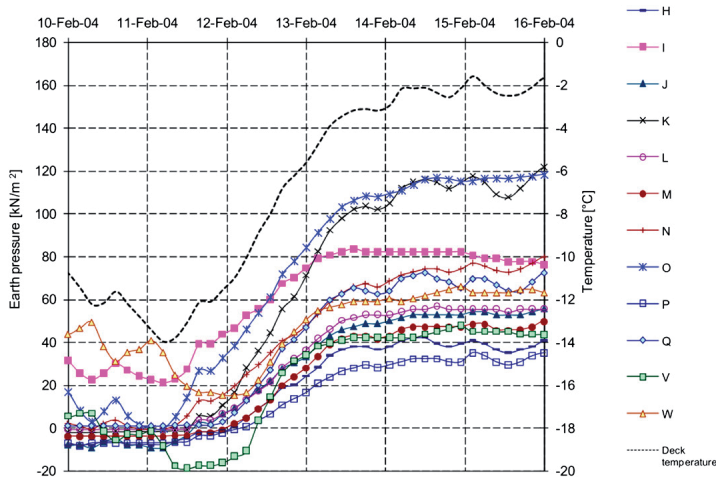

Fig. 9. Measured changes in average deck temperature and earth pressures on bridge abutments during 2004 between February 10 and 16 at earth-pressure cells H−W [kN/m^2; Kerokoski (2006) with permission]
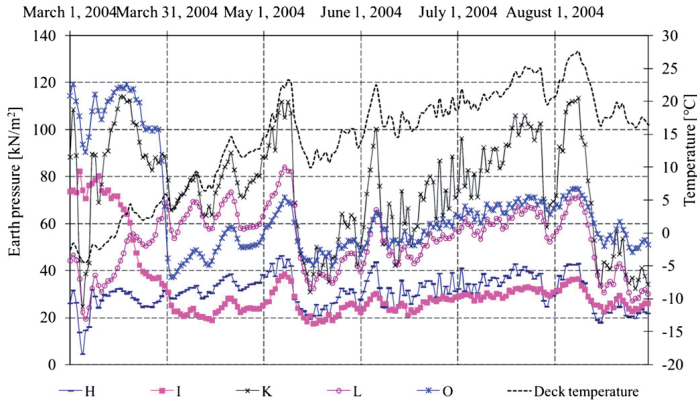
115

Fig. 10. Measured changes in average deck temperature and earth pressures on bridge abutments at midnight between March 1 and August 31, 2004 [Kerokoski (2006) with permission]
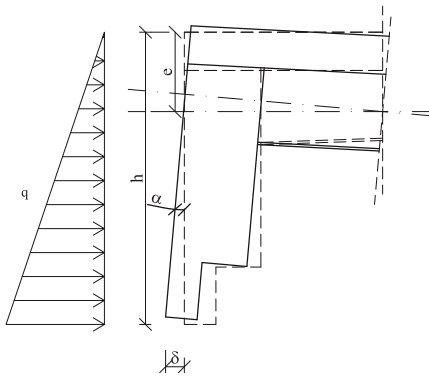

Fig. 11. Horizontal displacement δ and rotation angle α at the abutment

Table 1. Calculated Earth Pressures

Depth from road surface (including pavement), z (m)	At-rest pressure p_0 (kN/m²)	Passive pressure p_p (kN/m²)	Calculated earth pressure P (kN/m²)
1.24	9	147	71
2.1	14	245	118

Standardization 2004), which gives the same passive earth pressures as those given by Kerisel and Absi's earth-pressure theory. The passive earth-pressure coefficient $K_p = 8$ was determined using a soil internal friction angle $\phi = 38°$, as recommended by Finnra (1999a), and a wall friction angle of $\arctan(0.5 \cdot \tan 38°) = 21.3°$.

The passive earth-pressure distribution against the abutment was considered to be triangular, with a total force

Table 2. Modulus of Lateral Subgrade Reaction for the Abutment in Dense, Noncohesive Soil

Code	Horizontal displacement for passive earth pressure δ_p (mm)	Passive earth-pressure coefficient K_p	Modulus of lateral subgrade reaction $k_{s,average}$ (MN/m³)
Finnish code of practice	4.8	4.2	22
European standard		8	16.8
Swedish code of practice	12		
Measured value in the center of the abutment			15

$$P = 0.5 \cdot K_p \cdot \gamma \cdot h^2 \cdot b \qquad (5)$$

The average value was

$$k_{s,average} = P/(h \cdot b \cdot \delta) \qquad (6)$$

The measured average modulus of lateral subgrade reaction at the five earth pressure cells in the center of abutment T4 was $k_{s,T4} = 15$ MN/m³, as calculated previously. Using the Swedish code of practice (Table 2), the calculated figure showed a better agreement with this measured value. As a result of the high embankment stiffness behind the abutments, a simple model was developed to estimate the short-term significance of that stiffness to structural stresses.

Simple Model to Calculate Rotation Stiffness at the End of an Integral Abutment

Description of Model

The rotational restraint at the end of a jointless bridge, caused by the embankment, is seldom used by the engineer when designing

Paper III-Monitoring and Analysis of Abutment-Soil Interaction of Two Integral Bridges

a bridge with integral abutments. By neglecting the rotational stiffness of the embankment, the midspan moment is overestimated and more material than necessary is used in the bridge beam. In what follows, we present the description of a simple model to calculate the rotational stiffness at the end of a single-span bridge with integral abutments. For convenience, it is assumed that there is a triangular distribution of active earth pressure behind the abutment, as shown in Fig. 11. This earth pressure occurs when the abutment rotates because of traffic loads on the bridge and is proportional to the bottom edge displacement of the back wall. The maximum passive earth-pressure against the back wall is assumed to occur when the bottom edge displacement of the back wall, δ, is 1/200 of the height, h, of the back wall, as described in the Swedish code of practice (Vägverket 2004).

The increase in earth pressure Δq attributable to the movement of the abutment is

$$\Delta q = 200 \cdot \delta \cdot (K_p - K_0) \cdot \gamma \qquad (7)$$

where δ = horizontal displacement at the bottom of abutment (see Fig. 11); K_p = Rankine coefficient of passive earth pressure (apart from this use, this model does not reference the Rankine theory); K_0 = Rankine coefficient of at-rest pressure; and γ = unit weight of the soil behind the abutment. The moment that the earth pressure introduces in the beam can be calculated as

$$
\begin{aligned}
M &= \frac{\Delta q \cdot b \cdot h(2 \cdot h - 3 \cdot e)}{6} \\
&= \frac{200 \cdot \delta \cdot (K_p - K_0) \cdot \gamma \cdot b \cdot h \cdot (2 \cdot h - 3 \cdot e)}{6}
\end{aligned}
\qquad (8)
$$

where b = width of the abutment wall; h = height of the abutment wall; and e = distance between slab top and center of gravity of composite slab-beam structure. The rotation angle at the abutment is given by (see Fig. 11)
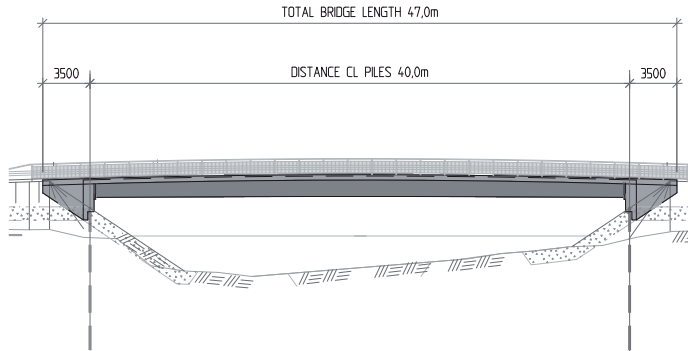
$$\alpha = \frac{\delta}{h - e} \qquad (9)$$
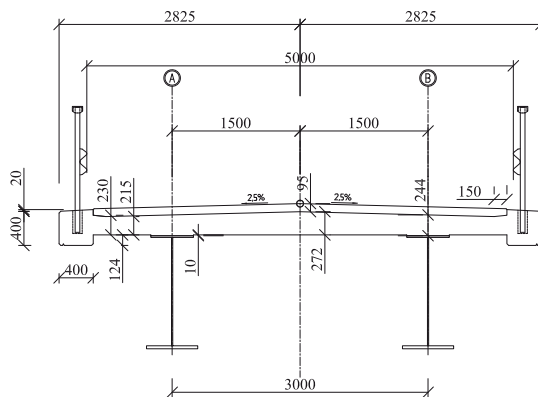

Fig. 12. Bridge over the Leduån

Fig. 13. Deck cross section of the bridge over the Leduån (dimensions in mm)

117

Design of steel piles for integral abutment bridges

Using Eqs. (10) and (11), the rotational stiffness of the abutment can be expressed as follows:

$$k_\alpha = \frac{M}{\alpha} = \frac{200 \cdot \delta \cdot (K_p - K_0) \cdot \gamma \cdot b \cdot h \cdot (2 \cdot h - 3 \cdot e) \cdot (h - e)}{6 \cdot \delta} \tag{10}$$

which can be rearranged into the equation

$$k_a = \frac{200 \cdot (K_p - K_0) \cdot \gamma \cdot b \cdot (2 \cdot h^3 - 5 \cdot h^2 \cdot e + 3 \cdot h \cdot e^2)}{6} \tag{11}$$

To verify the model, field tests were carried out as described later in this article. The current study did not include the long-term behavior of the embankment soil, the contraction of the bridge superstructure attributable to the creep and drying of the concrete, or the temperature change during the wintertime.

Bridge over Leduån, Sweden

Description

The bridge over the Leduån has a 40-m span with a deck that is 5.65 m wide including edge beams, as shown in Figs. 12 and 13. The superstructure of the bridge consists of two welded steel beams with a cast-in-place concrete deck, as shown in Fig. 12. Composite action is ensured by the use of 175-mm-long shear studs with a diameter $D = 22$ mm and with the average shear stud spacing being 14 studs/m. The height of the steel beams varies between 1.12 m at the supports and 1.32 m at the midspan. The dimensions of the steel beams are shown in Table 3. Each steel beam was manufactured using three pieces 11.2, 18, and 11.2 m long, with dimensions as shown in Fig. 13. The girder ends are embedded 0.62 m into the abutments, and the heights of the back walls are 3 m, as shown in Fig. 14. The wing walls are integral with the abutment, have a thickness of 0.35 m, and extend 3.0 m from the abutment. Piles are embedded 0.3 m into the bottom of the abutment with the pile length varying between 24.8 and 27.2 m.
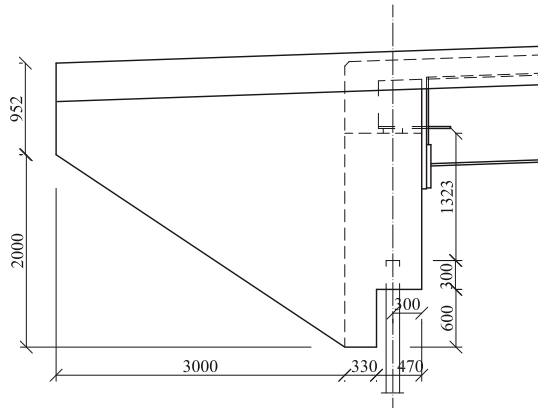
Four cross beams with UPE 300 profiles are evenly spaced along the bridge length and bolted to stiffeners on the two main girders.

Instrumentation

A number of sensors were installed on the bridge. In this research, the midspan displacements, the midspan strains, and the abutment rotations were studied. Detailed information on all gauges can be found in Nilsson (2008).

Displacement transducers were located on top of the bridge to measure deflection (see Fig. 15). A steel wire was attached to a weight resting on the river bottom, which acted as a reference. Thick steel plates were attached to the other end of the wire to keep it taut. The displacements used from the displacement transducers are the relative displacement readings between the unloaded bridge prior to loading and when the truck loaded the bridge. The weight on the river bottom is assumed to be still in this restricted time frame.

Strain gauges measured strains on the flanges in the middle of the bridge. This research examined data from the gauges that were located on the upper surface of the lower flange and on the lower surface of the upper flange.

To measure the abutment rotations, two displacement gauges that measured horizontal displacement along the bridge were used. The gauges were placed 1,500 mm apart along the vertical central line of the abutments (see Fig. 16).
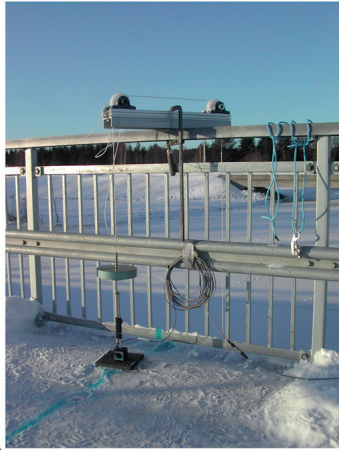
Load Test

The bridge was tested several times using heavy trucks (Pétursson et al. 2011); two of the tests are presented here. The axle loads were 71.1 kN on the front axle and 168.7 kN (made up of two masses of

Table 3. Dimensions of the Steel Beams

Distance from one end (m)	Upper flange (mm)		Web (mm)		Lower flange (mm)	
	t_{uf}	b_{uf}	t_w	h_w	t_{lf}	b_{lf}
0–11 and 29–40	25	500	13	1.051/1.221	36	800
11–29	25	600	11	1.212/1.255	45	800

Fig. 14. Abutment of the bridge over the Leduån (dimensions in mm and levels in m)

118

Paper III-Monitoring and Analysis of Abutment-Soil Interaction of Two Integral Bridges

(a)

(b)

Fig. 15. Displacement gauges used on the western and the eastern sides of the bridge; (a) shows the test setup with gauge, weights, steel wire, and tracked wheels for the wire; (b) shows where the gauge is in contact with the weight underneath it

Fig. 16. Picture showing the northern abutment; the metal housing covers the displacement transducers; the reference beam in front is supported by two steel piles placed at sufficient distance from the bridge to avoid being affected by the bridge movements

more accurate when comparing a measured value with a calculated value.

Young's modulus is taken to be 34 GPa (C35/45) for the concrete and 210 GPa for the steel. The restraint of the embankment is modeled with linear rotational springs. When calculating the moment of inertia, the concrete section is treated as an equivalent steel section giving the same stiffness.

Properties of the springs are calculated as follows: $b = 5$ m, $h = 3$ m, $e = 242$ mm (see Fig. 11), $K_p = 5.81$, $K_0 = 0.34$, and $\gamma = 18$ kN/m³. Based on Eq. (11), the rotational stiffness of the abutment becomes

$$k_a = \frac{200 \cdot (5.81 - 0.34) \cdot 18 \cdot 5 \cdot (2 \cdot 3^3 - 5 \cdot 3^2 \cdot 0.242 + 3 \cdot 3 \cdot 0.242^2)}{6}$$

$$= 7.16 \cdot 10^5 \text{ kNm/rad}$$

Results from the Load Test and Modeling

The results from the calculations show a reasonable agreement with the test results obtained in October 2007. All the results are tabulated in Tables 5 and 6. The measured values are lower than the calculated ones, indicating stiffer behavior in practice than in theory. The ratios of measured-to-calculated strain values are 0.84 for the lower flange strain and 0.68 for the upper flange strain. This indicates that the equivalent area of the deck slab that contributes to the stiffness is exaggerated in the calculation. A larger slab area means less strain in the steel for a given load and that the neutral axis is nearer to the slab, and thus, the strains in the upper flange will decrease more than in the lower flange.

The ratios of measured-to-calculated rotations are 0.88 and 0.83 for the southern and northern abutments, respectively, and 0.77 and 0.78 for the vertical displacements of the girders. The results indicate a stiffer soil than predicted by the model and/or a stiffer beam.

In the test conducted in January 2008, the bridge exhibited greater stiffness. The ratios of January's measurements to October's measurements are 0.48 and 0.65 for the southern and the northern abutment rotations, respectively.

In the test conducted in January 2008, the bridge exhibited greater stiffness. All measured values in January were lower than those in October except for the upper flange strain. The stiffer behavior during January is believed to have been caused by frozen soil making the embankment appear stiffer than it does in nonfrozen

84.35 kN) on the rear axle for the first test in October 2007. The second test in January 2008 used loads of 73.6 kN on the front axle and 164.6 kN (made up of two masses of 82.3 kN) on the rear axle. The distances between the axles are shown in Fig. 17. The truck was driven along the centerline of the bridge and stopped every 2 m to collect data.

Modeling of Bridge and Truck Load

A simple beam model was created to analyze the behavior of the bridge. The beam model consists of five beam elements with properties as shown in Table 4. The moment of inertia that is used in the calculation varies because of the varied height of the beam and because the dimensions of the steel beam change at 11 m away from the support. Although not usually considered in design calculations, both the edge beams and the 95-mm-thick concrete pavement are included in the beam properties, as it is believed to be

119

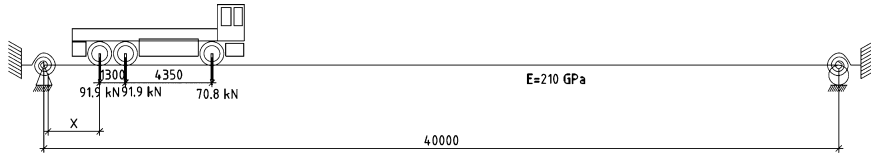# Design of steel piles for integral abutment bridges

Fig. 17. Load from the test truck and model of the bridge over the Leduån (dimensions in mm)

Table 4. Beam Properties of the Bridge Model

Distance from one end (m)	Cross-section area of beam element (m^2)	Moment of inertia at beam element ends (m^4)	Distance from center of gravity of cross section to upper surface of slab (m)
0–0.42 and 39.58–40	1	0.093	0.242
0.42–11 and 20–39.58	0.215	0.093–0.12	0.244–0.274
11–20	0.224	0.135–0.144	0.304–0.314

Table 5. Results from Measurements and Beam Model, Rotations and Deflections

Round	Maximum rotation southern (‰)	Maximum rotation in southern abutment (‰) (mean)	Maximum rotation northern (‰)	Maximum rotation northern (‰) (Mean)	Calculated rotation (‰)	Maximum deflection western beam (mm)	Calculated deflection (mm)	Maximum deflection eastern beam (mm)	Calculated deflection (mm)	Calculated deflection (mm)
October 2007 Round 1	0.44	0.46	0.46	0.43	0.52	6.62	7.12	8.25	7.17	9.2
October 2007 Round 2	0.44		0.43			7.67		6.20		
October 2007 Round 7	0.53		0.41			6.47		7.75		
October 2007 Round 8	0.43		0.42			7.74		6.17		
January 2008 Round 1	0.23	0.22	0.27	0.28		5.15	4.72	5.08	5.04	
January 2008 Round 2	0.22		0.27			4.57		5.06		
January 2008 Round 3	0.22		0.34			4.72		4.80		
January 2008 Round 4	0.22		0.24			4.42		5.23		

Table 6. Results from Measurements and Beam Model, Strains

Round	Maximum strain midspan lower flange (μ-strain)	Maximum strain midspan lower flange (μ-strain; mean)	Calculated strain in lower flange (μ-strain)	Minimum strain midspan upper flange (μ-strain)	Mean value strain in upper flange (μ-strain)	Calculated strain in upper flange (μ-strain)
October 2007 Round 1	68	62	74	−4.10	−4.20	−6.2
October 2007 Round 2	56			−4.65		
October 2007 Round 7	66			−3.86		
October 2007 Round 8	57			−4.17		
January 2008 Round 1	51	52		−4.61	−4.36	
January 2008 Round 2	52			−4.11		
January 2008 Round 3	50			−4.70		
January 2008 Round 4	55			−4.04		

120

Paper III-Monitoring and Analysis of Abutment-Soil Interaction of Two Integral Bridges

conditions. However, the fact that the neutral axis of the composite beam is shifted downward is an indication of a stiffer composite beam and can explain some of the discrepancy between the January and October tests. One reason for the stiffer behavior is that the concrete's Young's modulus is higher at low temperatures (Shoukry et al. 2011).

Summary and Conclusions

The calculation method presented here, taken from the Swedish code of practice, worked well in the evaluation of earth pressures against the abutments of the Haavistonjoki Bridge. The measured earth pressures were a little lower than the calculated pressures. The calculations ignored the effects of the transition slab within the embankment soil and the proximity to the bottom of the abutment.

The measured average modulus of lateral subgrade reaction values at Haavistonjoki were compared with the calculated values. As the passive earth pressures were calculated following Eurocode EN 1997-1 and the corresponding displacement calculated following the Swedish code of practice, the measured and calculated values were similar.

To study the significance of the stiffness of the embankments to midspan displacements, the abutment rotations and midspan strains on the Swedish bridge over the Leduån were measured while driving a truck over the bridge. The rotational stiffness of the abutments was determined according to a simple linear formula, based on the Swedish code of practice, which described horizontal soil-structure interaction. A simply supported beam with the same rotational stiffness at its ends as calculated for the bridge served as a structural model for the comparative analyses. The results with short-term live loads showed good agreement with the modeled values. However, the bridge generally showed a larger restraint than calculated, implying that the backfill was stiffer than expected. Furthermore, the differences between parameters such as the rotational stiffness measured in October 2007 and the rotational stiffness measured in January 2008 clearly indicate a stiffer behavior during wintertime.

References

Card, G. B., and Carder, D. R. (1993). "A literature review of the geotechnical aspects of the design of integral bridge abutments." *TRL Project Rep. 52*, Transport Research Library, Crowthorne, U.K.

Dicleli, M. (2005). "Integral abutment-backfill behavior on sand soil—Pushover analysis approach." *J. Bridge Eng.*, 10(3), 354−364.

European Committee for Standardization. (2004). "Eurocode 7: Geotechnical design. Part 1: General rules." *EN 1997-1*, Brussels, Belgium.

Finnra. (1999a). *Pohjarakennusohjeet sillansuunnittelussa [Guidelines for foundations of bridges],* Helsinki, Finland (in Finnish).

Finnra. (1999b). *Sillan osat. Siirtymälaatta [Type drawing: Transition slab 5 m],* Helsinki, Finland (in Finnish).

Horvath, J. S. (2000). "Integral-abutment bridges: Problems and innovative solutions using EPS geofoam and other geosynthetics." *Manhattan College Research Rep. No. CE/GE-00-2*, Civil Engineering Dept., Manhattan College, New York.

Kerokoski, O. (2006). "Soil-structure interaction of long jointless bridges with integral abutments." Ph.D. thesis, Tampere Univ. of Technology, Tampere, Finland.

Krizek, J. (2010). "Integral bridges soil-structure interaction." ⟨www.jaromirkrizek.eu⟩ (Aug. 11, 2011).

Laaksonen, A. (2004). "Soil-strcture interaction of jointless bridges." M.S. thesis, Tampere Univ. of Technology, Tampere, Finland (in Finnish).

Lehane, B. M., Keogh, D. L., and O'Brien, E. J. (1999). "Simplified elastic model for restraining effects of backfill soil on integral bridges." *Comput. Struc.*, 73(1−5), 303−313.

Mourad, S., and Tabsh, S. W. (1999). "Deck slab stresses in integral abutment bridges." *J. Bridge Eng.*, 4(2), 125−130.

Nilsson, M. (2008). "Evaluation of in-situ measurements of composite bridge with integral abutments." TkL, Luleå Univ. of Technology, Luleå, Sweden.

Pétursson, H., Collin, P., Andersson, J., and Veljkovic, M. (2011). "Monitoring of a Swedish integral abutment bridge." *Struct. Eng. Int.*, 21(2), 175−180.

Shoukry, S. N., William, G. W., Downie, B., and Riad, M. Y. (2011). "Effect of moisture and temperature on the mechanical properties of concrete." *Construct. Build. Mater.*, 25(2), 688−696.

Suomen geoteknillinen yhdistys. (1980). "Kairausopas: Painokairaus, tärykairaus, heijarikairaus [Weight sounding test, ram sounding test]." Vol. 1, Rakentajain kustannus, Helsinki, Finland (in Finnish).

Vägverket. (2004). "Bro 2004 [Bridge 2004. Code of practice]." *Swedish Road Administration Publication No. 2004:56*, Borlänge, Sweden (in Swedish).

121

Paper IV

Monitoring of a Swedish Integral Abutment Bridge

Hans Pétursson, Peter Collin, Milan Veljkovic and Jörgen Andersson

In paper IV, results obtained while monitoring the Swedish bridge over Leduån are presented. This paper is based on in-situ tests planned and partly evaluated by Pétursson, who also has been the author of this paper. Collin has contributed with his experiences, views and opinions through the whole process. Vejlkovic and Andersson contributed with data from the tests and some text in early stages of the work with the paper.

Monitoring of a Swedish Integral Abutment Bridge

Hans Pétursson, Lic Eng, Swedish Transport Administration, Borlänge, Sweden; **Peter Collin,** Prof., Luleå University of Technology/Ramböll, Luleå, Sweden; **Milan Veljkovic,** Prof., Luleå University of Technology, Luleå, Sweden; **Jörgen Andersson,** M.Sc., Luleå University of Technology, Luleå, Sweden. Contact: hans.petursson@trafikverket.se
DOI: 10.2749/101686611X12994961034291

Abstract

One of the most commonly discussed problems regarding bridges with integral abutments is the influence of longitudinal elongation of the superstructure as a result of seasonal temperature variations. A bridge built with integral abutments is often supported by a row of piles made of steel or concrete. The longitudinal elongation of the superstructure induces a displacement and a rotation at the top of the pile, which in turn may cause strains that exceeds the yield strain. Such seasonal variations may lead to low-cyclic fatigue failure in the pile. Therefore, it is of great interest to investigate the amplitude of these strains, as well as the general behaviour of the bridge. In 2005, the European R&D project, INTAB (RFSR-CT-2005-00041, "Economic and Durable Design of Bridges with Integral Abutments, 2005–2008") was started. Within the INTAB project a composite bridge was built and monitored in Northern Sweden.

Keywords: integral abutments; steel piles; composite bridges; monitoring; live load testing.

Introduction

The cost of maintenance is an ever-growing problem for road administrations around the world, and bridges are no exception. One way to reduce the need for future maintenance, as well as the investment cost, is to construct bridges without expansion joints and bearings; which in this paper is referred to as integral abutment bridges (see *Fig. 1*).

Conventional bridges are in general built with expansion joints and bearings, which can both be considered weak points in the bridge structure. Leaking joints are a common reason for corrosion problems in bridges. These joints need to be maintained, repaired and also often replaced several times during the service lifetime of the bridge. Therefore, if bridges are built without any expansion joints, it is possible to reduce the maintenance cost.

Integral abutment bridges have other benefits besides lower maintenance costs: there will be no expenditure on purchase of expansion joints and bearings. The foundation works can be simplified, which would result in lower construction costs. Furthermore, a shorter construction time saves money not only for the contractor but even more for the road users, a fact that is becoming increasingly important. No expansion joint also means less noise and higher comfort when a car enters or leaves the bridge.

As the piles are connected to the retaining walls of the bridge, the piles will follow the bridge's deformation with respect to both rotations and translations as a result of seasonal as well as daily temperature changes (see *Fig. 2*). This is also the case for

deformation caused by traffic on the bridge. Hence, in order to understand the mechanisms of integral abutment bridges, it is necessary to study the effect that movements in the abutment have on the stresses in the piles.

Analysing the stresses in the piles subjected to lateral movements is complex as it contains two co-dependent elements: the flexural pile and the soil. To further complicate matters, soils are often inhomogeneous. It is possible to obtain analytical solutions only for simple cases where the stiffness of the soil is constant along the pile, and the materials feature elastic behaviour. Expressions of the cases with constant or linear varying soil stiffness are given by the theories for beams on an elastic foundation. To handle more complex cases where soil stiffness varies with depth, an equivalent stiffness can be assumed.

In 2005, the European R&D project INTAB was started.[1] In May 2006, an international workshop on integral abutment bridges with participants from eight countries was organized by invitation and held in Stockholm.[2] The goal of the workshop was to share the experiences of the participants and to further increase the understanding of the design, construction, and maintenance of integral abutment bridges. During the workshop, it became clear that various approaches to the design of integral abutment bridges exists in different
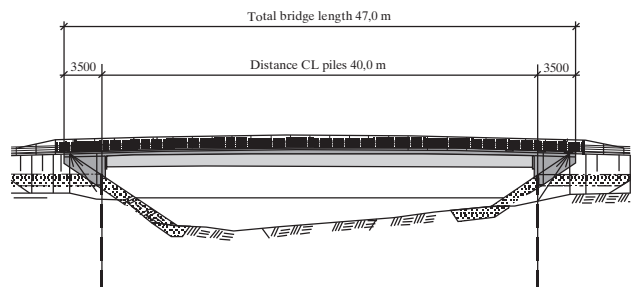
Fig. 1: The integral abutment bridge over Leduån (Units: m)

Within the figure: Total bridge length 47,0 m; Distance CL piles 40,0 m; 3500; 3500

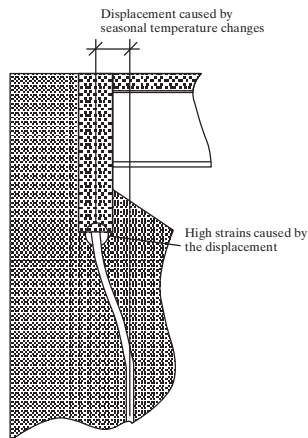# Design of steel piles for integral abutment bridges

Fig. 2: Pile deformation due to seasonal temperature variation induces strains in the steel pile

countries. Results of a European survey to illustrate the design criteria were compared to the best practice of transportation agencies in the United States.[3] There are many similarities in design assumptions and construction practices. Yet, there are also significant differences, especially regarding limits for the bridge length. Furthermore, the type of piling as well as the detailing of bridges differs much, from country to country.

Bridge over Leduån

Presently, there are no specific design rules existing for integral abutment bridges in Sweden and most European countries. In the future, bridges will be designed according to the Eurocodes. A common design criterion for the serviceability limit state is to restrict the allowable stresses to the yield limit (see EN 1993-2 7.3). This will curb the possibility to build longer integral abutment bridges founded on steel piles. EN 1990 3.4 states that "The limit states that concern: (a) the functioning of the structure or structural members under normal use; (b) the comfort of people; (c) the appearance of the construction works, shall be classified as serviceability limit states". None of these criteria are violated because of the fact that the pile experiences some inelastic strains. Some might consider the appearance of construction work as violated. But the part is hidden under the ground surface and will not make anyone using the bridge uncomfortable, and

it therefore need not be considered a violation of the rule. A structure's functionality can be endangered during normal use of piles only if cracks were to form in the steel piles. The bending strains in the piles are not necessary for the bridge to transfer the loads to the soil and would virtually vanish in a hinged pile, but a mechanism of this kind is both more expensive and susceptible to frequent maintenance problems. A pile joint without a hinge mechanism is therefore preferable in practice.

In order to investigate the stresses in the piles, the bridge behaviour as well as the accuracy of design models, a bridge was instrumented and monitored (see *Fig. 3*). The influence of both seasonal temperature variations and short-term traffic loads were studied.

Design and Construction

The bridge over Leduån is a 40 m single span integral abutment bridge. The composite superstructure comprises two I-shaped welded steel beams, and a one lane slab of concrete with characteristic compressive strength $f_{ck} = 40$ MPa (C40/50) (see *Fig. 4*). The superstructure is supported by end-bearing piles of steel pipe RR170 × 10 in S440 grade. Six piles are placed in a single row under each abutment. The piles were driven into the soil along a straight line perpendicular to the longitudinal axis of the bridge. The bearing piles were sheltered to a depth of 2 m under the lower end of an abutment by wider steel pipes of diameter 600 mm. Styrofoam plates were inserted inside the sheltering pipes and the remaining space was filled with loose

sand. A detailed description is given in the works of Nilsson[4] and Hällmark.[5]

The following sequence was used when constructing the bridge in order to reduce the effects of thermal movements on fresh concrete and to control moments induced into the supporting pile system:

1. The soil was excavated down to a level at which soft soil was wanted.
2. The piles were driven down in the ground.
3. The sheltering steel pipes and styrofoam plates were placed. The space between the steel piles and the steel pipes were filled with loose sand (see *Fig. 5*).
4. Blasted rock was filled around and up to the level of the top edge of the steel pipes, and then compacted.
5. The pile caps were poured to the required bridge seat elevation. Temporary bearings were installed.
6. The wing-walls were poured (see *Fig. 6*).
7. The beams were set and anchored to the abutment on temporary bearings. The bearings allow wide room for further dead load rotations.
8. The bridge deck was poured in the desired sequence, excluding the abutment retaining wall and the last portion of the bridge deck of length equal to the retaining wall width. In this manner, all dead load slab rotations occurred prior to locking the superstructure to the abutment, and no dead load moments were transferred to the supporting piles.
9. The retaining walls/pile caps were poured to full height. As no backfilling had yet been placed at this point, the abutment was free to move.
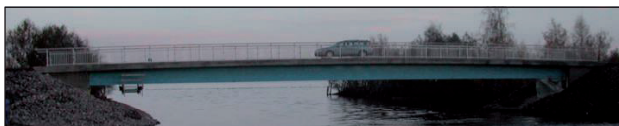

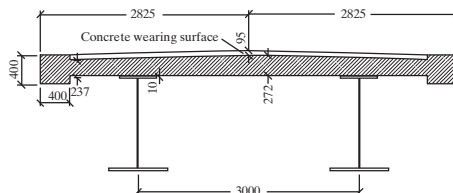Fig. 3: The bridge over Leduån in Northern Sweden

Fig. 4: Cross section of the bridge (Units: m)

126

Fig. 5: Piles have been driven. The pile to the right was later used for monitoring. The picture shows the loose sand and sty-rofoam plates that were used to achieve a less stiff surrounding for the upper part of the piles

Fig. 6: The bridge superstructure before it was launched in place

10. The soil behind the retaining walls was filled and compacted simulta-neously behind both abutments of the bridge.

Instrumentation of the Bridge

The bridge was monitored during a period of 18 months. Totally 34 gauges were placed on the bridge as shown in *Figs. 7 and 8*. Strain-gauges were welded to the bridge girder and to the piles. The strains in the piles were measured at five different levels with two strain-gauges at each level as shown in *Fig. 8*. The two strain-gauges in each section (position 5–9 in *Fig. 7*) were oriented and placed in such a way that the maximum strains of the cross section could be measured. At the upper four levels, the differ-ence in strain between two strain-gauges was stored (bending strain). Signals obtained from both pairs of strain-gauges at the fifth level were stored separately and an estimation of the axial force in the pile was made (*Table 2*).

The movement of the retaining walls was measured with level indicators, two at each side of the bridge (gauges 3 and 4 in *Fig. 7*). The level indicators were placed in a vertical plane along the centre line of the bridge at a verti-cal distance of 1,5 m between gauges on each abutment. With a known geometry of the abutment, rotation and displacement of the pile cap could be estimated from these measure-ments. Two strain-gauges (gauges 1 and 2 in *Fig. 7*) were welded at the steel girders' flanges, close to the south abutment, to get an indication of the moment constraint obtained at the bridge end. Strain-gauges were also welded to the upper and lower flanges at the mid-span of the bridge (position 10 and 11 in *Fig. 7*) for an estimation
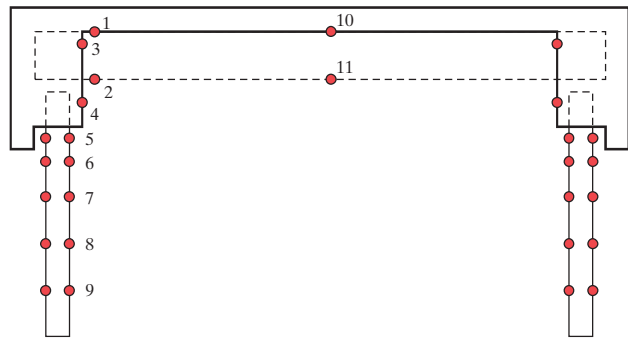

Fig. 7: A sketch showing the gauges that were used during the monitoring of the bridge

Part	Dimensions (mm)	Material
Upper flange	25 × 500/25 × 600	S460M
Web	13 × 1221/11 × 1234	S355J2G3
Lower flange	36 × 800/40 × 800	S460M

The length of each end part is 11,2 m and the middle part is 18 m. The height of the steel girder varies from 1073 to 1299 mm.

Table 1: The dimension of the bridge girders, end part/middle part

Gauge number according to *Fig. 4*	
1	Strains in upper flange at support
2	Strains in lower flange at support
3 and 4	Horizontal displacement of retaining wall, gauges placed on both abutments
5–8	Bending strains in the pile were measured with two gauges and the differences were recorded; strain-gauges were placed on one pile in the northern and one in the southern abutment
9	Strains in the pile measured with two gauges, signals from both were recorded; strain-gauges were placed on one pile in the northern and one in the southern abutment
10	Strains in top flange at mid-span
11	Strains in bottom flange at mid-span

Table 2: Explanations of what the gauges are used for

127

of the overall bridge behaviour. Temperature was measured at three locations in the concrete slab, in the steel flange and in the air. Detailed accounts of the gauges are given in the work by Nilsson.[4]
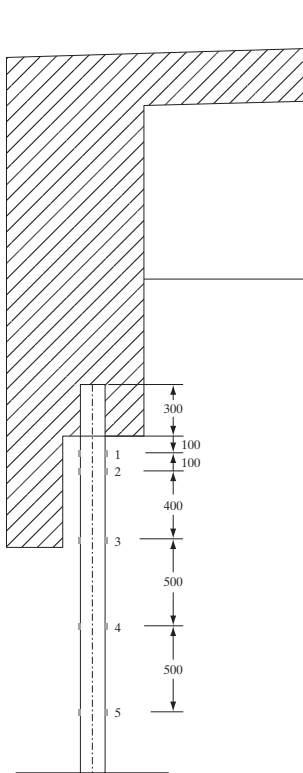

Fig. 8: Two strain-gauges were placed at five positions along the piles. For the upper four gauges the difference in strain between the two gauges was recorded (Units: mm)

Results from Monitoring

Long Term Monitoring

During the 18 months of monitoring the sampled data from strain measurements at the northern pile and the southern pile show a similar trend of variation. However, a clear difference in amplitudes exists. The maximum measured bending strain amplitudes are 881 μ-strain for the northern pile and 518 μ-strain for the southern pile (difference between two gauges in one section; see *Fig. 9*). With the assumption that Young's modulus is 210 GPa the corresponding bending stresses are ±93 and ±54 MPa for each pile, respectively. The measured temperature variation in the concrete deck was 43°C, which is much lower than the expected 50 years' maximum of 80°C (*Table 3*) according to Bro 2004.[6] Such a difference has to be statistically expected in a case where measurements are available only for a limited time period.

Short Term Monitoring and Comparison with Finite Element Analysis

Finite element analysis (FEA) was used to interpret the results of short-term measurements. The short-term measurements were made approximately every three months. A lorry with a maximum mass of about 25 t was used as test load (see *Fig. 10*). The strains were also measured on the bridge before loading, and after the

truck loading of the bridge. It was thus possible to get the strains due to just the truck load.

The soil characteristics were estimated by calibrating results of a simple two-dimensional finite element (FE) model with data from short-term measurements. A limited geotechnical investigation was made in-site and used to check the credibility of FEA.

Springs were used to model the support behind the retaining as well as the effects from the soil surrounding the piles (*Table 4*).

Recommendations from BRO 2004[6] were used as the starting value for the definition of the spring stiffness.

The spring stiffness, k, is given as:

$$k = k_k \cdot A_{\text{spring}} = k_k \cdot d \cdot s \qquad (1)$$

where A_{spring} is the projected pile-soil contact area related to one spring, d is the outer pile diameter, s is the distance between two springs and k_k (MN/m^3) is the sub-grade reaction modulus at the depth z. For friction-type soil the sub-grade reaction modulus is given by:

$$k_k = \frac{n_h \cdot z}{d} \qquad (2)$$

The constant of sub-grade reaction modulus, n_h (MN/m^3), can be found in BRO 2004.[6] According to the geotechnical investigation, the soil surrounding the piles was sand with a very low consistency. Thus n_h was taken as:

	Assumed Values in Design	Measured Values
Low temperature	−40°C	−16°C
High temperature	+40°C	+21°C
Temperature range	80°C	37°C
Stress range	269 MPa	93 MPa (Northern pile)
MPa/°C	3,36	2,58

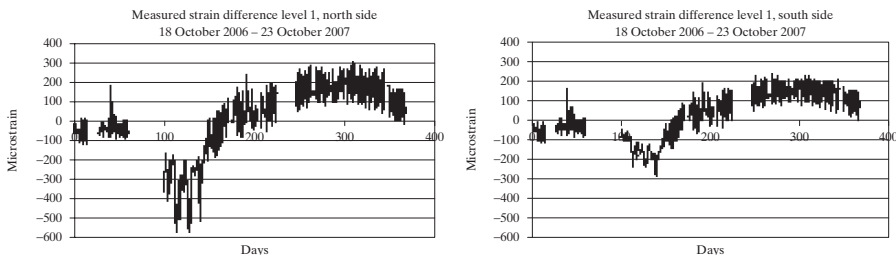*Table 3: Calculated and measured temperatures and stresses in the concrete slab*

Fig. 9: Measured strain difference between the northern and southern piles, for a period of 12 months
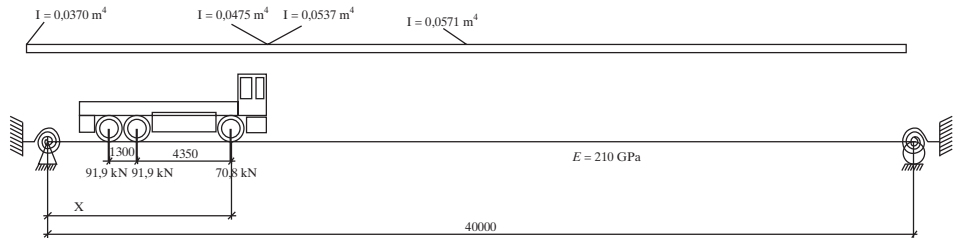
128

Fig. 10: The truck used for short-term monitoring. The theoretical moment of inertia of one composite bridge girder is also shown above (with the assumption that the ratio between Young's modulus is $E_{steel}/E_{concrete} = 7,2$)

| Below ground water level | Linear increase 0,00–1,71 m | $n_{hd} = 1,5$ MN/m³ |
| | Constant stiffness 1,71–6,00 m | $k_{kd} = 2,57$ MN/m² |

Table 4: Distribution of the soil properties along the pile, according to Bro 2004

– $n_h = 2,5$ MN/m³ over the ground water level;
– $n_h = 1,5$ MN/m³ under the ground water level.

In the considered soil model, the soil stiffness increases linearly with the depth until a maximum value of the product $k_k d$ is reached and then remains constant.

For sand with a very low consistency, these limits are:

– $(k_k d)_{max} = 4,28$ MN/m² over the ground water level;
– $(k_k d)_{max} = 2,57$ MN/m² under the ground water level.

Calibration of the FE model was made by varying the characteristics of soil properties.

The ground water level was assumed to be at the top of the pile.

The depth, z_c, at which the stiffness stops increasing and remains constant can be derived from $k_k d$ and n_h:

$$z_c = \frac{k_k \cdot d}{n_h} = \frac{4,28}{2,5} = 1,71 \text{ m} \qquad (3)$$

and the corresponding stiffness was:

$$k_c = (k_k d)_{max} \cdot s \qquad (4)$$

Results of FE calculations with soil properties used for design according to BRO 2004[6] indicated larger strains than the measured values, which could be explained by the fact that in the real bridge the piles are not rigidly fixed at the pile cap *(see Figs. 10 and 11)*.

The influence of springs supporting the piles is almost negligible for the

vertical displacement of the bridge measured while the empty lorry crossed the bridge (see *Fig. 12*).

Short-term measurements indicate that the deflections are asymmetric, as the deflections are consistently larger on the eastern side of the bridge, but the variations are quite small, 10–15%. The unsymmetrical deflections could probably be explained by some eccentricity in the loading and varying response of the back fill behind the abutment, or a combination of these factors.

The strains in the upper part of the piles (gauge 5 in *Fig. 7*) were measured in both summer (October) and winter (January) conditions, using the same lorry with a total weight of 24,0 t. In October, the maximum strain amplitudes were 95 μ-strain and 84 μ-strain for the northern pile and southern pile, respectively (*Table 5*). These strain differences correspond to the stress amplitude on each side of the pile of

20 MPa and 18 MPa, for each pile, respectively.

In January, the maximum strain amplitudes were 47 μ-strain and 45 μ-strain for the northern pile and southern pile, respectively. These strain differences correspond to the stress amplitude on each side of the pile of 10 MPa and 9,5 MPa, for each pile, respectively. The bending stresses in the piles during winter conditions were, according to the monitoring, 46 to 50% lower than for summer conditions (*Tables 6 and 7; see also Fig. 9*).
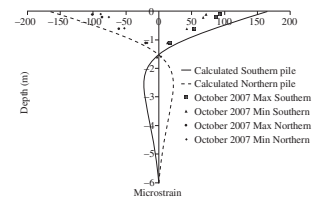

Fig. 11: Comparison between strains calculated by FEA and measured in the pile. The bridge is loaded by a truck according to Fig. 10
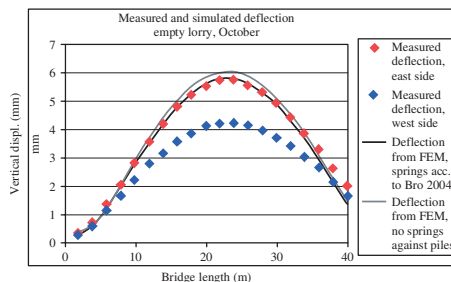

Fig. 12: Measured deflection compared to deflection modelled by FEM. The bridge was loaded by a truck as shown in Fig. 10

Design of steel piles for integral abutment bridges

	Northern pile (*μ*-strain)	Northern pile (MPa)	Southern pile (*μ*-strain)	Southern pile (MPa)	Deflections (mm)
October 2007	94,5	19,9	83,9	17,6	8
January 2008	46,9	9,9	45,3	9,5	5,8
Difference (%)		50,4		45,9	27,5

Load according to *Fig. 10.*

Table 5: Measured strains in the piles, gauges N5 and S5

	Upper flange (*μ*-strain)	Upper flange (MPa)	Lower flange (*μ*-strain)	Lower flange (MPa)
October 2007	−3,8	−0,8	74,8	15,7
January 2008	−4,2	−0,9	53,3	11,2

Load according to *Fig. 10.*

Table 6: Measured strains in the flanges at mid-span, gauges 10 and 11, at maximum deflection

	Upper flange (*μ*-strain)	Upper flange (MPa)	Lower flange (*μ*-strain)	Lower flange (MPa)
October 2007	−3,8	−0,8	−26,3	−5,5
January 2008	−6,1	−1,3	−31,4	−6,6

Load according to *Fig. 10.*

Table 7: Measured strains in the flanges at support, gauges 1 and 2, at maximum deflection

For the configuration giving maximum deflection in mid-span, the measured bending stresses are 28% larger for summer conditions compared to winter conditions. Also the deflections are larger in October, which could be explained by a larger restraint on the back wall when the soil around the bridge is frozen.

Conclusions

In this paper, results obtained while monitoring the Swedish bridge over Leduån have been presented. For this bridge, the response in the piles and the superstructure was measured for both thermal and traffic loading. Furthermore, a procedure for erecting integral abutment bridges, minimizing the bending stresses in the slender steel piles, has been described.

Part of the problem with integral abutment bridges is that, for all their simplicity of construction, they are complicated structural systems. To thoroughly analyse a given structure, the designer must not only design for primary loads (dead load, live load, wind load, etc.) but must also accurately account for secondary loads (creep, shrinkage, settlements, temperature effects, etc.). To further complicate the analysis, the response of the structure to a given set of forces is much dependent on the geometry, materials, configuration, soil interaction and construction details of the individual system. In order to avoid this complicated analysis, integral abutment bridges should typically be designed by using conservative methods and by building on field experience.

Despite these mentioned uncertainties, the measured values from Leduån with respect to deflection and pile stresses show a fair agreement with the FEA carried out with soil parameters according to BRO 2004.[6] The published research can be used as a knowledge base to determine reasonable guidance for the safe design of integral abutment bridges.

It is believed that integral abutment bridges will continue to gain ground in Europe. Although Eurocodes do not contain specific information on how to construct and design integral abutment bridges, they make it easier for engineers to transfer knowledge on the subject.

References

[1] Feldmann M, Naumes J, Pak D, Veljkovic M, Nilsson M, Eriksen J, Collin P, Kerokosi O, Petursson H, Verstraete M, Vroomen C, Haller M, Hechler O, Popa N. *Economic and Durable Design of Composite Bridges with Integral Abutments*. European Commission, Publications Office of the European Union: Luxembourg. ISBN 978-92-79-14598-8.

[2] Collin P, Veljkovic M, Petursson H. *International Work Shop on Bridges with Integral Abutments*. Technical Report 2006:14, Lulea University of Technology. ISSN 1402-1536. http://epubl.ltu.se/1402-1536/2006/14/LTU-TR-0614-SE.pdf.

[3] White H, Petursson H, Collin P. *Integral Bridges: The European Way*. Practice Periodical on Structural Design and Construction, Vol.15, No.3, pp.201-208, August 2010.

[4] Nilsson M. *Evaluation of In-situ Measurements of Composite Bridge with Integral Abutments*, Licentiate Thesis at Lulea University of Technology, 2008. http://epubl.ltu.se/1402-1757/2008/02/LTU-LIC-0802-SE.pdf.

[5] Hällmark R. *Low Cycle Fatigue of Steel Piles in Integral Abutment Bridges*, Master's Thesis at Lulea University of Technology, 2006. http://epubl.ltu.se/1402-1617/2006/291/index.html.

[6] Swedish Road Administration (Vägverket); BRO 2004, *Vägverket allmänna beskrivning för nybyggnad och förbättring av broar*, Vägverkets publikation, 2004, 56. ISSN 1401-9612.

Paper V

Low-Cycle Fatigue Strength of Steel Piles Under Bending

Hans Pétursson , Mikael Möller and Peter Collin

This paper describes bending tests and models of clamped piles demonstrating that a steel pipe pile can accommodate large inelastic deformations under strains six times greater than the yield strain for several hundred load cycles.

Low-Cycle Fatigue Strength of Steel Piles under Bending

Hans Petursson, Lic Eng., Swedish Transport Administration, Borlänge, Sweden; **Mikael Möller,** Prof. Steel Structures, Luleå University of Technology/AREVA, Helsingborg, Sweden; **Peter Collin,** Prof., Composite Structures, Luleå University of Technology Luleå, Sweden. Contact: hans.petursson@trafikverket.se

Abstract

Clamped abutment piles for integral abutment bridges experience both a compressive normal force and bending load cycles stemming from daily and yearly temperature variations. This paper describes experiments using full-scale models of clamped piles to demonstrate that a steel pipe pile can accommodate large inelastic deformations under strains six times greater than the yield strain for several hundred load cycles. This indicates that by permitting pile strains in excess of the yield strain (which is not permissible under most current design codes), integral abutment bridges could be erected with spans of up to 500 m and a projected service life of 120 years. The tests were carried out as a step towards the development of design rules for determining the capacity of piles for integral abutment bridges.

Keywords: integral bridges; low cycle fatigue; steel piles; bridge tests; jointless bridges.

Introduction

Steel piles in integral abutment bridges can experience severe strain during service due to soil restraint and annual fluctuations in bridge temperature, which displace and rotate the end of the pile that is clamped to the superstructure. These bending strains in the piles are not required for load transfer from bridge to soil and could be eliminated by using a hinged pile design. However, hinged piles are more expensive and might require frequent maintenance, making clamped pile joints preferable in practice. As a result, it would be desirable to know how repeated inelastic strains might affect the load-carrying capacity of a pile and whether it is possible to ignore such secondary effects without compromising the safety of the design.

Most design codes do not allow strains exceeding the yield point in the serviceability limit state. This conservative approach is rooted in a general fear of plasticization and concerns regarding low-cycle fatigue. However, in the ultimate limit state, current codes do not prohibit plasticization of the pile cross section. Full-scale static

tests conducted using X-shaped steel piles have demonstrated that piles are capable of carrying both the normal force and imposed deformations at the top.[1] Tests were conducted at Lulea University of Technology, Sweden, to demonstrate that steel pipe piles are in fact capable of withstanding cyclic strains that greatly exceed the yield strain for several hundred cycles without reducing their ability to safely carry the required axial loads over the designed service lifetime of 120 years for Swedish bridges.

It is important to distinguish between low-cycle fatigue and high-cycle fatigue. In high-cycle fatigue, there are millions of stress cycles prior to failure and the stresses are elastic. Conversely, low-cycle fatigue is typically characterised by large strains in the plastic range, and failure occurs after less than 10 000 cycles. High-cycle fatigue strengths of materials are often visualised using S–N diagrams. Low-cycle fatigue can

be visualised using a similar diagram in which the strain is plotted on the vertical axis instead of stress. Traffic over bridges causes them to undergo millions of stress cycles in the high-cycle fatigue domain, whereas temperature fluctuations and variations cause stress cycles in the low-cycle fatigue domain.

Some low-cycle fatigue tests have been reported in the literature. Five different structural steels with static yield strengths between 100 and 485 MPa were tested under cyclic plastic uni-axial strains with amplitudes ranging from ±1 to ±7%.[2] Cyclic hardening was observed in all steels and the maximum cyclic stress was found to be dependent on the steel type and the strain range. It was also found that steel types of similar manufacturing specifications exhibit rather similar cyclic stress–strain curves when subjected to cyclic inelastic strain, irrespective of the monotonic yield strength, and that the overall fatigue life was similar for all of the steels tested.

Low-Cycle Fatigue Tests

Test Set-Up

Two test specimens were made from 2100 mm long steel pipes that were cast into 600 mm long blocks of reinforced concrete with a square cross section 300 mm long on each side. The concrete was centred about the midpoint of the pipe (see *Fig. 1*). Each specimen was made with the steel pile cantilevering out of a concrete block in two directions as can be seen in *Fig. 3*. This made it possible to use each
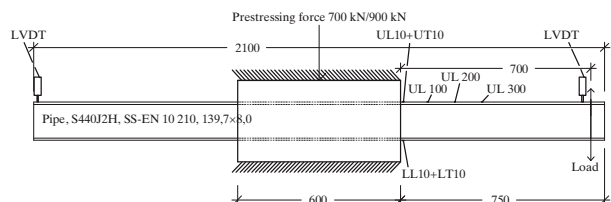
Fig. 1: The test set-up (units: mm)

	C	Si	Mn	P	S
Maximum	0,18	0,25	1,6	0,02	0,018
Typical	0,07	0,18	1,4	0,01	0,006

Table 1: Chemical composition of the steel in the tested piles (max. weight percent)[3]

Fig. 2: Photos of the test set-up from two different angles

Fig. 3: Graph of results from tensile tests with strains (%) on the x-axis and stress (MPa) on the y-axis. The dotted lines are calculated values with E = 210 GPa, one with origin at origo and the other with origin at $\sigma = 0$ MPa and $\varepsilon = 0,2\%$

specimen for two tests. To ensure that the steel pile was sufficiently clamped in the concrete block, to simulate actual situations in a satisfactory manner, 14 stirrups were used to reinforce the concrete. Eight φ12 stirrups were evenly spaced along the length of the concrete block surrounding the pile. Four were placed lengthwise, two φ12 stirrups on each side of the steel pile and one φ8 stirrup was placed over the steel pile and one beneath.

In reality, piles are subjected to a combination of axial forces and bending moments but in the tests, they are only subjected to bending. The reason for this, besides making testing easier, is the annual temperature cycle that mainly causes bending in the piles. The normal forces in piles are in compression and the strains are of smaller magnitude in real piles, at most half of the yield limit. It is therefore representative for describing the real problem in loading the piles in the test, purely in bending. Four tests may not be sufficient to draw far-reaching conclusions but is a step towards the development of design rules for determining the capacity of piles for integral abutment bridges.

The steel pipes were cold formed and had a longitudinal weld. The pile was oriented such that the weld was placed in the neutral axis during the tests. Each pipe was equipped with five strain gauges. Three of the gauges measured the longitudinal strains on top of the pipe at distances of 100, 200 and 300 mm from the concrete block end, respectively. Two additional gauges measured both longitudinal and transverse strains at a distance of 10 mm from the concrete block end, one at the bottom and the other at the top of the pipe's cross section. The deflection of the load point (at one pipe end) was measured with a displacement gauge, as was that of the unloaded end. The displacement gauges used are accurate to within 0,1%. The load (or displacement) was applied 700 mm from the near end of the concrete block by means of a servo hydraulic cylinder (Instron 270 kN) and a 250 kN load cell. A steel beam was placed along and on top
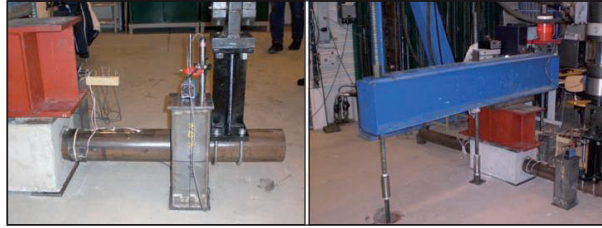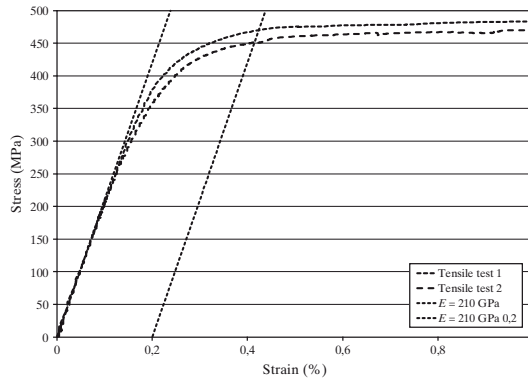
Diameter of pile (mm)	Thickness (mm)	Yield strength $f_{y0,2}$ (MPa)	Ultimate strength f_u (MPa)	Maximum elongation ε_{max} (%)
113,9	8	460	486	23

Table 2: Specifications of the tested piles. Three tensile tests were performed; the mean values are presented here

|	Unit	1	2	3
Date of casting		21 November 2008	21 November 2008	21 November 2008
Date of test		28 January 2009	28 January 2009	28 January 2009
Age at test	days	68	68	68
Length	mm	149,9	150,3	149,6
Width	mm	150,5	151	151,3
Height	mm	150,1	150,4	150
Mass	g	7768	7868	7786
Area	mm²	22560	22700	22630
Volume	dm³	3,386	3,413	3,395
Density	kg/m³	2294	2305	2293
Failure load	kN	1171	1196	1200
Compression strength	MPa	51,9	52,7	53
Load rate	kN/s	22,5	22,5	22,5

Table 3: Properties of the concrete blocks used in the tests
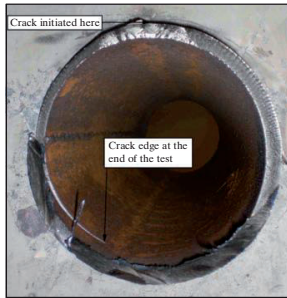
Fig. 4: Cross section of a cracked pipe after testing. After initiation it is possible to see marks after each cycle

Fig. 6: Load ranges applied during the tests

Test number	Displacement range (mm)
1	44,1
2	45,5
3	43,5
4	44,1

Table 4: Displacement range at tests

of the concrete block supported by the loading frame floor. A second steel beam was placed perpendicular to and on top of the first beam, and anchored to the frame floor using three 32 mm diameter Dywidag bars. The bars were pre-stressed to prevent the concrete block from moving and to ensure that the block remained in close contact with the floor during testing. The resultant force acting on the concrete block owing to pre-stressing was 900 kN. Pictures of the test set-up are shown in *Fig. 2*.

Materials

The piles used in the tests were constructed from a fine grain carbon–manganese structural steel with the designation S440J2H that has a typical carbon equivalent value (CEV) of 0,30 (maximum 0,39). The chemical composition of steel is shown in *Table 1* and the specifications of the piles are presented in *Table 2*. Three concrete test cubes were constructed from the same cast that was used for the concrete around the piles. Results from the concrete cube tests are presented in *Table 3*.

Three tensile tests were carried out. As shown in *Fig. 3*, Young´s modulus of the steel was approximately 210 GPa according to two of the tensile tests, the third was considered to be wrong and was not used. The tangent modulus starts to deviate from the initial value of Young's modulus at 200 to 300 MPa.
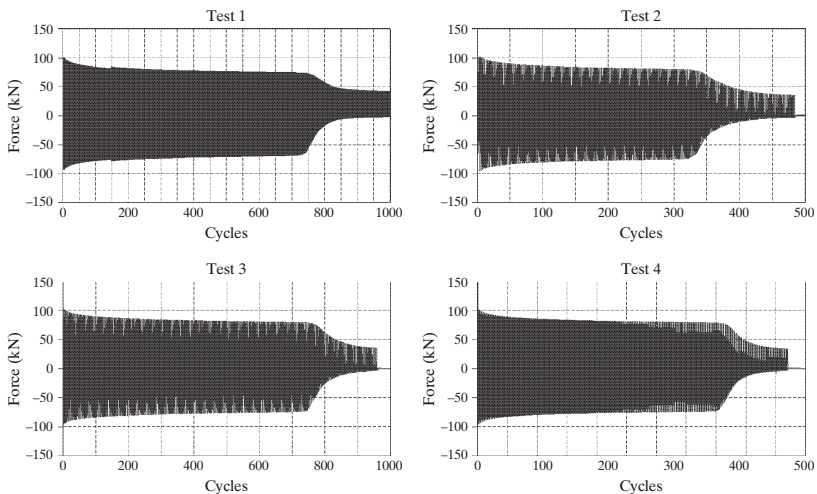

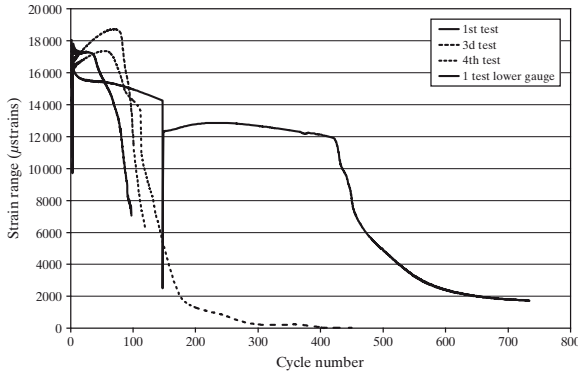Fig. 5: Changes in force applied over time during each test

135

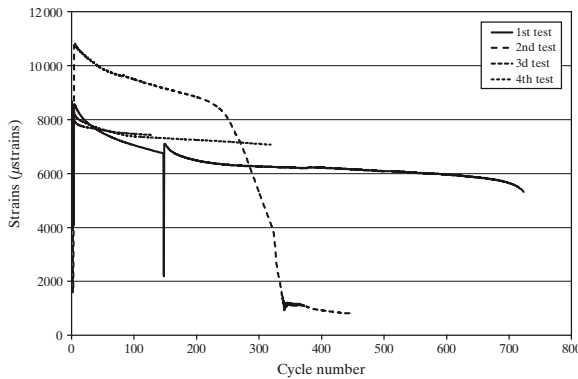*Fig. 7: Range of observed strains at the first strain gauge*

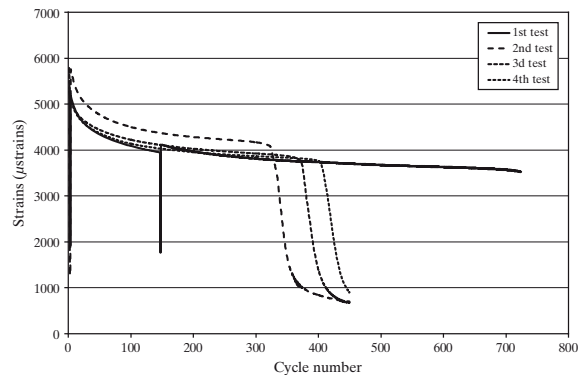*Fig. 8: Range of observed strains at the second strain gauge. The gauges failed part-way through tests 3 and 4*

Fig. 9: Range of observed strains at the third strain gauge

Test Procedure

The tests were started by slowly increasing the load on the pipe in the upward direction until the load–displacement curve began to plateau. This was achieved at a load of 100 kN in all tests, a value that is in good agreement with the theoretical plastic moment capacity of the cross section. The load was then reversed until a similar plateau was reached for downward loading. The plateau load for downward loading was –95 kN, which is somewhat smaller than that for the upward load. The measured displacements corresponding to the plateau loads were then used to control the displacement at the loading point of the pipe. For the first specimen, the loading point was subjected to cyclical displacements over a range of 44 mm. The pipe end displacement ranges used in the other three tests are shown in *Table 4*. In all tests, the loading frequency was maintained at 0,5 Hz.

Test Results

In all four tests, the failure mode for the steel pipes involved low-cycle fatigue cracking as shown in *Fig. 4*.

The cracks were initiated at the top of the pipe's cross section close to the end of the concrete block and initially grew through the pipe wall. The cracks were first observed after 711, 319, 366 and 402 cycles, respectively, in the four tests. Cyclic softening was observed during all tests, as can be seen in *Fig. 5*, which shows the vertical load applied to the pipe as a function of time for each test.

In all tests, the rate of softening was very high during the first 100 load cycles and decreased thereafter (*Fig. 6–10*). This could reflect softening of the steel itself but is more likely to originate from a softening of the concrete around the pipe. The first test was halted at 145 cycles as it was observed that the loaded part of the pipe was slowly but steadily moving out of the concrete block during each load cycle. As a result, the top and bottom strain gauges for the second test (i.e. those located 10 mm from the concrete block end; see *Fig. 1*) were destroyed and so could not be used in the test (*Fig. 7*). After this incident, the positions of the remaining pipes were fixed longitudinally by welding a small steel tab to the pipe wall, flush against the concrete along the pile's neutral axis. Crack initiation and early growth occurred
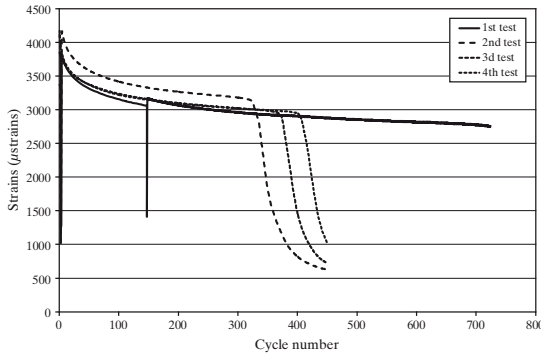
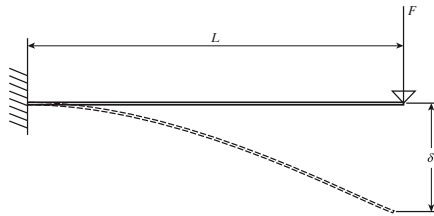*Fig. 10: Range of observed strains at the fourth strain gauge*

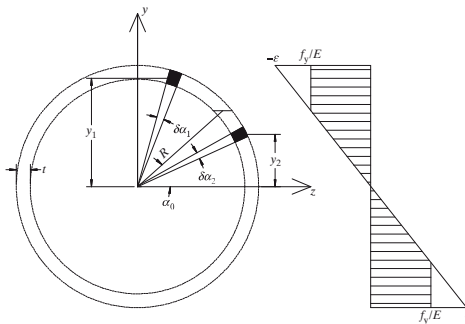*Fig. 11: A cantilever of length L under a vertical load F*

Fig. 12: Strain and stress distribution in circular cross section
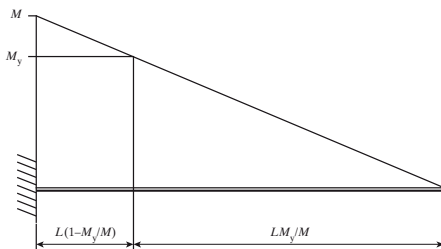

Fig. 13: Moment along a cantilever

after several hundred load cycles after which the pile's load-bearing capacity dropped rapidly over approximately 50 load cycles as the wall-through crack propagated in two opposite directions along the circumference of the pipe's cross section. At the end of the test, the crack had typically propagated across approximately 60% of the circumference of the cross section. The residual load-bearing capacity is not symmetric with respect to the direction of the load. Thus, under a crack-closing load, the residual load was approximately 40% of that for an undamaged pipe. This implies that the crack is not closing ideally, which in turn indicates significant plastic deformation around the crack tips. Conversely, crack-opening loads reduce the residual load bearing to almost zero. The strain ranges measured during the tests are shown in *Figs. 7–10*.

Analysis

In order to analyse the damage caused by bending strains in an integral abutment pile, it is necessary to calculate the magnitude of the strains. The strains in a pile in a bridge with integral abutments are controlled by the abutment displacements and rotations. In the case of low-cycle fatigue, it is the annual temperature variations that give the highest strains and hence the horizontal displacement is of most interest. Therefore, the expressions in these tests are derived for the strain as a function of moment and displacement as a function of strain.

Calculating the Strain

For the part where the strain is greater than the yield strength, the contribution to the moment in the cross section is (see *Fig. 12*):

$$dM1 = f_y \sin(\alpha)\, tR^2\, d\alpha \qquad (1)$$

For the part where the strain is equal to or less than the yield strain, the contribution to the moment is:

$$dM2 = \varepsilon E \sin^2 \alpha tR^2 d\alpha \qquad (2)$$

These expressions are then integrated:

$$M(\alpha_0) = 4\left(\int_0^{\alpha_0} \varepsilon E \sin^2 \alpha tR^2 d\alpha \right.$$
$$\left. + \int_{\alpha_0}^{\frac{\pi}{2}} f_y tR^2 \sin \alpha d\alpha \right) \qquad (3)$$

where α_0 is the central angle with sides passing through a point with zero strain and the nearest point with yield strain is:

$$M(\alpha_0) = 4R^2 t \left(f_y \left| 1 - \cos \alpha \right|_{\alpha_0}^{\frac{\pi}{2}} + E\varepsilon \left| \frac{\alpha}{2} - \frac{\sin 2\alpha}{4} \right|_0^{\alpha_0} \right) = 4R^2 t \left(f_y \cos \alpha_0 + E\varepsilon \left(\frac{\alpha_0}{2} - \frac{\sin 2\alpha_0}{4} \right) \right) \qquad (4)$$

$\varepsilon(\alpha_0) = \varepsilon_y / \sin \alpha_0$ in which $\varepsilon(\alpha_0)$ denotes the strain in the extreme fibre for a specific angle α_0.

Moreover, it holds that $\cos \alpha - (\sin 2\,\alpha / 4\sin \alpha) = \cos(\alpha/2)$ and that the plastic moment $M_p = 4f_y R^2 t$ in expression (4) can be rewritten as:

$$M(\alpha_0) = M_p \left(\frac{\alpha_0}{2\sin \alpha_0} + \frac{\cos \alpha_0}{2} \right) \qquad (5)$$

It is not possible to arrive at a closed form solution of Eq. (5). In order to facilitate a closed form relationship between strain and bending moment, the right hand side of Eq. (5) is approximated with a second order polynomial according to:

$$M(\alpha_0) = M_p \left(a\alpha_0^2 + b\alpha_0 + c \right) \qquad (6)$$

Obviously a more extensive power series or a Fourier series may be a more precise approximation but considering the overall precision in the analysis of this problem, a second-order polynomial is judged sufficient. From Eqs. (5) and (6) it holds:

$$a\alpha_0^2 + b\alpha_0 + c = \frac{\alpha_0}{2\sin \alpha_0} + \frac{\cos \alpha_0}{2} \qquad (7)$$

When $\alpha_0 = 0$, the moment is M_p and thus $c = 1$:

$$\alpha_0 = -\frac{b}{2a} + \sqrt{\left(\frac{b}{2a} \right)^2 - \frac{1}{a}\left(1 - \frac{M}{M_p} \right)} \qquad (8)$$

When $M = \pi f_y R^2 t$ the angle $\alpha_0 = \pi/2$:

$$\frac{\pi}{2} = -\frac{b}{2a} + \sqrt{\left(\frac{b}{2a} \right)^2 - \frac{1}{a}\left(1 - \frac{\pi}{4} \right)} \qquad (9)$$

$$M\left(\frac{\pi}{4} \right) = M_p \left(\frac{\pi\sqrt{2}}{8} + \frac{1}{2\sqrt{2}} \right) = M_p \frac{\pi + 2}{4\sqrt{2}} \qquad (10)$$

$$\frac{\pi}{4} = \frac{b}{2a} + \sqrt{\left(\frac{b}{2a} \right)^2 - \left(1 - \frac{\pi + 2}{4\sqrt{2}} \right)} \qquad (11)$$

With $a = -0,02629$ and $b = -0,09533$ the following expression is obtained:

$$\alpha_0 = -\frac{-0,095}{2 - 0,026}$$
$$+ \sqrt{\left(\frac{-0,095}{2 - 0,026} \right)^2 - \frac{1}{-0,026}\left(1 - \frac{M}{M_p} \right)}$$
$$= -1,8 + \sqrt{3,3 + 38\left(1 - \frac{M}{M_p} \right)} \qquad (12)$$

$$\varepsilon(\alpha_0) = \frac{\varepsilon_y}{\sin(\alpha_0)} \qquad (13)$$

$$\varepsilon(M) = \frac{\varepsilon_y}{\sin\left(-1,8 + \sqrt{3,3 + 38\left(1 - \frac{M}{M_p} \right)} \right)} \qquad (14)$$

Calculating the Displacement

To calculate the displacement, the pile is treated as a cantilever with length L (see *Fig. 11*) and a moment distribution as shown in *Fig. 13*. The corresponding curvature, κ, along the cantilever is shown in *Fig. 14*.

The curvature is approximated as being linear between the curvature at yield and the maximum curvature. The displacement can then be calculated as follows (Eq. 18).

$$\delta = \int_0^L \kappa x\, dx = \int_{L\frac{M_y}{M}}^L \left(\kappa_y + (\kappa - \kappa_y)\left(\frac{x - L\frac{M_y}{M}}{L\left(1 - \frac{M_y}{M} \right)} \right) \right) x\, dx + \int_0^{L\frac{M_y}{M}} \kappa_y \frac{x}{L\frac{M_y}{M}} x\, dx$$

$$= \frac{L^2 \left(\kappa \left(2 - \frac{M_y}{M} - \left(\frac{M_y}{M} \right)^2 \right) + \kappa_y \left(1 + 2\frac{M_y}{M} - 2\left(\frac{M_y}{M} \right)^2 \right) \right)}{6} + \frac{L^2 \kappa_y \left(\frac{M_y}{M} \right)^2}{3} \qquad (15)$$

$$\delta(M) = \frac{L_2 \kappa}{6}\left(2 - \frac{M_y^2}{M^2} - \frac{M_y}{M} \right) + \frac{L^2 \kappa_y}{6}\left(1 + \frac{M_y}{M} \right) \qquad (16)$$

$$\kappa = \frac{\varepsilon}{R} \qquad (17)$$

$$\delta(M) = \frac{L^2}{6R}\left(\varepsilon\left(2 - \frac{M_y^2}{M^2} - \frac{M_y}{M} \right) + \varepsilon_y\left(1 + \frac{M_y}{M} \right) \right) \qquad (18)$$

By substituting M with Eq. (5) and $\alpha_0 = \text{asin }(\varepsilon_y/\varepsilon)$, the following expression is obtained (Eq. 19).

$$\delta(\varepsilon) = \frac{L^2 \varepsilon_y}{6R}\left(\frac{\varepsilon}{\varepsilon_y}\left(2 - \frac{\pi^2}{4\left(\frac{\varepsilon}{\varepsilon_y}\text{asin}\left(\frac{\varepsilon_y}{\varepsilon} \right) + \sqrt{1 - \left(\frac{\varepsilon_y}{\varepsilon} \right)^2} \right)^2} - \frac{\pi}{2\left(\frac{\varepsilon}{\varepsilon_y}\text{asin}\left(\frac{\varepsilon_y}{\varepsilon} \right) + \sqrt{1 - \left(\frac{\varepsilon_y}{\varepsilon} \right)^2} \right)} \right) + 1 \right.$$
$$\left. + \frac{\pi}{2\left(\frac{\varepsilon}{\varepsilon_y}\text{asin}\left(\frac{\varepsilon_y}{\varepsilon} \right) + \sqrt{1 - \left(\frac{\varepsilon_y}{\varepsilon} \right)^2} \right)} \right) \qquad (19)$$

The output of Eq. (19) cannot be compared to the measured values directly. This is because the clamping of the pile is not rigid and the displacement is therefore larger in the tests than a result from an analytical calculation will provide. In *Fig. 15* the result from expression (19) is compared to the finite element (FE) model shown in *Fig. 16*.

The FE-model consists of 1680 shell elements. The pipe that is modelled has radius 66 mm and thickness 8 mm. The material properties are perfectly elastic–plastic with yield stress at 460 MPa, Young's modulus 210 GPa and Poisson's ratio 0,3. The distances between the supports are 700 mm and loading is prescribed as a deflection of the middle supports.
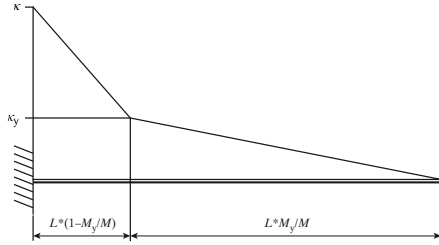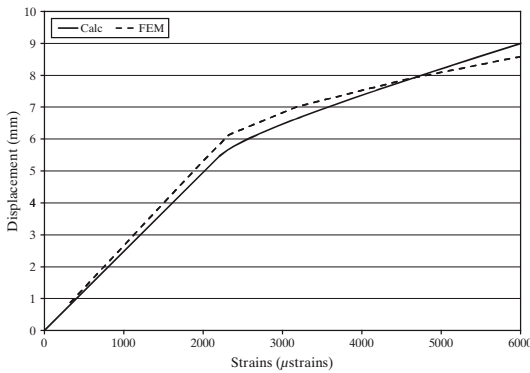
Fig. 14: Curvature along a cantilever

Fig. 15: Comparison between calculation with analytical expression (19) and FEM for a 700 mm pipe cantilever with radius 66 mm and thickness 8 mm
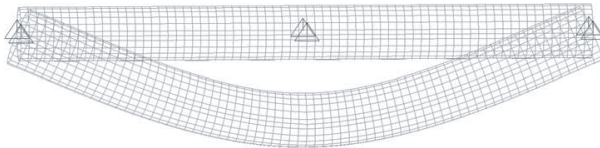

Fig. 16: Finite element model

Conclusion

This work provides experimental evidence demonstrating that a steel pipe pile loaded in bending can withstand several hundred cycles at strain ranges that exceed the yield strain by a factor of six.

The results presented herein constitute an important step towards the development of simple and safe design rules for determining the capacity of piles for integral abutment bridges.

References

[1] Pétursson H, Collin P. Innovative solution for integral abutments. *10th Nordic Steel Construction Conference 2004,* Copenhagen, 2004; 349–359.

[2] Dusicka P, Itanib AM, Buckleb IG. Cyclic response of plate steels under large inelastic strains. *J. Constr. Steel Res.* 2007; **63**: 156–164.

[3] Jokiniemi H, Harju T. Ruukki Construction, *Applicability of Ruukki's Steel Grade S440J2H for Piling Purposes*, PM written 20.03.2006, 2006; 4.

Paper VI

Simulation of Low-Cycle Fatigue in Integral Abutment Piles

Robert Hällmark, Peter Collin, Hans Pétursson and Bernt Johansson

Published in:

Proceedings for IABSE Symposium – Improving Infrastructure Worldwide, September 19-21, 2007, Weimar, Germany

In Paper VI a model to simulate strain variations caused by temperature variations and traffic loads was created from real temperature data and traffic loads measured by Bridge-Weigh-In-Motion technology. The work was carried out as a M.Sc. project by Hällmark initiated and supervised by Pétursson and Collin.

Simulation of Low-cycle Fatigue in Integral Abutment Piles

Robert Hällmark
M.Sc. Civ. Eng.
Ramböll Sverige AB
Luleå, Sweden
Robert.Hallmark@ramboll.se

Peter Collin
Professor
LTU / Ramböll Sverige AB
Luleå, Sweden
Peter.Collin@ramboll.se

Hans Pétursson
Lic. Techn.
Ramböll Sverige AB
Falun, Sweden
Hans.Petursson@ramboll.se

Bernt Johansson
Professor
Luleå Univ. of Technology
Luleå, Sweden
Bernt.Johansson@ltu.se

Summary

Integral abutment bridges are bridges without any expansion joints, and their largest benefits are the lower construction- and maintenance costs. In order to build longer integral bridges it might be necessary to allow plastic hinges to be developed in the piles. Lateral thermal movements are the major reason to plastic deformations, and since temperature variations are cyclic it has to be proved that low-cycle fatigue will not occur. A simulation of the pile strain spectra should be able to take into account the strains caused by temperature variations and traffic loads. Such a model has been created from real temperature data and traffic loads measured by Bridge-Weigh-In-Motion technology. Monte Carlo simulations have been performed in order to simulate daily and annual temperature changes as well as the varying traffic loads. Piles strains have been calculated, and their fatigue effect has been evaluated.

Keywords: Integral abutments, jointless bridges, low cycle fatigue, Monte Carlo simulation.

1. Introduction

Integral abutment bridges are bridges without any expansion joints, and their largest benefits are the lower construction- and maintenance costs. This paper deals with a type of integral abutment shown in Fig. 1 with concrete end walls supported by steel piles. The top of the piles will experience lateral displacements as well as rotations, as a result of thermal movements, temperature gradients, and traffic loads. In order to build longer integral bridges, it is necessary to allow the development of plastic strains in the piles. Lateral thermal displacements are the major reason to plastic strains, and since the temperature variations are cyclic it must be proved that low-cycle fatigue failure will not occur.

A calculation method called the Equivalent Cantilever Method (see 2.2) has been used in order to create a model of the abutment-pile-soil interaction. The pile strains were expressed as a function of varying parameters such as effective bridge temperature, traffic load, and temperature gradient. The effective bridge temperature was simulated by using a mathematical temperature model which had been adapted to real temperature measurements. Daily maximum and minimum temperatures are generated for every single day during the bridge service lifetime, giving daily- as well as annual strain cycles. Traffic loads are simulated by using a traffic load model based on the gross weight distribution of the lorries that crosses the bridge. Data from measurements of traffic intensity and lorry gross weights, at two Swedish roads, have been used to create the traffic simulation model.

2. Low-cycle Fatigue Simulation Model

Thermal expansion and contraction of bridge decks are normally handled by expansion joints. In an integral abutment bridge the abutments will be pushed towards the backfill or pulled away, as a result of the bridge longitudinal expansion. Variations in bridge temperature will appear both daily and seasonally and lead to a cyclic loading procedure of the piles. The piles will deflect under the

loading and plastic deformations may occur now and then. Low-cycle fatigue may be a possible failure mode, which may reduce the bridge's lifetime [1]. The ability of the piles to take lateral movements will be a very important parameter, as well as the lateral stiffness of the soil that surrounds the upper part of the piles.

2.1 Example Bridge – Leduån Bridge

The bridge that has been used as a model in all of the simulations is a 40 m long one span integral abutment bridge. The bridge is a two lane roadway bridge, designed to be a crossing over the Leduån River close to the Swedish town Nordmaling, see Fig. 1. The piles used in the construction are steel pipe piles, $\varnothing170x10$, which are driven in straight lines perpendicular to the longitudinal bridge axis. Six end bearing piles are supporting each abutment. In order to study how the bridge behaves under traffic loads, temperature displacements etc. it is monitored continuously by Luleå University of Technology, since the end of 2006.
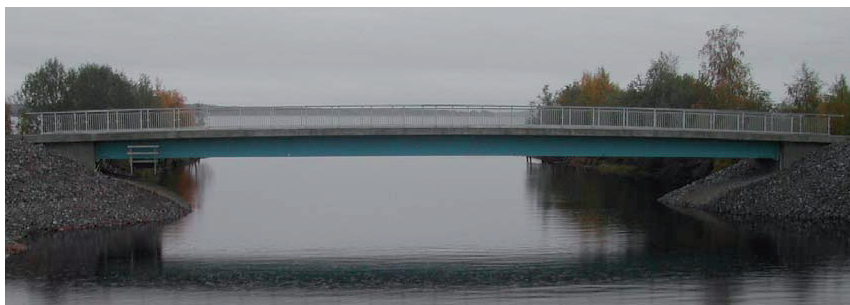

Fig. 1 *View of the Leduån River Bridge.*

2.2 Calculation Model

The interaction between piles and soil has been modelled by the Equivalent Cantilever Method described in [2] [3]. In this model, piles are replaced by equivalent cantilevers. The length of the pile in the equivalent cantilever model, L_{equ}, is a function of pile- and soil properties. How L_{equ} is calculated is described in [2] [3]. Two different L_{equ} are used in the pile strain calculations, one for horizontal stiffness and one for bending moment. The first one is based on the assumption that the lateral pile stiffness of the equivalent cantilever pile equals the lateral stiffness of a pile embedded in soil. The other assumption says that the maximum moment in the equivalent cantilever equals the maximum moment in a pile embedded in soil. The pile strains were calculated according to the following expression,

$$\varepsilon_P = \frac{\left(N_{pile}^{dead} + N_{pile}^{traffic}\right)}{A_{pile} \cdot E} + \left(\frac{3 \cdot \varnothing}{L_{equ,h}^2}\right) \cdot \left(\Delta_{abut} + H\left(\theta_{\Delta T} + \theta_{traffic} + \theta_{dead}\right)\right) + \left(\frac{2 \cdot \varnothing}{L_{equ,m}}\right) \cdot \left(\theta_{\Delta T} + \theta_{traffic} + \theta_{dead}\right). \tag{1}$$

N_{pile}	normal force in a single pile	θ	abutment rotations
A_{pile}	pile area	$L_{equ,h}$	equivalent cantilever length, horizontal stiffness
E	the modulus of elasticity	$L_{equ,m}$	equivalent cantilever length, moment
$\varnothing$	pile diameter	H	distance between the superstructures gravity centre
Δ_{abut}	lateral abutment displacement		and the level where the piles enter the abutment

2.3 Temperature Simulations

2.3.1 Shade Air Temperature

Shade air temperature measurements from different places indicate that seasonal temperature changes are varying almost like a sinus wave [1] [4]. Temperature measurements, in Stockholm, during a period of 5 years are used to illustrate the cyclic behaviour, see Fig. 2. The input data has been compiled in [5].

The temperature has been studied at five locations in Sweden, and a mathematical model has been developed in order to perform a Monte Carlo 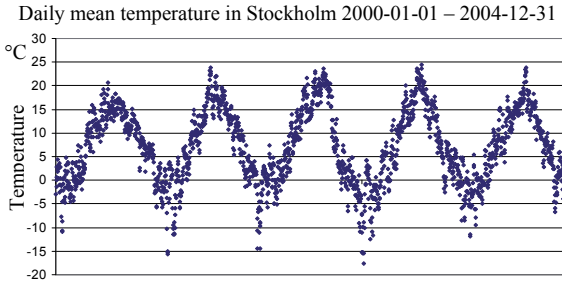simulation of the annual temperature changes as well as the daily changes. The annual temperature variation is modelled by two separate sine curves: one which describes the daily maximum temperature and one which describes the daily minimum temperature. In order to deal with the randomness that is associated with temperatures, normal distributions are used. These are adapted to the mean daily maximum and minimum temperatures for each month, and to the extreme temperatures that occur once in fifty years at the studied locations. The following expression is suggested to be used, (2).

Daily mean temperature in Stockholm 2000-01-01 – 2004-12-31

Fig. 2 *Seasonal temperature changes in Stockholm during a period of five years.*

$$T_{d,\max/\min} = T_{\max/\min\,amp} \cdot \sin\left(\frac{t_d}{365} \cdot 2\pi - t_0\right) + T_{\max/\min\,m} + N(\mu, \sigma_{\max/\min}).$$ (2)

$T_{d\,\max/\min}$	simulated daily maximum respectively minimum temperatures
$T_{\max/\min\,amp}$	annual amplitude of the daily maximum respectively minimum temperatures
t_d	time measured in days
t_0	factor introduced to shift the sinus curve horizontally to adjust it to measured temperature data
$T_{\max/\min\,m}$	annual mean value of daily maximum and minimum temperatures
$N(\mu, \sigma_{\max/\min})$	normal distributions adapted to extreme temperatures and mean daily max/min temperatures

The mean values of the simulated daily temperature variations have been compared to measured temperatures, and it has been observed that the mathematical model is rather conservative concerning daily temperature variations. The daily temperature changes are overestimated by 10-17%, at the five studied locations.

2.3.2 Temperature Differences between Deck and Girders.

One negative and one positive temperature difference has been simulated every day during the bridge service lifetime. A conservative assumption has been used, saying that the positive and negative temperature differences will coincide with the daily minimum and maximum bridge temperature. Two log-normal distributions are used to model the temperature differences. The probability distributions are adapted to the extreme temperature differences that occur once in a year and once in fifty years according to ENV 1991-2-5. Fig. 3 illustrates a result from a simulation of negative and positive temperature differences during a period of 50 years.
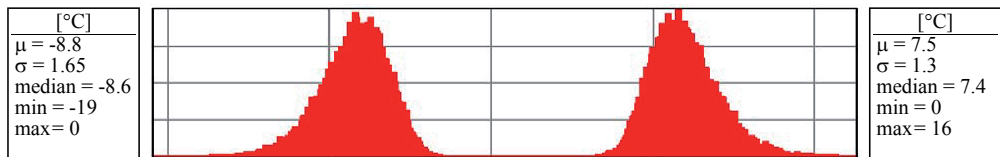

[°C]
μ = -8.8
σ = 1.65
median = -8.6
min = -19
max = 0

[°C]
μ = 7.5
σ = 1.3
median = 7.4
min = 0
max = 16

Fig. 3 *Log-normal distributions, illustrated by the result from a Monte Carlo simulation.*

2.3.3 Effective Bridge Temperature

Longitudinal thermal movements of a bridge are mainly governed by the effective bridge temperature (EBT). The simulated shade air temperatures are therefore transformed into EBTs, in this case by using the EBT model given in EN1991-1-5. The only input needed to this model is the shade air temperature and type of superstructure. The Leduån Bridge that has been used in this

Design of steel piles for integral abutment bridges

study is classified as a Group 2 bridge according to EN1991-1-5, and the EBT can be calculated according to the following expression,

$$T_{EBT\,max/min} = 4 + T_{shade\,max/min} \qquad [°C]. \tag{3}$$

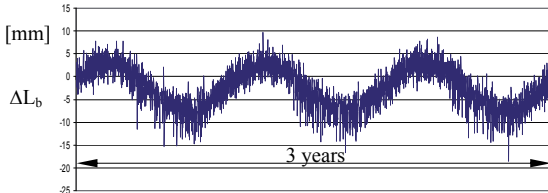### 2.3.4 Temperature Movements

Fig. 4 *Variation of bridge length for a composite bridge with a single span of 40.0 m, located in Kiruna.*

The abutment displacements, as a result of the expansion and contraction of the superstructure, can be described as

$$\Delta_{abut} = \frac{\alpha \cdot \Delta T_{EBT} \cdot L_b}{2}, \tag{4}$$

where α is the thermal coefficient of the superstructure and L_b the length of the bridge. In *Fig. 4*, thermal movements are plotted over a period of time in order to illustrate the results from the temperature simulations.

2.4 Traffic Load Simulation

A traffic load model has been developed in order to study the real loads which the piles in an integral bridge will be subjected to. The load model is based on lorry loads from Bridge Weigh In Motion (BWIM) measurements and Annual Average Daily Traffic (AADT) values, measured with the Metor 2000 system. Second hand information has been used, and most of the information has been collected from [6]. Measurements from two Swedish roads have been studied. The roads and locations that have been studied is E22 close to the Swedish town Strängnäs and National Road 67 close to Tillberga. The traffic fatigue load model given in [7] has also been used in the calculations, in order to study the differences.
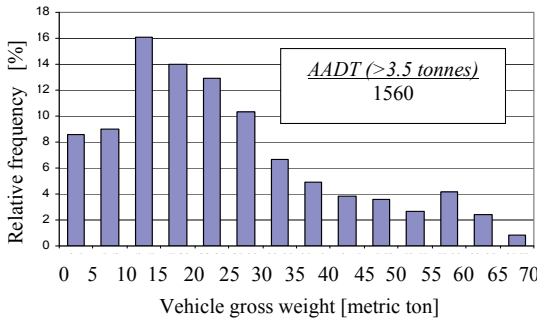

Fig. 5 *Vehicle gross weight distribution at road E22-Strängnäs.*

If the load is doubled then the fatigue effect increases eight times. The weight of a passenger car is only a few percentage of the weight of a heavily loaded lorry. The passenger cars contribution to the fatigue will therefore be insignificant. Only vehicles with a weight above 3.5 tonnes are taken into consideration in the traffic fatigue load model. The AADT for vehicles with a weight >3.5 tonnes are used together with the gross weight distribution among these vehicles. An example of a gross weight distribution that has been used is shown in Fig. 5.

2.4.1 Vehicle Models

The vehicles with a gross weight >3.5 tonnes are divided into four groups, depending on their gross weight. One vehicle model is used to represent all vehicles in one group. When the vehicle models were created, the allowable vehicle loads according to the Swedish Traffic Regulation were taken into consideration, as well as results from a similar study [8]. Gross weight overloads of 6-25% were allowed, since [6] states that 13.8% of the lorries (weighed by the BWIM-technique in Sweden during 2005) were overloaded. [6] states also that every third vehicle above 35 tonnes, was overloaded at least on one axel. A distributed lane load from traffic queues was also taken into consideration. The traffic load model works according to the following schedule, see Fig. 6.

- Vehicle weight, W, is generated from a gross weight distribution
- W $\Rightarrow$ Vehicle type 1, 2, 3 or 4
- Queue weight, q, is generated
- Normal force is calculated in the most exposed pile
- Rotation due to the traffic load is calculated
- Pile strain caused by the traffic load is calculated

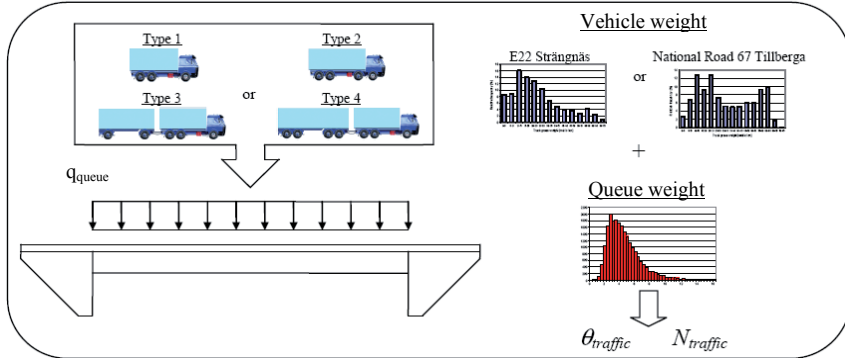| Weight interval [ton]	
Type 1:	$3.5 < W < 28$
Type 2:	$28 \leq W < 38$
Type 3:	$38 \leq W < 55$
Type 4:	$55 \leq W < 75$

Fig. 6 *Schematic illustration of traffic load model.*

The six steps in the generation of pile strain cycles, due to traffic loads, are repeated every time a lorry crosses the bridge. In the example with road E22, there will be 1560 daily cycles, which gives 68 million cycles during the bridge service lifetime of 120 years. A Monte Carlo simulation is used to simulate 100 000 traffic loads cycles for each road. These load cycles are taken as representative for the whole lifetime and repeated until the required number of cycles is achieved.

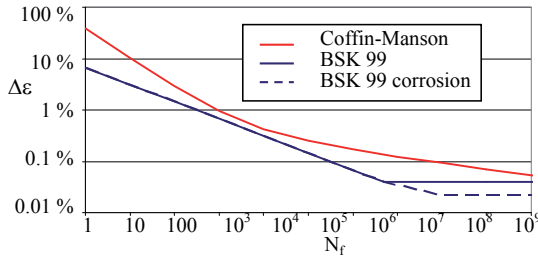## 3. Fatigue Calculations

3.1 Fatigue Model

Fig. 7 *Extrapolated ε_f - N_f curve from [8] compared to Coffin-Manson's equation.*

The fatigue calculations are strain based, since plastic deformations are allowed to occur. Two different models to evaluate the low-cycle fatigue have been studied, Coffin-Mansons's equation and the extrapolated ε_f - N_f curves from [9]. The latter was chosen since it is more conservative and simpler to use in the calculations. Fig. 7 illustrates the relationship between the suggested models, in a specific case where the detail fatigue category factor, C, equals 112 MPa.

The cumulative fatigue is calculated according to the Palmgren-Miner's model,

$$\sum_{i=1}^{n} \frac{n_i}{N_{fi}} \leq 1 . \tag{5}$$

n_i the number of times a certain strain cycle is repeated
N_{fi} the number of cycles until failure for a strain cycle with a certain amplitude.

3.2 Definition of Strain Cycles

The total strain in the piles is a function of variables with frequencies that spans from seconds up to a year. To be able to analyse the fatigue with the available computer programs, the total pile strain must be separated into different cycles. Two groups of cycles are identified, see Fig. 8.
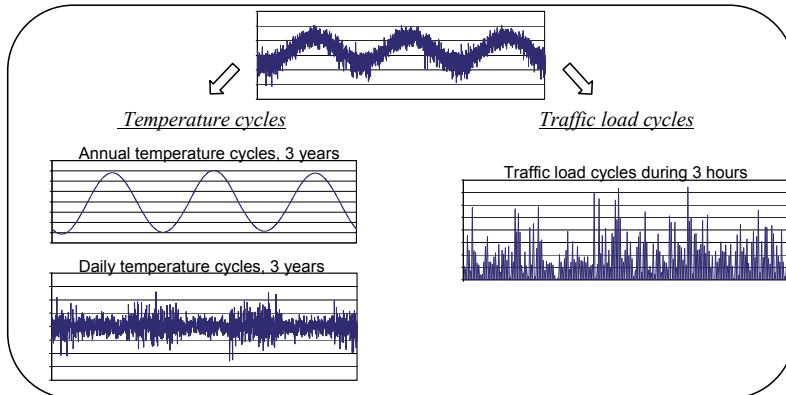

Fig. 8 *Illustration of how the total pile strains can be separated into different type of cycles.*

3.3 Identification and Calculation of Cycles

The amplitudes of daily strain cycles are varying a lot in contrast to the annual cycles, which are almost the same from one year to another. The temperature cycles are analysed together, which means that the daily variations have been superposed on the annual cycles. The simple ranges between peaks and valleys are known from the simulations, but it is harder to identify the cycles among these variations. A number of different techniques can bee used to identify cycles for irregular loading. [10] states that an agreement appears to have been reached that the preferable method is the rain-flow method. The rain-flow counting technique has therefore been used to identify the temperature cycles in this study.

Strain cycles caused by traffic loads are counted separately, since the period of such a cycle is very short compared to the temperature cycles. There is no need of any cycle counting technique either, since every single traffic load is modelled as one complete cycle with loading and unloading. If the traffic cycles should be superposed on the temperature cycles it would be necessary to use a time scale in seconds. This would give enormous amounts of data since the temperature and the traffic load has to be defined every time a vehicle crosses the bridge. A simplification with a separate analysis of temperature cycles and traffic load cycles will not affect the result too much, since all cycles still will be taken into consideration. If one unique vehicle load should be generated for every vehicle, it would give 68 million traffic cycles which has to be recorded. The traffic load distributions are not that complex, and a simulation of 100 000 cycles are taken as representative for all of the traffic cycles.

The traffic loads will however give a contribution to the daily maximum strains. In order not to underestimate the maximum amplitudes of the daily cycles, a traffic strain is added to the daily maximum temperature strain. The minimum values will not be affected since the traffic always gives positive rotations and translations. Fig. 9 illustrates how the temperature strain cycles are combined with the traffic strain cycles. In the upper left corner, the varying strain due to daily temperature changes are illustrated during seven days. In the upper right corner, the varying traffic strain cycles during 12 hour is illustrated. The traffic strains during 12 hours are superposed on a part of the temperature strain curve, in order to illustrate the contribution from the traffic loads. The daily maximum strain will be higher and the minimum strain will not be affected.
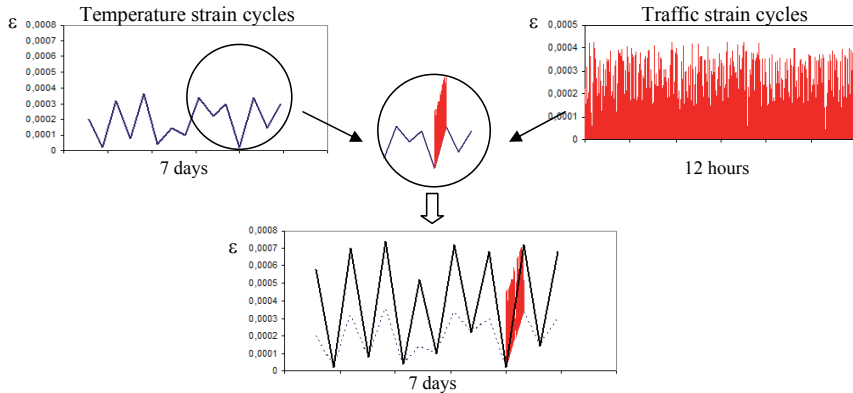
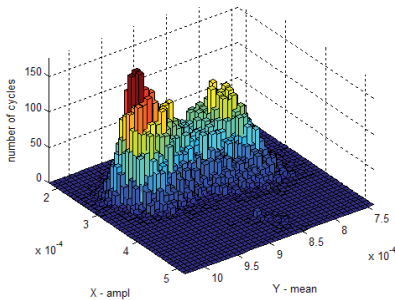Fig. 9 *Illustration of how daily strain ranges are modelled.*

Fig. 10 *3D-model of the distribution of both amplitudes and mean values for temperature induced strain cycles during 60 years.*

A Matlab-script [11] has been used to identify the strain cycles, count them and sort them into bins. The number of cycles until failure will not be calculated for each individual cycle, since there are about 44 000 temperature cycles during the bridge service lifetime. The temperature strain cycles are instead sorted according to their amplitude, and divided in 40 intervals. When the cumulative fatigue is calculated, all cycles within an interval are assumed to have the highest amplitude in that interval. Fig. 10 illustrates a result from rain-flow counting of simulated temperature strain cycles during 60 years.

3.4 Fatigue Simulations Results

The cumulative fatigue has been simulated during 120 year for the pile which will suffer the highest strain variations. The following parameters have been varied:

- Corrosion   No corrosion $\rightarrow$ 2.4 mm corrosion depth
- Bridge length $40 \rightarrow 200$ m
- Soil model   Two different soil models
- Bridge location   Five different locations in Sweden.
- Pile cross-section   RR170x10 and HEM120

The soil models are based on the specific soil condition at Leduån Bridge, in which the upper part of the piles was surrounded by pipes ($\varnothing$600 mm). The piles were wrapped in styrofoam sheets and loose sand was filled between the styrofoam sheets and the sheltering pipes. The undisturbed soil consists of fine sandy silt and silty fine sand, down to a depth of 6 m. The soil below this depth will not affect the pile strains at the top. In this case there was silt/clay down to a depth of about 20 m. [2] and [3] suggests that a properly filled pre-drilled hole shall be treated as soil without any lateral stiffness. This assumption has been used in one of the soil models, the original soil model. The alternative soil model is more conservative, since the filling in the pre-drilled hole is given the same properties as loose sand in-situ. The soil stiffnesses are calculated according to [7].

Some examples of results from the simulation processes are shown in *Table 1*. The bridge length has been varied in this case, while the other parameters have been kept constant.

Design of steel piles for integral abutment bridges

Table 1 *Example of results from cumulative fatigue simulations, with the original soil model.*

$L_{equ.\ m}$	3.143 m	*Cumulative fatigue - Extrapolated ε - N_f curves*				
$L_{equ.\ h}$	2.773 m					
Corrosion:	2.4 mm	*Bridge length*	*60 m*	*80 m*	*100 m*	*150 m*	*200 m*
Location:	Karesuando		*0.3851*	*0.5668*	*0.8292*	*1.884*	*3.694*

4.   Discussion and Conclusion

The aim of this study was to investigate if, how and when low-cycle failure may occur in piles supporting integral abutment bridges. The conclusion is that low-cycle fatigue does not seem to be a problem at all in piles in integral bridges. At least as long as the length of the bridge does not exceed 100 m, according to the calculation models that have been used. The effect of the location in Sweden does not seem to be very important. The maximum bridge length will however be a bit shorter in the north mountain regions. H-piles oriented for weak axis bending seems to be more suitable for integral abutment bridges than pipe piles with the same cross-sectional area. The large influence of the lateral soil stiffness can also be noted, higher soil stiffness decreases the fatigue lifetime considerably. In order to build longer integral bridges, lateral soil stiffness will be a key factor to deal with. The soil stiffness can for instance be lowered by using pre-drilled holes backfilled with loose sand or other soft materials, or by designing the back wall in a way which makes it possible for the piles to pass through the open air before they enter the abutments.

References

[1]   DICLELI, M. and ALBHAISI, S. (2004). Effect of cyclic thermal loading on the performance of steel H-piles in integral bridges with stub abutments, *Journal of Constructional Steel Research*, 60, 161-182

[2]   ABENDROTH, R.E. and GREIMANN, L.F. (1989). Rational Design Approach for Integral Abutment Brige Piles, *Transportations Research Record 1223*, 12-23

[3]   ABENDROTH, R.E. and GREIMANN, L.F. (2005). *Field Testing of Integral Abutments*, Iowa DOT Project HR-399, Iowa State University and Iowa Department of Transportation, Iowa.

[4]   ARSOY, S. (2000). *Experimental and Analytical Investigations of Piles and Abutments of Integral Bridges*, Doctoral Thesis, Virginia Polytechnic Institute and State University, Blacksburg, Virginia

[5]   MOBERG, A. (2005). *Daily temperature data for Stockholm old observatory 1756-2004*, Available at: http://www.smhi.se/sgn0102/n0205/jordens_klimat/stockholm_daily.zip

[6]   VÄGVERKET. (2006). *BWIM-mätningar 2005 sammanfattning (BWIM-measurements 2005 Summary)*, Vägverket Publikation 2006:14, Borlänge, Sweden, ISSN: 1401-9612

[7]   VÄGVERKET (2004). BRO2004 (the Swedish Bridge Code), Vägverket Publikation 2004:56, Borlänge, Sweden, ISSN: 1401-9612

[8]   GETACHEW, A. (2003). *Traffic Load Effects on Bridges*, Doctoral Thesis, Royal Institute of Technology, Stockholm

[9]   BOVERKET. (2003). Swedish Manual for Steel Structures – BSK99, Boverket, Karlskrona, ISBN: 91-7147-816-7

[10] ASM INTERNATIONAL. (1996). ASM Handbook Vol 19, Fatigue and Fracture, ASM International, Ohio, ISBN: 0-87170-385-8

[11] NIESŁONY, A. (2003). *Rain flow for Matlab*, Available at: http://www.mathworks.com/ matlabcentral/fileexchange/loadFile.do?objectId=3026&objectType=FILE# (2006-07-16)